# Generation of Oxidative Radicals by Advanced Oxidation Processes (AOPs) in Wastewater Treatment: A Mechanistic, Environmental and Economic Review

Sara Feijoo[a], Xiaobin Yu[a], Mohammadreza Kamali[a], Lise Appels[a], and Raf Dewil[a,b,*]

[a]KU Leuven, Department of Chemical Engineering, Process and Environmental Technology Lab, Jan Pieter de Nayerlaan 5, 2860 Sint-Katelijne-Waver, Belgium

[b]University of Oxford, Department of Engineering Science, Parks Road, Oxford, OX1 3PJ, United Kingdom

[*]Corresponding author: Raf Dewil, raf.dewil@kuleuven.be

***Keywords***— Advanced oxidation processes, wastewater treatment, oxidative radicals, economic review, environmental assessment

## Abstract

In light of the rising presence of contaminants of emerging concern (CECs) in water streams, in recent decades, advanced oxidation processes (AOPs) have received significant research interest, as the generation of oxidative radicals allows for the effective degradation of recalcitrant compounds. This review paper provides insights into the most relevant generation methods of several oxidative species, with a main emphasis on hydroxyl, sulfate, chlorine and iodine radicals. Understanding the strengths and pitfalls of each generation route is essential to set the baseline for future industrial applications. To this end, this review presents a comprehensive summary of how different techniques result in distinct radical types, and in addition to the principles and mechanisms of formation, the environmental and economic aspects behind the different methods are discussed.

**Abbreviations** – *AFT*: Anodic Fenton treatment, *AOP(s)*: Advanced oxidation process(es), *BDD*: Boron-doped diamond, *CDRs*: Chlorine-derived radicals, *CECs*: Contaminants of emerging concern, *COD*: Chemical oxygen demand, *DSAs*: Dimensionally stable anodes, *eAOPs*: Electrochemical advanced oxidation processes, *EDDS*: [S,S]-ethylene-diamine-disuccinic acid, *EDTA*: Ethylene-diamine-tetra-acetic acid, *EE2*: Ethinylestradiol, *FCE*: Freeze concentration effect, *FFA*: Furfuryl alcohol, *GAC*: Granular activated carbon, *LGSFY*: Light green SF yellowish, *MMO*: Mixed metal oxide, *NOM*: Natural organic matter, *PDS*: Peroxydisulfate, *PFOA*: Perfluorooctanoic acid, *PMS*: Peroxymonosulfate, *PPCP(s)*: Pharmaceuticals and personal care product(s), *RNS*: Reactive nitrogen species, *SR-AOP(s)*: Sulfate radical-based advanced oxidation process(es), *TN*: Total nitrogen, *TOC*: Total organic carbon, *UV*: Ultraviolet, *WAO*: Wet air oxidation, *(n)ZVI*: (nano) Zero-valent ion.

# Table of Contents

# 1 Introduction

The main challenge faced by existing wastewater treatment plants is the potential toxicological effects derived from the recurring and increasing presence of refractory compounds in their effluents, ranging from conventional surfactants, dyes, heavy metals and household chemicals to contaminants of emerging concern (CECs). CECs are mainly micropollutants, such as residues from pharmaceuticals, personal care products and pesticides (Tran et al., 2018; Vidal-Dorsch et al., 2012). Current treatment technologies have not been designed to effectively remove CECs, and their inevitable release into the environment may cause severe adverse effects, not only to aquatic life but also to human health (Herrero et al., 2012; Tran et al., 2018). This imminent worldwide threat is particularly exacerbated by rising water scarcity due to climate change and by the water consumption rate in an ever-growing population (Boretti and Rosa, 2019; Martí et al., 2010). Therefore, to ensure a safe and abundant water supply, there is an urgent need to develop low-cost, efficient and scalable techniques to drive the commercialization of more sustainable and effective wastewater treatment technologies (Balkema et al., 2002; Muga and Mihelcic, 2008).

Several methods have been developed and implemented to address highly polluted wastewater, which can be categorised into biological and physicochemical treatments (Crini and Lichtfouse, 2019). Biological treatment technologies are currently considered popular options, especially for sewage wastewater treatment, due to several showcased qualities, such as being (1) simple in operation, (2) efficient in removing biodegradable organic matter and nitrogen compounds, (3) effective in attenuating the final effluent colour, (4) economically attractive and (5) well accepted by the public. Nonetheless, biological methods generally fail to effectively deal with influents that contain recalcitrant compounds such as CECs, requiring complementary physicochemical treatment (Crini and Lichtfouse, 2019; Weber et al., 1970). Physicochemical treatment technologies on their own have also been introduced as a wastewater treatment solution, covering a broad portfolio of techniques, from conventional membrane filtration, coagulation, precipitation, solvent extraction, evaporation, carbon adsorption or ion exchange to more complex advanced oxidation processes (AOPs) (Crini and Lichtfouse, 2019; Wang et al., 2005). In recent years, there has been a notable trend in the development of multiple AOP-based technologies (Fig. 1) as techniques to degrade complex organic compounds mediated by the generation of powerful oxidative radicals (Deng and Zhao, 2015; Garrido-Cardenas et al., 2020; Macías-Quiroga et al., 2020; Ushani et al., 2020). In fact, they have proven to be effective in the removal of a wide range of contaminants, both at low and high concentrations, and applicable to wastewater effluents of multiple origins (Garrido-Cardenas et al., 2020).

This review elaborates on the principles and mechanisms involved in the generation of the most common oxidative radicals to degrade CECs. Several activation methods are explained, comprising the type and origin of radicals formed, their suitable operating conditions and relevant considerations for industrial applications. Critical discussions are provided regarding the environmental and economic aspects of the different alternatives.

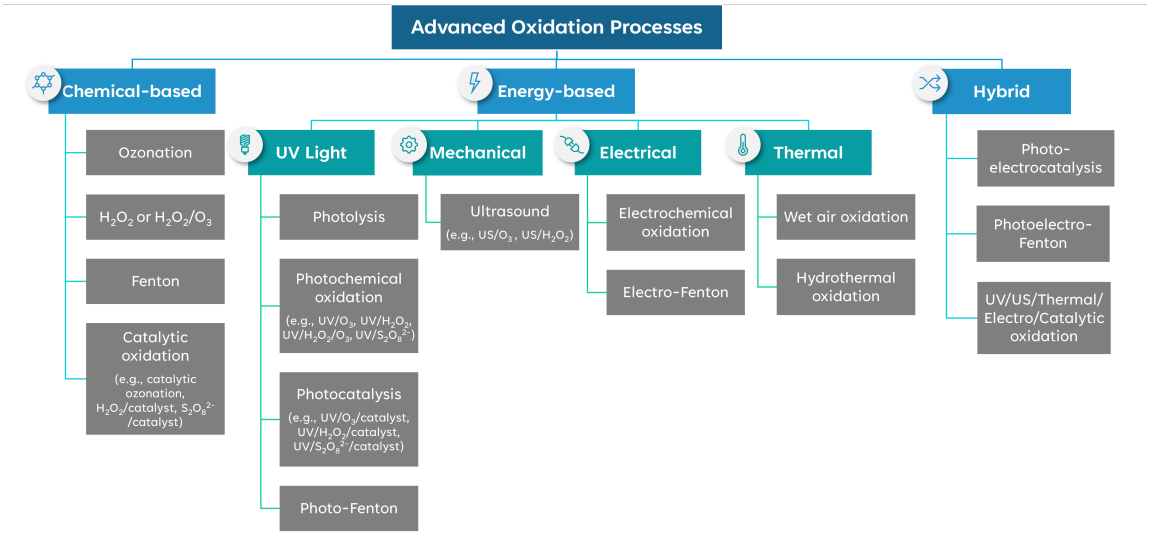


**Figure 1:** High-level classification of advanced oxidation processes in terms of their main activation method (Amor et al., 2019; Jiménez et al., 2019; Sharma et al., 2019).

# 2 Generation methods

## 2.1 Hydroxyl radicals

Hydroxyl radicals ($^{\bullet}OH$) (Fig. 2) present a high standard redox potential (between +1.80 and +2.85 V) (Wardman, 1989), are highly non-selective and react rapidly with most organic pollutants, showing rate constants in the order of $10^8$ to $10^{10}$ $M^{-1}s^{-1}$ (Deng and Zhao, 2015). The underlying reaction mechanisms may take place via electrophilic addition, hydrogen abstraction or electron transfer pathways, depending on the organic pollutant at hand (Scaria and Nidheesh, 2022).

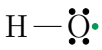

**Figure 2:** Structure of hydroxyl radical, $^{\bullet}OH$ (• unpaired electron) (Mailloux, 2015).

Conventionally, $^{\bullet}OH$ radicals are generated by the addition of a precursor such as hydrogen peroxide ($H_2O_2$) or ozone ($O_3$) to the reaction medium. These precursors need to be activated either via physical methods such as UV light and cavitation, through catalytic reactions, via electrochemical routes or under a hybrid combination of different techniques (Fernandes et al., 2019b; Poyatos et al., 2009; Shah et al., 2018). $^{\bullet}OH$ radicals have also been generated directly from water molecules, mainly via electrochemical-based technologies. The key features of these activation methods are discussed in further detail in the following sections.

### 2.1.1 Chemical activation of $O_3$ and $H_2O_2$

$O_3$ is a well-known oxidising agent that is particularly used for disinfection purposes (Hoigné, 1988; Kim et al., 1999). $O_3$ is mostly produced by the dissociation of molecular oxygen via electrical or photochemical methods (Hoigné, 1988; Masschelein, 1998; Schmitz, 2017), with

electrical discharge (also known as corona discharge) being the most popular route due to its higher efficiency (Considine and Considine, 2007; Summerfelt, 2003). Given that generating $O_3$ is a highly energy-consuming process (approximately 10 kWh is needed to produce 1.0 kg of $O_3$ (Summerfelt, 2003)), ozonation has typically been applied as a tertiary treatment for polishing purposes, so the removal of recalcitrant compounds is technically and economically feasible (Arzate et al., 2019).

In mechanistic terms, the ozonation reaction can be accomplished via two pathways, referred to as direct and indirect ozonation (Chiang et al., 2006). In the first type, oxidation is highly selective to specific contaminants and driven by molecular ozone (Eq. 1), showing first-order kinetics and rate constants in the range of $10^{-3}$ to $10^{9}$ $M^{-1}s^{-1}$ (Hoigné, 1988). In indirect oxidation, secondary radicals (Fig. 3), mainly $^{\bullet}OH$ and $HO_2^{\bullet}$, are formed by a set of reactions in the decomposition of $O_3$ (Eqs. 2 - 8) and lead to pollutant degradation with relatively low selectivity and fast reaction rates ($10^{9}$ to $10^{10}$ $M^{-1}s^{-1}$) (Chiang et al., 2006; Chong et al., 2012; Hoigné, 1998).

$$O_3 + M \longrightarrow M_{oxid} \tag{1}$$

$$O_3 + OH^- \longrightarrow O_2 + HO_2^- \longleftrightarrow H_2O_2 \tag{2}$$

$$O_3 + HO_2^- \longrightarrow HO_2^{\bullet} + O_3^{\bullet -} \tag{3}$$

$$HO_2^{\bullet} \longleftrightarrow H^+ + O_2^{\bullet -} \tag{4}$$

$$O_3 + O_2^{\bullet -} \longrightarrow O_3^{\bullet -} + O_2 \tag{5}$$

$$O_3^{\bullet -} + H^+ \longrightarrow HO_3^{\bullet} \tag{6}$$

$$HO_3^{\bullet} \longrightarrow {}^{\bullet}OH + O_2 \tag{7}$$

$${}^{\bullet}OH + O_3 \longrightarrow HO_2^{\bullet} + O_2 \tag{8}$$

Ozonation processes are normally operated at ambient temperature and pressure (Chong et al., 2012). Additionally, several studies have pointed out that their oxidation efficiency is optimised under alkaline conditions, since indirect ozonation prevails over the direct mechanism and leads to a higher concentration of $^{\bullet}OH$ radicals resulting from the self-decomposition of $O_3$ in the presence of $OH^-$ ions (Eqs. 9 - 11) (Alaton et al., 2002; Chiang et al., 2006; Katsoyiannis et al., 2011; Poyatos et al., 2009). Additionally, at basic pH, the formation of intermediate conjugate bases that affect the lifetime of $O_3$, namely, perhydroxyl ions ($HO_2^-$), is mitigated,

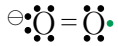

**(a)** Superoxide radical, $O_2^{\bullet -}$

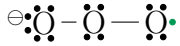

**(b)** Ozonide radical, $O_3^{\bullet -}$

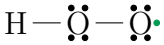

**(c)** Hydroperoxyl radical, $HO_2^{\bullet}$

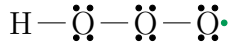

**(d)** Hydridotrioxygen radical, $HO_3^{\bullet}$

**Figure 3:** Structures of (a) superoxide radical (Yogranjan et al., 2017), (b) ozonide radical (ChemSpider, 2021), (c) hydroperoxyl radical (PubChem, 2021) and (d) hydridotrioxygen radical (Liang et al., 2013) (• unpaired electron).

and the generation of oxidative radicals is not jeopardised (Chong et al., 2012; Hoigné, 1998). Hence, ozonation is suitable for the treatment of wastewater streams with an alkaline nature (Saeli et al., 2019).

$$O_3 + OH^- \longrightarrow O_3^{\bullet -} + {}^{\bullet}OH \tag{9}$$

$$O_3^{\bullet -} \longrightarrow O_2 + O^{\bullet -} \tag{10}$$

$$O^{\bullet -} + H^+ \longrightarrow {}^{\bullet}OH \tag{11}$$

$H_2O_2$ is another strong oxidation agent that has already been successfully applied in the treatment of wastewater of various origins (Guo et al., 2018; Kim et al., 2009). Conventionally, it is used for the degradation of a variety of pollutants, such as sulfur and nitrogen oxides, as well as in disinfection and biodegradation processes (Zaharia et al., 2009). Similar to ozonation, the oxidation reaction can take place via direct (Eqs. 12 and 13) or indirect mechanisms (Eq. 14) (Joshi et al., 1995; Pardieck et al., 1992). However, oxidation by $H_2O_2$ alone fails to degrade several recalcitrant compounds (e.g., highly chlorinated compounds and cyanides) due to low reaction rates at feasible $H_2O_2$ concentrations (Neyens and Baeyens, 2003). The selection of the pH in the $H_2O_2$ treatment is also a key design parameter for successful operation. Under alkaline pH, $H_2O_2$ reacts with hydroxyl ions ($OH^-$) to generate $HO_2^-$ ions (Eq. 15), which have a lower redox potential (i.e., +0.79 V) than ${}^{\bullet}OH$ radicals (Wardman, 1989). Therefore, acidic conditions are preferred (Fernandes et al., 2019b).

$$H_2O_2 + X^- \longrightarrow H_2O + XO^- \tag{12}$$

$$H_2O_2 + XO^- \longrightarrow H_2O + O_2 + X^- \tag{13}$$

$$H_2O_2 + H^+ + e^- \longleftrightarrow H_2O + {}^{\bullet}OH \tag{14}$$

$$H_2O_2 + OH^- \longleftrightarrow HO_2^- + H_2O \tag{15}$$

As discussed, direct ozonation is a highly selective reaction towards unsaturated electron-rich bonds in specific functional groups, such as aromatics, olefins and amines (Chiang et al., 2006). It also displays a preference for attacking ionised and dissociated compounds rather than the neutral form of the contaminants. To mitigate such strict selectivity, both $H_2O_2$ and $O_3$, also known as peroxone ($H_2O_2/O_3$), can be used simultaneously, and due to their synergistic effects, the degradation efficiencies attained with this oxidising combination (Eq. 16) are higher than those obtained separately (Alaton et al., 2002; Deng and Zhao, 2015; Fernandes et al., 2019b; Katsoyiannis et al., 2011). The presence of $H_2O_2$ in the peroxone-driven oxidation introduces a major advantage compared to ozonation alone, which circumvents bromate formation in bromide-containing wastewater (Supplementary Material, Appendix A.1) (Fischbacher et al., 2015). Given the difference in the behaviour of $O_3$ and $H_2O_2$ under alkaline conditions, it is, however, not straightforward to define the optimal pH conditions for the peroxone process. Different values have been reported in the literature, as it is a parameter that depends on the nature of the pollutant under study, its susceptibility to degradation by either precursor and the original $H_2O_2/O_3$ molar ratio (Li et al., 2015; Popiel et al., 2009).

$$H_2O_2 + O_3 \longrightarrow {}^{\bullet}OH + HO_2^{\bullet} + O_2 \tag{16}$$

Finally, it should be noted that the presence of other ions in the wastewater matrix can negatively affect the overall degradation efficiency of contaminants, as they may act as scavengers and directly react with $^{\bullet}OH$ radicals to form other species with a lower oxidative power (Chiang et al., 2006). An overview of $^{\bullet}OH$ scavengers can be found in Appendix D.1 of the Supplementary Material. For a deeper analysis of the influence of the wastewater composition on $^{\bullet}OH$-based AOPs, the reader is referred to the review by Lado Ribeiro et al. (2019) (Lado Ribeiro et al., 2019).

### 2.1.2 Activation via UV irradiation

Both $H_2O_2$ and $O_3$ can be activated via UV irradiation to release $^{\bullet}OH$ radicals, as shown in reactions (17) and (18), which can eventually lead to the degradation of contaminants (Eq. 19) or to recombination to produce more $H_2O_2$ (Eq. 20). The typically used wavelength for this purpose is 254 nm (Poyatos et al., 2009; Robl et al., 2012).

$$H_2O_2 \xrightarrow{hv} 2\,{}^{\bullet}OH \tag{17}$$

$$O_3 + H_2O \xrightarrow{hv} 2\,{}^{\bullet}OH + O_2 \tag{18}$$

$${}^{\bullet}OH + RH \longrightarrow H_2O + R^{\bullet} \tag{19}$$

$$2\,{}^{\bullet}OH \longrightarrow H_2O_2 \tag{20}$$

In the case of $H_2O_2$, subsequent propagation reactions take place, in which hydroperoxyl radicals ($HO_2^{\bullet}$) are formed and regenerate $H_2O_2$ as follows (Liao and Gurol, 1995):

$$H_2O_2 + {}^{\bullet}OH \longrightarrow HO_2{}^{\bullet} + H_2O \tag{21}$$

$$H_2O_2 + HO_2{}^{\bullet} \longrightarrow {}^{\bullet}OH + O_2 + H_2O \tag{22}$$

$$2\,HO_2{}^{\bullet} \longrightarrow H_2O_2 + O_2 \tag{23}$$

Wastewater treatment through $H_2O_2$ combined with UV allows for the degradation of organic pollutants that display low reactivity towards $O_3$ and ${}^{\bullet}OH$ radicals while presenting high photoactivity. UV/$H_2O_2$ is especially suitable for streams with a high bromide ($Br^-$) content, as this method also inhibits $BrO_3{}^-$ formation (Katsoyiannis et al., 2011). It is also possible to combine both $H_2O_2$ and $O_3$ with UV light (Eq. 24). When both types of precursors are used, degradation rates are accelerated, and the amount of ${}^{\bullet}OH$ radicals produced is also increased (Poyatos et al., 2009). Other enhancements of the peroxone process have been attained when combined with $TiO_2$-based photocatalysis (Fernandes et al., 2019a, 2020).

$$H_2O_2 + 2\,O_3 \xrightarrow{hv} 2\,{}^{\bullet}OH + 3\,O_2 \tag{24}$$

### 2.1.3 Activation via cavitation

Cavitation consists of the transition from liquid to vapour phase (i.e., the formation of bubbles in the bulk of a liquid) as a result of low-pressure regions (Gagol et al., 2018). This generation method can be further categorised into acoustic and hydrodynamic cavitation. The former type of cavitation is induced by ultrasound acoustic wave discharge, whereas the latter takes place by forcing the liquid through constraining structures or by dropping the pressure below its critical point (Fedorov et al., 2022). During cavitation, ${}^{\bullet}OH$ radicals can be formed by using either $H_2O_2$ or $O_3$ as a precursor (Duan et al., 2020; He et al., 2007; Soumia and Petrier, 2016). In the case of cavitation combined with ozonation, $O_3$ decomposes due to the increased temperature inside the bubbles, leading to the formation of molecular and atomic oxygen (Eq. 25) (Kang and Hoffmann, 1998). Together with the decomposition of water molecules (Eq. 26) and subsequent propagation reactions (Eqs. 27 - 32), enhanced ${}^{\bullet}OH$ radical and $H_2O_2$ yields have been observed compared to ozonation and cavitation alone (Destaillats et al., 2000; He et al., 2007). The combination of $H_2O_2$ and cavitation has also been studied to enhance ${}^{\bullet}OH$ formation (Eqs. 33 - 35), although high $H_2O_2$ loadings may form low reactive radicals, such as $HO_2{}^{\bullet}$, and therefore cause a scavenging effect (Fedorov et al., 2022; Shemer and Narkis, 2005). Recently, hydrodynamic cavitation was highlighted as an attractive solution for industrial applications given several advantages (i.e., fast, effective and robust) and especially in combination with other AOPs due to the high synergistic effects observed (Cako et al., 2020; Fedorov et al., 2022). In addition, sonocatalytic degradation of pharmaceuticals using novel ZnO nanostructures has reported promising results (Soltani et al., 2019a,b). Nonetheless, recent evidence on toxic

byproduct formation (e.g., 4-methylbenzaldehyde and p-nitrotoluene) during cavitation should not be overlooked when developing these treatments further (Gagol et al., 2020).

$$O_3 \xrightarrow{)))} O_{2(g)} + O(^3P) \tag{25}$$

$$H_2O \xrightarrow{)))} {}^{\bullet}OH + H^{\bullet} \tag{26}$$

$$O(^3P)_{(g)} + H_2O \longrightarrow 2\,{}^{\bullet}OH \tag{27}$$

$$O_3 + {}^{\bullet}OH \longrightarrow O_2 + HO_2{}^{\bullet} \tag{28}$$

$$O_2 + H^{\bullet} \longrightarrow HO_2{}^{\bullet} \tag{29}$$

$$O_3 + HO_2{}^{\bullet} \longrightarrow 2\,O_2 + {}^{\bullet}OH \tag{30}$$

$$2\,{}^{\bullet}OH \longrightarrow H_2O_2 \tag{31}$$

$$HO_2{}^{\bullet} + {}^{\bullet}OH \longrightarrow H_2O + O_2 \tag{32}$$

$$H_2O_2 \xrightarrow{)))} 2\,{}^{\bullet}OH \tag{33}$$

$$H_2O_2 + O_2 \xrightarrow{)))} 2\,HO_2{}^{\bullet} \tag{34}$$

$$H_2O_2 + {}^{\bullet}OH \longrightarrow HO_2{}^{\bullet} + H_2O \tag{35}$$

### 2.1.4 Activation via catalysis

#### 2.1.4.1 Fenton

Fenton processes are a catalytic set of reactions where $^{\bullet}OH$ radicals are generated from the interaction between $H_2O_2$ and an iron catalyst (Eqs. 36-41) (Ameta et al., 2018; Brillas et al., 2009). Electron transfer is the mechanism behind reaction (36) to generate $^{\bullet}OH$. Nonetheless, radical production can be negatively affected, as depicted in reactions (37) and (38). Therefore,

it is crucial to optimise the molar ratio of the Fenton reagents in the system to avoid such scavenging. In addition, the iron catalyst is regenerated during the Fenton process by the reaction of Fe(III) with the remaining $H_2O_2$ (Eq. 42) but at a dramatically lower rate (up to $9{\cdot}10^7$ times slower than Eq. 36). Consequently, it becomes a critical bottleneck in the process, as it may hinder iron from being available for the main reactions and therefore reduce the amount of $^{\bullet}OH$ radicals generated for degradation (Deng and Zhao, 2015; Vasquez-Medrano et al., 2018).

$$Fe^{2+} + H_2O_2 \longrightarrow Fe^{3+} + {}^{\bullet}OH + OH^- \tag{36}$$

$$^{\bullet}OH + H_2O_2 \longrightarrow HO_2{}^{\bullet} + H_2O \tag{37}$$

$$Fe^{2+} + {}^{\bullet}OH \longrightarrow Fe^{3+} + OH^- \tag{38}$$

$$Fe^{3+} + HO_2{}^{\bullet} \longrightarrow Fe^{2+} + O_2 + H^+ \tag{39}$$

$$Fe^{2+} + HO_2{}^{\bullet} + H^+ \longrightarrow Fe^{3+} + H_2O_2 \tag{40}$$

$$2\,{}^{\bullet}OH \longrightarrow H_2O_2 \tag{41}$$

$$H_2O_2 + Fe^{3+} \longrightarrow Fe^{2+} + HO_2{}^{\bullet} + H^+ \tag{42}$$

The designation of Fenton-like reactions is given to those in which other metals, such as copper and cobalt at low oxidation states, are used as catalysts instead of iron (Eq. 43) (Ameta et al., 2018; Bokare and Choi, 2014). Similar degradation rates have been attained in Fenton and Fenton-like processes (Hsueh et al., 2005; Wang, 2008), although Fenton-like reactions impose the additional hurdle of preventing metal leaching into the effluent. As additional variations of the conventional Fenton process, some studies have also revealed that under specific complexation conditions, for instance, if the Fe(III)-phloroglucinol complex is formed when degrading phloroglucinol, Fenton-like reactions carried out under alkaline conditions can also yield successful degradation results (Wang et al., 2017; Zhao et al., 2017).

$$H_2O_2 + Cu^+ \longrightarrow Cu^{2+} + {}^{\bullet}OH + OH^- \tag{43}$$

The main pitfall of the conventional Fenton process is its strong dependence on factors such as pH and reagent dosages to attain the desired degradation efficiencies. More specifically, to avoid the precipitation of iron as a hydroxide ($Fe(OH)_3$) and the degradation of $H_2O_2$ into $H_2O$ and $O_2$, the reaction must be carried out under acidic conditions (i.e., pH 3–4). Most importantly, the ratio of $H_2O_2$ and Fe(II) is a key design consideration, not only with an impact on

scavenging effects as previously discussed but also on operational costs. In fact, the optimum concentration of $H_2O_2$ is defined by the chemical oxygen demand (COD) of the influent, and an accumulation of iron can lead to complexation with carboxylate species, which has a negative effect on the degradation rates and increases the amount of iron sludge requiring post-treatment (Babuponnusami and Muthukumar, 2014; Pignatello et al., 2006; Vasquez-Medrano et al., 2018). Additionally, attention has been given to opting for heterogeneous catalysts rather than for homogeneous systems, as they are more easily separated and reused, operate at wider pH ranges, and help reduce iron sludge formation (Thomas et al., 2021; Zárate-Guzmán et al., 2019). To this end, catalysts made of composite materials of magnetite and ferrites, zero-valent iron (ZVI) and iron minerals supported on clay, carbon derivatives, zeolites and metal-organic frameworks have been studied (Nidheesh, 2015; Thomas et al., 2021). Additional process enhancements have been explored through physical means, such as through new catalyst morphologies (e.g., nanoparticles, single-atom catalysts), as well as through combinations with cavitation, electrochemical treatments, semiconductors and plasmonic materials (Huang et al., 2021; Rayaroth et al., 2022; Zhu et al., 2019).

#### 2.1.4.2 Photo-Fenton

The drawbacks of the conventional Fenton process can be mitigated by using a more advanced version consisting of its combination with UV irradiation, the so-called photo-Fenton process (Vasquez-Medrano et al., 2018). The photo-Fenton reaction (Eq. 44) is carried out at wavelengths from UV up to 600 nm and, in comparison to the conventional Fenton process, leads to the production of additional $^{\bullet}OH$ radicals as well as to a reduction of the photocatalyst by UV light (O'Dowd and Pillai, 2020). As a result, the photolysis of the possible iron complexes allows for Fe(II) regeneration, while in parallel degrading organic ligands ($L$), such as $RCOO^-$, $RO^-$ and $RNH^+$, at higher rates (Eq. 45) (Malato-Rodríguez, 2004; Vasquez-Medrano et al., 2018). A variation to the photo-Fenton process is the solar photo-Fenton process, which consists of the substitution of UV lamps by sunlight. It allows for a self-sustaining wastewater treatment process where environmental impacts can be reduced (Arzate et al., 2019; Morone et al., 2019; Särkkä et al., 2015; Vasquez-Medrano et al., 2018; Zepon Tarpani and Azapagic, 2018).

$$H_2O + Fe^{3+} \xrightarrow{hv} Fe^{2+} + {}^{\bullet}OH + H^+ \tag{44}$$

$$Fe^{3+}L_n \xrightarrow{hv} Fe^{2+}L_{n-1} + L^{\bullet} \tag{45}$$

#### 2.1.4.3 Catalytic ozonation

Since the utilisation efficiency of the ozonation process is low due to its low solubility in water and the mineralisation of organic pollutants has been proven to be ineffective by generating additional toxic byproducts, catalytic ozonation has arisen as an alternative process to overcome these issues (Wang and Chen, 2020). Similar to the Fenton process, iron is a known catalyst in ozonation (Eqs. 46 and 47) (Poyatos et al., 2009). Other metal ions have also shown an enhancement in the decomposition of $O_3$ for radical generation, both in homogeneous and heterogeneous catalysis (Wang and Chen, 2020). Since $O_3$ is highly unstable in aqueous media, its

decomposition is already spontaneous to generate free $^{\bullet}OH$ radicals, and the use of a catalyst is not imperative (Poyatos et al., 2009). However, when ozonation is coupled with photocatalysis, an increase in efficiency and a decrease in reaction time have been observed. It also allows for a reduction in the $O_3$ dosage needed, leading to lower operational costs and reduced formation of $O_3$ byproducts (Mecha and Chollom, 2020).

$$O_3 + Fe^{2+} \longrightarrow FeO^{2+} + O_2 \tag{46}$$

$$FeO^{2+} + H_2O \longrightarrow Fe^{3+} + {}^{\bullet}OH + OH^- \tag{47}$$

#### 2.1.4.4 Photocatalytic oxidation

The semiconductor titanium dioxide ($TiO_2$) is the most commonly used catalyst in photocatalytic oxidation. At wavelengths lower than 380 nm, $TiO_2$ particles are excited to produce positive holes in the valence band ($h^+$) by promoting electrons from the valence to the conduction band ($e^-$) with oxidative and reductive abilities, respectively (Eq. 48). These can trigger a set of propagation reactions on the catalyst surface to generate $^{\bullet}OH$ radicals by decomposing either $H_2O_2$ (Eq. 49) or $O_3$ (Eqs. 50 - 52) as well as $O_2{}^{\bullet-}$ radicals from adsorbed $O_2$ (Eq. 53) (Deng and Zhao, 2015; Poyatos et al., 2009).

$$TiO_2 \xrightarrow{hv} TiO_2\,(h^+ + e^-) \tag{48}$$

$$H_2O_2 + e^- \longrightarrow {}^{\bullet}OH + OH^- \tag{49}$$

$$O_3 + e^- \longrightarrow O_3{}^- \tag{50}$$

$$O_3{}^- \longrightarrow O_2 + O^- \tag{51}$$

$$O^- + H_2O \longrightarrow OH^- + {}^{\bullet}OH \tag{52}$$

$$O_{2\,(ad)} + e^- \longrightarrow O_2{}^{\bullet-} \tag{53}$$

$TiO_2$ may also generate $^{\bullet}OH$ from adsorbed water molecules or $OH^-$ ions (Eqs. 54 and 55). In addition, when excited at wavelengths lower than 242 nm, the photolysis of water may be triggered and allow for $^{\bullet}OH$ radical formation (Eq. 56) (Deng and Zhao, 2015). Other $TiO_2$ photoanodes doped with metals such as Ni, Co and Zn, as well as dimensionally stable anodes (DSAs) and novel electrodes such as $TiNbO_5$ and $Ti/TiO_2/WO_3$, have also been investigated for this in situ generation. Nevertheless, mineralisation efficiencies have been shown to be

considerably lower than in other treatments since mass and energy transport limitations hinder the overall degradation process (Brillas and Martínez-Huitle, 2015; Sirés et al., 2014).

$$h^+ + \mathrm{H_2O}_{(ad)} \longrightarrow {}^{\bullet}\mathrm{OH} + \mathrm{H}^+ \tag{54}$$

$$h^+ + \mathrm{OH}^-_{(ad)} \longrightarrow {}^{\bullet}\mathrm{OH} \tag{55}$$

$$\mathrm{H_2O} \xrightarrow{hv} {}^{\bullet}\mathrm{OH} + \mathrm{H}^{\bullet} \tag{56}$$

An important disadvantage to be considered when applying photocatalytic oxidation is that a critical loss in degradation efficiency occurs because the electrons promoted to the valence band can recombine, either with unreacted positive holes (Eq. 57) or with adsorbed $^{\bullet}$OH radicals (Eq. 58). To suppress such recombination processes, an external electric field can be applied so that photo-induced electrons are continuously extracted from the anode and injected into the cathode, leading to a higher number of positive holes and $^{\bullet}$OH radicals, and as a result, photoelectrocatalytic oxidation has been shown to be more efficient than photocatalysis in several lab-scale studies (Brillas and Martínez-Huitle, 2015; Sirés and Brillas, 2012). In addition, the replacement of UV lamps by solar energy has been implemented, and solar photoelectrocatalytic oxidation provides the additional advantage that it circumvents the additional costs and safety requirements derived from UV irradiation (Peleyeju and Arotiba, 2018).

$$e^- + h^+ \longrightarrow \mathrm{TiO_2} + heat \tag{57}$$

$$e^- + {}^{\bullet}\mathrm{OH} \longrightarrow \mathrm{OH}^- \tag{58}$$

### 2.1.5 Electrochemical activation

The main advantage of electrochemical advanced oxidation processes (eAOPs) is that, compared to other treatments, eAOPs make use of a reagent considered to be much cleaner: electrons. In addition, eAOPs are versatile, safe and energy-efficient setups that are easily operated under mild conditions. On the other hand, current obstacles limiting their implementation are the costs derived from the power supply and the production and maintenance of the electrodes, as well as the lack of an overarching understanding of the reaction mechanisms that yield byproducts that may be even more toxic than the original pollutant. Additionally, wastewater typically presents a low conductance, and therefore, the addition of electrolytes and pH modifiers is often required (Anglada et al., 2009; Sirés and Brillas, 2012).

When discussing eAOPs that rely on activating a chemical precursor, electro-Fenton, anodic Fenton treatment (AFT) and electro-Peroxone processes have been developed. In the electro-Fenton treatment, the reagents needed to generate $^{\bullet}$OH radicals, that is, $H_2O_2$ and iron catalysts, are formed and regenerated by electrochemical means, respectively. The electro-Fenton process is therefore based on the continuous feed of $O_2$ or air through the wastewater so

that $H_2O_2$ is produced electrochemically through the cathodic reduction of dissolved $O_2$ on a carbon electrode (Eq. 59). In parallel, soluble Fe(III) can be cathodically reduced to Fe(II) (Eq. 60), which is a fast reaction that accelerates the production of $^{\bullet}OH$ radicals through the Fenton reaction (Eq. 61) (Brillas et al., 2009; Oturan and Oturan, 2018; Poyatos et al., 2009). Regarding anodic Fenton treatment, the cathode is made of iron material to release Fe(II) ions, and $H_2O_2$ is continuously added as an external chemical for the Fenton reaction to take place (Sirés and Brillas, 2012). A membrane-divided cell is also required during AFT so that the formation of $OH^-$ ions from water reduction at the cathode is avoided, and consequently, the pH can be maintained at acidic values. Finally, the electro-Peroxone process involves the electrogeneration of $H_2O_2$ from cathodic $O_2$ reduction during conventional ozonation. By installing a pair of electrodes in the ozonation reactor, in situ generated $H_2O_2$ and $O_3$ can react and produce $^{\bullet}OH$ radicals to improve the degradation of $O_3$-resistant pollutants. Furthermore, in situ $H_2O_2$ has been shown to significantly reduce the amount of $BrO_3{}^-$ formed in bromine-containing water, as previously discussed (Zhou et al., 2018).

$$O_{2(g)} + 2\,H^+ + 2\,e^- \longrightarrow H_2O_2 \tag{59}$$

$$Fe^{3+} + e^- \longrightarrow Fe^{2+} \tag{60}$$

$$Fe^{2+} + H_2O_2 \longrightarrow Fe^{3+} + {}^{\bullet}OH + OH^- \tag{61}$$

Electro-Fenton is an appealing alternative to the conventional Fenton process from an economic and environmental point of view. The continuous (re)generation of the reactants increases the efficacy of the process, avoiding extra operational costs and mitigating the environmental implications derived from the transport, use and storage of chemicals. Other specific advantages are the higher degradation efficiencies observed, the ease of regulating $H_2O_2$ production in the system and the elimination of parasitic reactions that consume $^{\bullet}OH$ radicals (Brillas and Martínez-Huitle, 2015; Sirés et al., 2014). Additionally, it is a versatile system that has been successfully implemented in both divided and undivided electrochemical cells under various types of anode (e.g., graphite, platinum, BDD) and cathode (e.g., graphite, gas diffusion electrodes) materials (Sirés and Brillas, 2012). To further accelerate the degradation rates, electro-Fenton can also be irradiated with UV light, which helps mitigate the accumulation of iron species and, therefore, regenerate Fe(II) ions, as previously discussed (Eq. 45). This method is known as the photoelectro-Fenton method, and despite its advantageous synergistic effects and the accelerated mineralisation rates observed, there is an excessive cost associated with the use of UV lamps (Brillas and Martínez-Huitle, 2015; Sirés and Brillas, 2012). Therefore, process enhancement with solar power sources has been developed in the so-called solar photoelectro-Fenton (Olvera-Vargas et al., 2015; Steter et al., 2018).

Without the addition of chemical precursors, pollutants in wastewater can be degraded by the $^{\bullet}OH$ radicals formed under direct electron transfer from water molecules at the anode surface (Eq. 62), which is a process coupled with the corresponding reduction of $O_2$ at the cathode (Eq. 63). This treatment is referred to as electrochemical oxidation and can be performed in divided or undivided electrochemical cells. Very different behaviours depending on the cell configuration, cathode properties, electrolyte composition and pollutant nature have been reported

in the literature (Amadelli et al., 2000; Brillas et al., 2009; Sirés and Brillas, 2012). Among the process influencing factors, the selection of the electrode material is a determinant design parameter to safeguard the efficiency, selectivity and biocompatibility of this oxidation route. In broad terms, anodes can be categorised as active and non-active, depending on whether the interaction with $^{\bullet}OH$ radicals on their surface is strong or weak (i.e., chemisorbed vs physisorbed species), respectively. Generally, the weaker the interaction is, the higher the reactivity and oxidant power, and therefore, non-active electrodes are more suitable for organics degradation (Garcia-Segura et al., 2018; Martínez-Huitle and Ferro, 2006; Sirés and Brillas, 2012). Example materials in this category can be found among mixed metal oxide (MMO) electrodes, also known as dimensionally stable anodes (DSAs). They consist of a metal oxide coating, such as $RuO_2$, $IrO_2$, and $SnO_2$, over a base material resistant to corrosion, such as Ti. Non-active MMOs are those with $PbO_2$ and $SnO_2$ as coatings, for instance (Wu et al., 2014). Nevertheless, the most effective type of non-active electrode to degrade organic contaminants is the boron-doped diamond (BDD) electrode. Despite their much higher cost compared to MMOs, they display a higher reactivity, stability and $O_2$ overpotential, allowing for higher degradation efficiencies (Comninellis and Chen, 2010; Loos et al., 2018; Martínez-Huitle and Ferro, 2006; Radjenovic and Sedlak, 2015; Sirés and Brillas, 2012). In recent years, new electrode materials and configurations have been developed at the laboratory scale, although their stability and operational costs have not yet been optimised for industrial roll-out (Brillas and Martínez-Huitle, 2015; Särkkä et al., 2015). In addition, it should be noted that the active or non-active nature of the anodic material is not exclusive, and mixed behaviours can also occur and be adapted depending on the desired application (Garcia-Segura et al., 2018). Finally, it is noteworthy that the formation of hydrogenated byproducts is of great concern in electrochemical oxidation due to the toxicity of these compounds, especially chlorate ($ClO_3^-$), perchlorate ($ClO_4^-$) and bromate ($BrO_3^-$) when the corresponding halides are present in solution (Supplementary Material, Appendix A.2) (Kurokawa et al., 1990; Srinivasan and Thiruvenkatachari, 2009; Steffen and Wetzel, 1993).

$$H_2O \xrightarrow{anode} H^+ + (^{\bullet}OH)_{ad} + e^- \tag{62}$$

$$O_2 + 2\,H^+ + 2\,e^- \xrightarrow{cathode} H_2O_2 \tag{63}$$

The commercialization of electrochemical AOPs is still hindered by low current efficiencies and limited yield of degradation attained per unit volume and time. As a result, high energy consumption and costs are tied to this type of operation, especially when mass transfer phenomena are limited and high current densities are needed to ensure effective degradation. To mitigate such drawbacks, it is recommended to avoid the use of plate-and-frame filter press reactors since the electrolyte and current flows are perpendicular to each other and a thin stagnant boundary layer can be formed on the electrode surface (Radjenovic and Sedlak, 2015). Instead, it is preferred to use flow-through electrochemical reactors with 3-D particle and granular electrodes, where adsorption-electrochemical oxidation occurs at a large specific surface area that allows for a reduction in energy consumption (Arevalo and Calmano, 2007; Can et al., 2014). In addition, reducing the electrode interdistance, working with current modulation and preventing electrode fouling by polarity reversal can help reduce mass and charge transfer limitations (Radjenovic and Sedlak, 2015; Scialdone et al., 2011; Urtiaga et al., 2014).

## 2.2 Sulfate radicals

Sulfate radical ($SO_4^{\bullet-}$) based AOPs, also known as SR-AOPs, promote the formation of $SO_4^{\bullet-}$ radicals (Fig. 4). This branch of AOPs has received great interest over the past decades, as it has been proven to effectively eliminate recalcitrant contaminants, such as pharmaceuticals, endocrine disruptors, dyes and perfluorinated compounds (Han et al., 2019; Oh et al., 2016). In addition, $SO_4^{\bullet-}$ radicals present several distinct advantages. First, their redox potential is in the range of +2.43 to +3.10 V depending on the pH (Devi et al., 2016; Wardman, 1989), which is higher than that of $^{\bullet}OH$ radicals (i.e., +1.80 to +2.85 V) and $O_3$ (i.e., +1.04 to +1.80 V) (Wardman, 1989). Second, $SO_4^{\bullet-}$ radicals can maintain their reactivity over a wider pH range, including acidic (pH 2) and alkaline (pH 8) conditions. In fact, SR-AOPs may be effectively operated at neutral pH while reaching a higher standard redox potential than $^{\bullet}OH$ radicals under the same conditions. In this way, the need to add extra chemicals to alter the pH and the subsequent generation of waste can be avoided (Guerra-Rodríguez et al., 2018). Finally, $SO_4^{\bullet-}$ radicals present a reasonably long lifetime in water, between $1.5{\cdot}10^3$ and $2{\cdot}10^3$ times longer than that of $^{\bullet}OH$ radicals (Ghanbari et al., 2016; Ushani et al., 2020). They have also displayed fast reaction rates (Tang et al., 2019), better selectivity towards specific functional groups directly related to molecular ecotoxicity, such as perfluorinated compounds (Lutze et al., 2015), and lower scavenging and self-scavenging effects (Supplementary Material, Appendix D.2) (Duan et al., 2020).

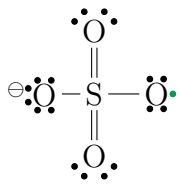

**Figure 4:** Structure of sulfate radical, $SO_4^{\bullet-}$ (• unpaired electrons) (Moad and Solomon, 1989).

The most common precursors used to generate $SO_4^{\bullet-}$ radicals are peroxymonosulfate (PMS, ${SO_5}^{2-}$) and peroxydisulfate or persulfate (PDS, ${S_2O_8}^{2-}$) (Fig. 5) (Lee et al., 2020), which are typically commercialised in the form of sodium salt ($NaHSO_5$) and as triple potassium salt (2 $KHSO_5{\cdot}KHSO_4{\cdot}K_2SO_4$) under the brand name Oxone, respectively (Sigma Aldrich, 2020; Zhang et al., 2015). The major distinction between both precursors is that PDS generates only $SO_4^{\bullet-}$ radicals, whereas PMS also induces the formation of $^{\bullet}OH$ (Giannakis et al., 2021). PDS has surpassed PMS in commercial applications, given that it is a very stable and soluble salt in water as well as more economical and efficient. In fact, all sulfate groups in its structure are activated, as opposed to what occurs with PMS (Ike et al., 2018a), and their redox potentials are +1.10 V and +1.60 V for PMS and PDS, respectively (Wardman, 1989). In addition, PDS has been found to be effective in solid waste and sludge treatment, remediation of soil and groundwater, resource recovery, metal extraction, synthesis and regeneration of ecomaterials, and disinfection applications (Lin et al., 2022). Nonetheless, for both PDS and PMS, the reaction rates for the degradation of CECs are so slow that without being activated, none of these compounds are considered reactive, as they do not naturally release $SO_4^{\bullet-}$ radicals (Liang and Bruell, 2008). Their formation typically takes place by breaking their peroxide bonds (O-O) either via cleavage using heat or light (Eqs. 64 and 65) by an oxidation-reduction process with radiolysis of $H_2O$ (Eqs. 66 - 68) or under low-valent transition metals, such as Fe(II) and Ag(I) (Eqs. 69 and 70) (Duan et al., 2020; Giannakis et al., 2021; Guerra-Rodríguez et al., 2018; Waldemer et al., 2007). Recent studies on antibiotics degradation have shown that PDS and

PMS are particularly effective at low pollutant concentrations, although the removal efficiency is also dependent on the antibiotic chemical structure (Honarmandrad et al., 2023). Similarly, increasing the concentration of PDS and PMS enhances $SO_4^{\bullet-}$ radical production up to the limits of 0.7 mM and 2 mM, respectively, as scavenging effects may take place (Honarmandrad et al., 2023). Alternatively, $SO_4^{\bullet-}$ radicals may also be generated from sulfate ions ($SO_4^{2-}$) typically present in wastewater, without the need to add an external precursor. In fact, $SO_4^{2-}$ has been identified in surface and groundwater in concentrations up to 630 mg $L^{-1}$ and 230 mg $L^{-1}$, respectively, and previous works in the field have proven to generate $SO_4^{\bullet-}$ at lower $SO_4^{2-}$ concentrations (i.e., 150 mg $L^{-1}$) via electrochemical treatment (Farhat et al., 2015; Radjenovic and Petrovic, 2016, 2017).

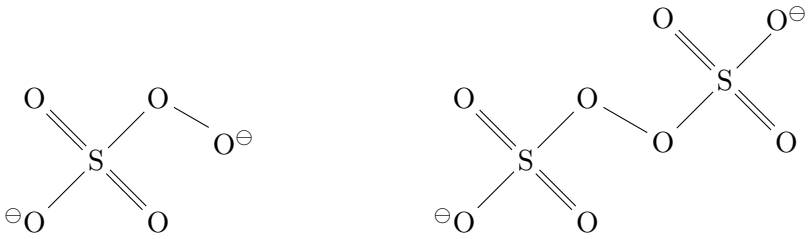

**(a)** PMS, $SO_5{}^{2-}$ **(b)** PDS, $S_2O_8{}^{2-}$

**Figure 5:** Structures of (a) PMS and (b) PDS (Arellano et al., 2019).

$$S_2O_8{}^{2-} \xrightarrow{\Delta/\,hv} 2\,SO_4{}^{\bullet-} \tag{64}$$

$$HSO_5{}^{-} \xrightarrow{\Delta/\,hv} SO_4{}^{\bullet-} + {}^{\bullet}OH \tag{65}$$

$$H_2O \xrightarrow{\Delta/\,hv} H^{\bullet} + {}^{\bullet}OH \tag{66}$$

$$S_2O_8{}^{2-} + H^{\bullet} \longrightarrow SO_4{}^{\bullet-} + SO_4{}^{2-} + H^{+} \tag{67}$$

$$HSO_5{}^{-} + H^{\bullet} \longrightarrow SO_4{}^{\bullet-} + H_2O \tag{68}$$

$$S_2O_8{}^{2-} + M^{n+} \longrightarrow SO_4{}^{\bullet-} + SO_4{}^{2-} + M^{(n+1)+} \tag{69}$$

$$HSO_5{}^{-} + M^{n+} \longrightarrow SO_4{}^{\bullet-} + {}^{\bullet}OH + M^{(n+1)+} \tag{70}$$

In terms of pollutant degradation mechanisms, several pathways have been postulated, including single electron transfer, hydrogen abstraction and radical addition (Duan et al., 2020; Xiao et al., 2018). It is believed that electron transfer is the predominant pathway since it

has been observed that aromatic and unsaturated compounds showed greater degradation efficiencies by $SO_4^{\bullet-}$ than saturated hydrocarbons and halogenated alkanes, suggesting that $SO_4^{\bullet-}$ radicals have a greater tendency to abstract electrons than H atoms (Giannakis et al., 2021; Neta et al., 1988; Ushani et al., 2020). In addition, $SO_4^{\bullet-}$ also interacts with other radicals and oxidants present in the bulk to initiate a chain of reactions leading to other reactive species, including $^{\bullet}OH$ radicals (Eqs. 71 - 77) (Devi et al., 2016; Duan et al., 2020; Matzek and Carter, 2016; Waldemer et al., 2007).

$$SO_4{}^{\bullet-} + H_2O \longrightarrow {}^{\bullet}OH + H^+ + SO_4{}^{2-} \tag{71}$$

$$SO_4{}^{\bullet-} + OH^- \longrightarrow {}^{\bullet}OH + SO_4{}^{2-} \tag{72}$$

$$2\,SO_4{}^{\bullet-} \longrightarrow S_2O_8{}^{2-} \tag{73}$$

$$SO_4{}^{\bullet-} + {}^{\bullet}OH \longrightarrow HSO_5{}^{-} \tag{74}$$

$$2\,{}^{\bullet}OH \longrightarrow H_2O_2 \tag{75}$$

$$H_2O_2 \longrightarrow H_2O + \frac{1}{2}\,O_2 \tag{76}$$

$$H_2O_2 + S_2O_8{}^{2-} \longrightarrow 2\,H^+ + 2\,SO_4{}^{2-} + O_2 \tag{77}$$

Despite the promising characteristics of $SO_4^{\bullet-}$ radicals and the successful results attained in the degradation of specific pollutants, further studies are required to elucidate the precise underlying mechanisms and enable SR-AOP scale-up and industrial roll-out. More specifically, it is crucial to overcome limitations such as the generation of toxic byproducts (i.e., halogenated and nitro-products) and scavenging side-reactions (Dewil et al., 2017; Duan et al., 2020; Rayaroth et al., 2022). Therefore, understanding the different alternatives together with their environmental and economic aspects is imperative to set the ground for further technological improvements. In this regard, an analysis of the literature in this field is presented in the following sections, where the focus was on the activation of either $SO_4{}^{2-}$ or PDS rather than PMS, since, as previously discussed, they are more attractive from a commercialization point of view. For more information on PMS activation methods, the reader is referred to the recent studies of Oh et al. (2016), Ghanbari and Moradi (2017) and Honarmandrad et al. (2023) (Ghanbari and Moradi, 2017; Honarmandrad et al., 2023; Oh et al., 2016).

### 2.2.1 Thermal activation

Applying heat has been shown to successfully activate PDS, where the thermal scission of the O-O bond results in the release of $SO_4^{\bullet-}$ radicals for the degradation of a wide variety of pollutants

(Duan et al., 2020; Ushani et al., 2020). Even though contaminant degradation in wastewater typically obeys a pseudo-first order kinetics and can be accurately fitted under the Arrhenius equation, it is not the case for SR-AOPs that the higher the temperature is, the faster the degradation. For each contaminant, there is a threshold in temperature after which radical-radical and scavenging reactions are favoured over those radical-contaminants due to the higher radical concentration in the bulk (Devi et al., 2016; Guerra-Rodríguez et al., 2018; Matzek and Carter, 2016). Several studies have reported that PDS can be activated at temperatures in the range of 60 to 90°C, being more effective than when it is activated via catalytic routes (Ike et al., 2018b; Milh et al., 2020; Oh et al., 2009; Zhao et al., 2013). This is primarily due to two reasons: (1) as shown in Eq. (64), the stoichiometry of the formation reaction yields two moles of $SO_4^{\bullet-}$ radicals per mole of PDS activated, whereas the reaction with transition metal ions obeys a 1:1 relationship (Eq. 69); and (2) in the case of transition metal ion activation, unreacted ions may compete with the target contaminants and further react with $SO_4^{\bullet-}$ (Eq. 78) (Oh et al., 2009; Rodriguez et al., 2014).

$$SO_4{}^{\bullet-} + M^{n+} \longrightarrow SO_4{}^{2-} + M^{(n+1)+} \tag{78}$$

### 2.2.2 Activation via UV irradiation

UV light mediated methods are considered an economical and harmless option to activate PDS (Duan et al., 2020). The reason is that, similar to thermal treatments, UV activation theoretically yields the generation of two moles of $SO_4^{\bullet-}$ per activated mole of PDS (Eq. 64). In addition, the fact that UV light is already used in wastewater treatment and disinfection facilities is a major advantage in terms of future process integration. Consequently, it is a well-known and established technology that has received much attention in studies focused on $SO_4^{\bullet-}$ production (Ao and Liu, 2017; Dhaka et al., 2017; Duan et al., 2017; Guan et al., 2011; Herrmann, 2007; Tan et al., 2014). In addition, the risk of generating toxic $BrO_3{}^-$ is mitigated in the presence of natural organic matter (NOM) at typical concentrations; therefore, this crucial challenge during ozonation meets its solution with UV and SR-AOPs (Lutze et al., 2014).

A key design factor in UV treatment is the selection of a suitable wavelength. It has been found that the molar extinction coefficient of PDS and the $SO_4^{\bullet-}$ quantum yield are inversely proportional to the UV wavelength irradiated (Herrmann, 2007; Lin et al., 2011). The wavelength that has been more extensively used is 254 nm due to the attained degradation efficiencies and reduced reaction times as well as its availability and energy requirements (Chen et al., 2017; Duan et al., 2017, 2020; He et al., 2013; Lin et al., 2013, 2011; Luo et al., 2016). In addition, pH is another important factor to be taken into play during UV irradiation. Discrepancies in the selection of the optimal pH can be found in the literature, mainly because the properties of the target pollutant have a major influence. For contaminants more readily degraded by $SO_4^{\bullet-}$ than $^{\bullet}OH$ radicals, it has been reported that neutral or acidic conditions would be optimum. This is because at neutral pH, both types of radicals coexist, while at acidic pH, $SO_4^{\bullet-}$ radicals are claimed to be dominant, and vice versa for alkaline conditions (Gao et al., 2012; Guo et al., 2014; Ismail et al., 2017; Matzek and Carter, 2016).

### 2.2.3 Activation via cavitation

Similar to the generation of $^{\bullet}OH$ radicals, both acoustic and hydrodynamic cavitation have been used to activate $SO_4^{\bullet-}$ precursors such as PDS and $SO_4{}^{2-}$ (Fedorov et al., 2020, 2021; Rayaroth et al., 2022; Wei et al., 2017). Inside the cavitation bubbles, the precursor molecules are trapped and brought to an excited state at extreme temperatures and pressures, up to 5,200 K and 500 atm, respectively, releasing radicals to react with the pollutant species either in the cavities or in the bulk (Duan et al., 2020; Fedorov et al., 2021; Soumia and Petrier, 2016). It has been reported that cavitation promotes the reaction of generated $SO_4^{\bullet-}$ radicals with $H_2O$, and therefore, degradation through $^{\bullet}OH$ radicals is more dominant in these systems (Rayaroth et al., 2022; Wei et al., 2017). Nonetheless, the addition of an $SO_4^{\bullet-}$ precursor showed increased degradation efficiencies compared with the use of the precursor or cavitation independently (Fedorov et al., 2020, 2021). In addition, limiting PDS concentrations has been identified to not trigger scavenging effects (Fedorov et al., 2020), and cavitation for $SO_4^{\bullet-}$ generation has also been investigated in combination with other methods, such as UV light or catalysis, to attain higher efficiencies (Chakma et al., 2017; Fedorov et al., 2020).

### 2.2.4 Activation via gamma radiation

Gamma radiation has also been studied for the generation of $SO_4^{\bullet-}$ radicals from activated PDS to degrade several contaminants (Alkhuraiji et al., 2017; Paul (Guin) et al., 2014; Wang and Wang, 2018b). From a sustainability point of view, human health and safety concerns are the main drawbacks for the commercialization of this technique. Therefore, keeping a future practical implementation in mind, this method can be outperformed by the other techniques discussed in this review.

### 2.2.5 Activation via catalysis

Effective $SO_4^{\bullet-}$ radical formation from catalyst-activated PDS has been investigated through numerous transition metals acting as electron donors, such as $Cu^{2+}$, $Mn^{2+}$, $Ni^{2+}$, $Co^{2+}$, $V^{3+}$ and $Ru^{3+}$ (Ushani et al., 2020). However, it is worth mentioning the repercussions of the studies from Anipsitakis and Dionysiou (2003) and Anipsitakis and Dionysiou (2004), in which the rate of oxidation of PDS, PMS and $H_2O_2$ by multiple metal ions was investigated. From their observations, Co(II) and Ag(I) were found to be optimum homogeneous catalysts compared to the other metals for the activation of PMS and PDS, respectively (Anipsitakis and Dionysiou, 2003, 2004b). More recently, Ike et al. (2018) reviewed postulated techniques and mechanisms of PDS activation in silver catalysts, suggesting novel insights as well as discrepancies in the field (Ike et al., 2018a). Briefly, activation of PDS is presumed to occur as depicted in Eq. (79), although the association with the catalyst itself as an intermediary step has also been proposed as a plausible mechanism (Eq. 80) (House, 1962; Sharpe, 1992). Other authors have also suggested the generation of a radical ion pair, as shown in Eq. (81) (Anipsitakis and Dionysiou, 2004a; Gansäuer and Bluhm, 2000). Additionally, a more advanced degradation pathway has been proposed where PDS is oxidised in Ag(I), releasing not only Ag(II) but also Ag(III) ions that may subsequently react with $H_2O$ to generate $^{\bullet}OH$ radicals (Eqs. 82 and 83) (Xu et al., 2008).

$$Ag^{+} + S_2O_8{}^{2-} \longrightarrow Ag^{2+} + SO_4{}^{\bullet -} + SO_4{}^{2-} \tag{79}$$

$$Ag^{+} + S_2O_8{}^{2-} \longrightarrow AgS_2O_8{}^{-} \longrightarrow Ag^{2+} + SO_4{}^{\bullet -} + SO_4{}^{2-} \tag{80}$$

$$Ag^{+} + S_2O_8{}^{2-} \longrightarrow [Ag^{II}(SO_4{}^{\bullet})]^{+} + SO_4{}^{2-} \tag{81}$$

$$Ag^{2+} + H_2O \longrightarrow Ag^{+} + {}^{\bullet}OH + H^{+} \tag{82}$$

$$Ag^{3+} + 2\,H_2O \longrightarrow Ag^{+} + 2\,{}^{\bullet}OH + 2\,H^{+} \tag{83}$$

The review from Ike et al. (2018) also discusses the use of iron ions as catalysts, since it has been observed that Fe(0)/Fe(II)/Fe(III) have been more extensively investigated over the past years for this purpose, regardless of their slightly lower efficiency compared to silver (Guerra-Rodríguez et al., 2018; Ike et al., 2018a). The rationale behind this preference is due to the affordability of iron, its biocompatibility, lower toxicity and its capacity for the rapid and controllable activation of PDS in its various valence states (Duan et al., 2020; Liang et al., 2004a). In addition, PDS activated in iron catalysts has also been further proposed as an efficient method for water disinfection purposes (Wordofa et al., 2017). Fe(II) has been observed to rapidly activate PDS, as shown in Eq. (84), where generated $SO_4^{\bullet -}$ radicals may subsequently react with the target pollutant or with excess Fe(II) still present in the bulk (Eq. 85) (Liang et al., 2004a; Matzek and Carter, 2016; Neta et al., 1988; Xu and Li, 2010). Typically, at least a 1:1 PDS to iron ratio is needed for the degradation of contaminants (Eq. 69), although the optimal proportion may vary across treatments (Matzek and Carter, 2016). Since the degradation of the CECs is always desired over scavenging in Eq. (85), several methods have been developed to promote one reaction over the other. For instance, Fe(II) was gradually added to control its concentration in the bulk, incorporating a reducing agent, such as thiosulfate ($S_2O_3{}^{2-}$), or using organic chelators (Liang et al., 2004a,b). It should be noted that despite the ease of adding a chelating agent to the reaction, the selection of a suitable compound is crucial in terms of the overall environmental friendliness of the process. Previously used chelators such as ethylene-diamine-tetra-acetic acid (EDTA) and [S,S]-ethylene-diamine-disuccinic acid (EDDS) display low biodegradability, and therefore, alternatives such as citric acid ($C_6H_8O_7$) have been preferred (Matzek and Carter, 2016; Yan and Lo, 2013).

$$Fe^{2+} + S_2O_8{}^{2-} \longrightarrow Fe^{3+} + SO_4{}^{\bullet -} + SO_4{}^{2-} \tag{84}$$

$$Fe^{2+} + SO_4{}^{\bullet -} \longrightarrow Fe^{3+} + SO_4{}^{2-} \tag{85}$$

Despite the great degradation efficiencies attained, cobalt is a highly toxic metal with fatal consequences for both the environment and human health (Han et al., 2019; Leyssens et al., 2017). Therefore, its use as a homogeneous catalyst requires subsequent rigorous removal of

trace metals in the effluent of a wastewater treatment plant (Jawad et al., 2015). In this day and age, such associated environmental risks and operational costs have favoured its use in heterogeneous forms (Li et al., 2022), where further studies on stability, toxicity and regeneration are needed to determine their suitability for implementation (Dewil et al., 2017; Hu and Long, 2016; Li et al., 2022; Oh and Lim, 2019).

In terms of other heterogeneous catalysts to activate PDS, a wide variety of structures have also been investigated, such as nano zero-valent iron (nZVI) (Kang et al., 2018; Kim et al., 2018a; Matzek and Carter, 2016; Tan et al., 2018), metal-free carbon materials (e.g., biochar, activated carbon, graphene and carbon nanotubes) (Chen et al., 2018b; Duan et al., 2018; Xiao et al., 2018), and transition metal oxides (e.g., iron oxides, manganese oxides, cobalt oxides and copper oxides); the latter are both non-immobilised and immobilised on inorganic- or carbon-based supports (Duan et al., 2020; Matzek and Carter, 2016; Wang and Wang, 2018a; Xiao et al., 2018). These combinations have been proven to alter the physicochemical properties of the catalysts and induce new catalyst-specific functionalities. Nevertheless, some limitations have still not been overcome for further applications. For instance, during the activation process of Fe(0) in the nZVI setup, it is partially oxidised to Fe(III), which displays a poor ability as an activator in solution (Rastogi et al., 2009). Metal leaching, corrosion and aggregation phenomena are still issues when dealing with transition metal oxides, while carbon-based materials have poor catalytic stability, complex synthesis methods, regeneration requirements and high costs (Brienza and Katsoyiannis, 2017; Duan et al., 2020; Guerra-Rodríguez et al., 2018).

Finally, recent developments in photocatalysis have also taken place for SR-AOPs, involving photocatalysts based on iron, $TiO_2$, other metals and carbonaceous materials. The reader is referred to the comprehensive review from He et al. (2022) for more information on PDS activation mechanisms via these heterogeneous photocatalysts (He et al., 2022). One of the advantages of developing novel photocatalysts lies in coupling pollutant degradation with renewable energy production, as in the observed cogeneration of $H_2$ via solar light responsive Eosin-$TiO_2$ photocatalysis treatment (Khan et al., 2020).

### 2.2.6 Electrochemical activation

When applied to the generation of $SO_4^{\bullet -}$ radicals from PDS, electrochemical treatment has proven to effectively degrade recalcitrant organic pollutants that were found to be non-degradable via PDS alone (Antonin et al., 2015; Carter and Farrell, 2008; Matzek and Carter, 2016). For this purpose, primarily boron-doped diamond (BDD) electrodes have been investigated (Tröster et al., 2002). However, the underlying mechanisms are not yet fully discerned. Some authors refute the intervention of $SO_4^{\bullet -}$ and suggest that PDS reacts with BDD-adsorbed $^{\bullet}OH$ radicals to produce other reactive species, such as singlet oxygen ($^1O_2$) and superoxide ($O_2^{\bullet -}$) (Eqs. 86 and 87) (Bu et al., 2017; Zhang et al., 2014; Zhou et al., 2015). Others propose a non-radical oxidation where PDS is activated on the BDD surface, creating a highly reactive transition state structure that can degrade organic contaminants (Eqs. 88 and 89). Such proposed mechanisms are also claimed to enhance the production of $^{\bullet}OH$ via water dissociation, which would also contribute to the degradation of pollutants (Farhat et al., 2015; Song et al., 2018).

$$2\,^{\bullet}\mathrm{OH} + \mathrm{S_2O_8}^{2-} \xrightarrow{BDD} 2\,\mathrm{SO_4}^{2-} + {}^1\mathrm{O_2} + 2\,\mathrm{H}^+ \tag{86}$$

$$4\,^{\bullet}\mathrm{OH} + \mathrm{S_2O_8}^{2-} \xrightarrow{BDD} 2\,\mathrm{SO_4}^{2-} + 2\,\mathrm{O_2}^{\bullet-} + 4\,\mathrm{H}^+ \tag{87}$$

$$\mathrm{BDD} + \mathrm{PDS} \longrightarrow \mathrm{BDD(PDS^{\bullet})} \tag{88}$$

$$\textit{Pollutant} + \mathrm{BDD(PDS^{\bullet})} \longrightarrow \textit{Degradation products} \tag{89}$$

Electrochemical processes stand out as a promising method for generating $SO_4^{\bullet-}$ radicals from $SO_4^{2-}$ ions that may already be present in the wastewater. Consequently, the need for additional reactants and the generation of secondary waste streams are avoided. This type of treatment is, however, limited in terms of operating conditions, as boron-doped diamond (BDD) electrodes have been primarily used to generate $SO_4^{\bullet-}$ in situ (Farhat et al., 2015; Radjenovic and Petrovic, 2016, 2017). Alternative materials such as blue-$TiO_2$ and self-doped $TiO_2$ nanotube array electrodes have also been recently reported as effective generators of $^{\bullet}OH$ and $SO_4^{\bullet-}$, although the body of literature in this branch is not as extensive (Cai et al., 2019; Divyapriya and Nidheesh, 2021; Kim et al., 2018b). When using BDD electrodes, the formation of PDS has also been observed, which is postulated to occur due to the recombination of the $SO_4^{\bullet-}$ radicals produced during either direct electron oxidation at the anode or during the reaction of other sulfate-containing compounds with the BDD-adsorbed $^{\bullet}OH$ radicals (Eqs. 90 - 93) (Cañizares et al., 2009b; Serrano et al., 2002; Song et al., 2018). Either of the indirect generation routes has been observed more often in experimental studies (Divyapriya and Nidheesh, 2021). Several studies have also reported that the $SO_4^{\bullet-}$ radicals involved in the reaction chain (Eqs. 90 - 93) are not only intermediates of PDS production but also actively participate in the degradation of organic pollutants, as occurs in the other activation methods for SR-AOPs (Chen et al., 2018a; Farhat et al., 2015, 2017; Radjenovic and Petrovic, 2017). In this way, it is proven that it is not necessary to add a precursor such as PDS to generate oxidative radicals, as long as the wastewater matrix contains $SO_4^{2-}$ ions.

$$\mathrm{SO_4}^{2-} \longrightarrow \mathrm{SO_4}^{\bullet-} + e^- \tag{90}$$

$$\mathrm{HSO_4}^- + {}^{\bullet}\mathrm{OH} \longrightarrow \mathrm{SO_4}^{\bullet-} + \mathrm{H_2O} \tag{91}$$

$$\mathrm{H_2SO_4} + {}^{\bullet}\mathrm{OH} \longrightarrow \mathrm{SO_4}^{\bullet-} + \mathrm{H_3O}^+ \tag{92}$$

$$\mathrm{SO_4}^{\bullet-} + \mathrm{SO_4}^{\bullet-} \longrightarrow \mathrm{S_2O_8}^{2-} \tag{93}$$

## 2.3 Chlorine radicals

Chlorine radicals ($Cl^{\bullet}$) (Fig. 6) and their derivatives (CDRs), which present redox potentials up to +2.60 V (Wardman, 1989), have also been used for the degradation of complex organic

compounds. Furthermore, it has been observed that $Cl^{\bullet}$ is more selective towards the decomposition of aromatics, aniline and phenolic compounds than $^{\bullet}OH$ (Pan et al., 2017). Regarding scavenging compounds, an overview of their reaction rates can be found in Appendix D.3 of the Supplementary Material. Several studies have reported that single electron transfer, Cl-adduct formation and hydrogen abstraction are the main mechanisms involved in the removal of pollutants when these radicals are present (Cai et al., 2020; Minakata et al., 2017). For their generation, activation via UV or visible light, other oxidation agents such as peroxymonosulfate (PMS) and electrochemical treatment are presented in the following sections.

**Figure 6:** Structure of chlorine radical, $Cl^{\bullet}$ (● unpaired electron).

### 2.3.1 Activation via UV irradiation

The formation of chlorine species using UV irradiation has been of interest for multiple researchers in recent years (Belghit et al., 2020; Du et al., 2020; Guo et al., 2018; Huang et al., 2017; Nikravesh et al., 2020; Pan et al., 2017), as it is also a well-known inactivation method for water-borne pathogens (Raviv and Antignus, 2004). Hypochlorous acid (HClO) and hypochlorite ions ($ClO^-$) can be activated with UV to generate $^{\bullet}OH$ and $Cl^{\bullet}$ radicals (Cai et al., 2020). Additionally, secondary radicals such as $Cl_2^{\bullet -}$, $ClO^{\bullet}$ and $O^{\bullet -}$ are generated in these processes (Nikravesh et al., 2020). Reactions (94) - (101) illustrate the generation of various types of chlorine-derived radicals (CDRs) under UV irradiation (Belghit et al., 2020).

$$HClO \longleftrightarrow ClO^- + H^+ \tag{94}$$

$$HClO \xrightarrow{hv} {}^{\bullet}OH + Cl^{\bullet} \tag{95}$$

$$ClO^- \xrightarrow{hv} O^{\bullet -} + Cl^{\bullet} \tag{96}$$

$$Cl^{\bullet} + Cl^- \longleftrightarrow Cl_2^{\bullet -} \tag{97}$$

$$HClO + {}^{\bullet}OH \longrightarrow H_2O + ClO^{\bullet} \tag{98}$$

$$ClO^- + {}^{\bullet}OH \longrightarrow OH^- + ClO^{\bullet} \tag{99}$$

$$HClO + Cl^{\bullet} \longrightarrow HCl + ClO^{\bullet} \tag{100}$$

$$ClO^- + Cl^\bullet \longrightarrow Cl^- + ClO^\bullet \tag{101}$$

When using HClO and $ClO^-$ as precursors, Zhang et al. (2020) indicated that the presence of $Br^-$ ions could lead to the formation of HBrO and $BrO^-$ (Eqs. 102 and 103), which by direct photolysis generate $^\bullet OH$, $O^{\bullet -}$ and $Br^\bullet$ radicals (Eqs. 104 and 105). Further reactions between these species may form free bromine as well (Eq. 106) (Zhang et al., 2020a). In addition, the presence of transitional metals such as copper and iron may also lead to additional radicals, as shown in reactions (107) - (111) (Nikravesh et al., 2020). Similarly, a UV/HClO system can also favour the generation of carbonate radicals ($CO_3^{\bullet -}$) and hence facilitate the degradation of compounds such as amine-containing contaminants, which can readily react with $CO_3^{\bullet -}$ (Eqs. 112 and 113).

$$HClO + Br^- \longrightarrow HBrO + Cl^- \tag{102}$$

$$ClO^- + Br^- \longrightarrow BrO^- + Cl^- \tag{103}$$

$$HBrO \xrightarrow{hv} {}^\bullet OH + Br^\bullet \tag{104}$$

$$BrO^- \xrightarrow{hv} O^{\bullet -} + Br^\bullet \tag{105}$$

$$HBrO + Br^- + H^+ \longleftrightarrow Br_2 + H_2O \tag{106}$$

$$Fe^{2+} + HClO \longrightarrow Fe^{3+} + {}^\bullet OH + Cl^- \tag{107}$$

$$Fe^{2+} + HClO \longrightarrow Fe^{3+} + OH^- + Cl^\bullet \tag{108}$$

$$Cu^{2+} + HClO \longrightarrow Cu^+ + H^+ + ClO^\bullet \tag{109}$$

$$Cu^+ + HClO \longrightarrow Cu^{2+} + {}^\bullet OH + Cl^- \tag{110}$$

$$Cu^+ + HClO \longrightarrow Cu^{2+} + OH^- + Cl^\bullet \tag{111}$$

$$Cl^\bullet + HCO_3{}^- \longrightarrow H^+ + Cl^- + CO_3{}^{\bullet -} \tag{112}$$

$$Cl_2^{\bullet -} + HCO_3^- \longrightarrow H^+ + 2\,Cl^- + CO_3^{\bullet -} \tag{113}$$

In addition to the traditional types of chlorine oxidation agents, other precursors have been explored. For instance, Chuang et al. (2017) indicated that chloramines could be efficiently used for the degradation of 1,4-dioxane ($C_4H_8O_2$), benzoate ($C_7H_6O_2$) and carbamazepine ($C_{15}H_{12}N_2O$) under UV irradiation, especially at pH 7–8 (Chuang et al., 2017).

Recently, there has been a trend in the application of visible light for the treatment of polluted wastewater via AOPs (Pinedo Escobar et al., 2020; Yun et al., 2017). One of the main reasons is the advantage of benefiting from solar irradiation as a clean and renewable source of energy, which can satisfy economic and environmental requirements. The production of $^{\bullet}OH$ and $ClO^{\bullet}$ was reported for the first time under visible light irradiation by Cheng et al. (2020) using graphitic carbon nitride (g-$C_3N_4$) (Cheng et al., 2020). Since g-$C_3N_4$ is a low-cost non-metallic photocatalyst (Yin et al., 2015), visible light activation of chlorine can be an advantageous option for the treatment of effluents from various origins. Integration of UV/chlorine systems with other treatment technologies was explored by Du et al. (2020), where its combination with real reverse osmosis concentrates presenting a high chloride and alkaline content could considerably enhance the degradation of organic compounds with a high molecular weight (Du et al., 2020).

### 2.3.2 Activation via peroxymonosulfate (PMS)

The application of peroxymonosulfate (PMS) has also enabled the generation of chlorine-derived species in recent studies. The reaction of PMS with $Cl^-$ ions results in the formation of HClO (Eq. 114), which under acidic conditions can be transformed to $Cl_2$ via Eq. (115) (Yuan et al., 2011). PMS can also form $Cl^{\bullet}$ radicals and HClO in the presence of a high concentration of $Cl^-$ (Eq. 116) (Yuan et al., 2011), while the decomposition of HClO is responsible for singlet oxygen generation (Eq. 117) (Khan and Kasha, 1994). The reaction of PMS with HClO may also result in the formation of singlet oxygen (Eq. 118). In a recent study, Wang et al. (2020) reported the treatment of the membrane filtration concentrate of coking effluents where all these oxidative species were involved (Wang and Wang, 2020).

$$Cl^- + HSO_5^- \longrightarrow SO_4^{2-} + HClO \tag{114}$$

$$Cl^- + HClO + H^+ \longrightarrow Cl_2 + H_2O \tag{115}$$

$$2\,Cl^- + HSO_5^- \longrightarrow SO_4^{2-} + HClO + Cl^{\bullet} \tag{116}$$

$$2\,HClO \longrightarrow {}^1O_2 + 2\,H^+ + 2\,Cl^- \tag{117}$$

$$HSO_5^- + HClO \longrightarrow {}^1O_2 + Cl^- + SO_4^{2-} + 2\,H^+ \tag{118}$$

### 2.3.3 Electrochemical activation

The wide range of concentrations in which $Cl^-$ has been found in various effluents is a key incentive for the in situ CDR formation that electrochemical treatment entails (Eqs. 119 - 121) (Cho et al., 2014; Garcia-Segura et al., 2018; Wang et al., 2020; Xiao et al., 2009). To this end, active anode materials are preferred over non-active materials, as the latter lead to undesired non-oxidising chlorine species (Garcia-Segura et al., 2015). In addition, faster degradation rates have been observed under acidic pH conditions (Garcia-Segura et al., 2018). Nonetheless, the higher the Cl-content of the influent wastewater is, the higher the risk of toxic organo-chlorinated transformation products being formed (Radjenovic and Sedlak, 2015).

$$Cl^- \longrightarrow Cl^\bullet + e^- \tag{119}$$

$$2\,Cl^- \longrightarrow Cl_{2(aq)} + 2\,e^- \tag{120}$$

$$Cl_{2(aq)} + H_2O \longrightarrow HClO + Cl^- + H^+ \tag{121}$$

There are also studies focused on the combination of eAOPs with other chlorine activation methods (Zhang et al., 2020b). Xiao et al. (2009) combined an electrochemical process with UV using non-photoactive dimensionally stable anodes (DSAs) in the presence of chlorides for ammonia ($NH_3$) degradation (Xiao et al., 2009). Salmerón et al. (2020) applied an electrochemical process for the treatment of wastewater with high salinity assisted by solar energy (Salmerón et al., 2020). Recent studies have also indicated the possibility of electricity co-generation during the in situ formation of CDRs. As an example, Zhang et al. (2018) illustrated the possibility of simultaneous TOC and TN removal as well as electricity co-generation from nitrogen-containing wastewater by the catalytic reactions of $^\bullet OH$ and $Cl^\bullet$ radicals (Zhang et al., 2018). They showed that it was possible to produce electricity by employing a hybrid photoanode comprised of $WO_3$ electrodes and silicon photovoltaic cells (Zhang et al., 2018). Simultaneous degradation of organic pollutants and electricity co-generation using such a hybrid photoanode has also been further investigated for the oxidation of phenol ($C_6H_6O$) and ammonium-N ($NH_4{}^+$-N) (Ji et al., 2017). Photo-generated holes at $WO_3$ are responsible for the conversion of $H_2O$ to $^\bullet OH$ and $Cl^-$ to $Cl^\bullet$. Here, $Cl^\bullet$ radicals played the most important role in the oxidation of $NH_4{}^+$-N (Ji et al., 2017).

## 2.4 Iodine radicals

Periodate ($IO_4{}^-$) is used as a precursor of iodine-derived radicals such as $IO_3{}^\bullet$ and $IO_4{}^\bullet$ (Fig. 7), with $IO_3{}^\bullet$ being more effective for the decomposition of organic compounds (Lee et al., 2016b). A summary of the recent findings on the application of $IO_4{}^-$ activation systems is depicted in Table B.1. As a key takeaway, it can be argued that iodine radicals can selectively decompose organic matter even in the presence of other compounds, such as chlorine nitrate ($ClNO_3$). These systems can be effectively used for the treatment of water matrices with humic acid ($C_{187}H_{186}O_{89}N_9S$) and minerals. Finally, considering that the existence of molecular oxygen can play a key role in promoting the formation of oxidising singlet oxygen (Bokare and Choi,

2015), additional air purges can be added to enhance process efficiency (Du et al., 2019). Under such conditions, complete reduction of $IO_4^-$ to $IO_3^-$ can potentially prevent the formation of toxic iodinated byproducts.

**(a)** Iodate radical, $IO_3^\bullet$ **(b)** Periodate radical, $IO_4^\bullet$

**Figure 7:** Structures of (a) iodate radical and (b) periodate radical (• unpaired electron).

### 2.4.1 Activation via UV irradiation

The activation of $IO_4^-$ via photolysis allows for the generation of distinct types of radicals as well as non-radical species, including $H_2O_2$ and $O_3$ (Kläning and Sehested, 1978). In these treatments, it is believed that $IO_3^\bullet$ and $IO_4^\bullet$ play the most important role in the degradation of organic compounds (Bendjama et al., 2018). The reactions involved in the photolysis of $IO_4^-$, including initiation (Eqs. 122 and 123), propagation (Eqs. 124 - 129) and termination (Eqs. 130 - 135), are illustrated below. Alternatively, visible light can also be used instead of UV irradiation to generate iodine radicals. As an example, Yun et al. (2017) discussed the mechanism of visible light activation for the degradation of rhodamine B dye (Yun et al., 2017). They reported that electrons were transferred between the excited dye and $IO_4^-$, resulting in the generation of dye radicals further oxidised with existing dissolved oxygen, and that generated $IO_4^-$ ions were reduced to $IO_3^\bullet$, leading to the effective degradation of organic compounds (Fig. B.1). When using $IO_3^-$ as a precursor, flash photolysis also forms iodine radicals, especially under neutral pH conditions (Kläning et al., 1981).

$$IO_4^- + hv \longrightarrow IO_3^\bullet + O^{\bullet -} \tag{122}$$

$$IO_4^- + hv \longrightarrow IO_3^\bullet + O(^3P) \tag{123}$$

$$O^{\bullet -} + H^+ \longrightarrow {}^\bullet OH \tag{124}$$

$$O(^3P) + O_2 \longrightarrow O_3 \tag{125}$$

$$IO_4^- + IO_3^\bullet \longrightarrow IO_4^\bullet + IO_3^- \tag{126}$$

$$IO_4^- + {}^\bullet OH \longrightarrow IO_4^\bullet + OH^- \tag{127}$$

$$IO_3^- + {}^\bullet OH \longrightarrow HIO_4^- \tag{128}$$

$$IO_3^- + {}^\bullet OH \longrightarrow IO_3^- + OH^- \tag{129}$$

$${}^\bullet OH + {}^\bullet OH \longrightarrow H_2O_2 \tag{130}$$

$$O(^3P) + O(^3P) \longrightarrow O_2 \tag{131}$$

$$IO_3^\bullet + IO_3^\bullet \longrightarrow I_2O_6 \tag{132}$$

$$IO_4^\bullet + IO_4^\bullet \longrightarrow I_2O_8 \tag{133}$$

$$I_2O_6 + H_2O \longrightarrow IO_4^- + IO_3^- + 2\,H^+ \tag{134}$$

$$I_2O_8 + H_2O \longrightarrow IO_4^- + IO_3^- + 2\,H^+ + O_2 \tag{135}$$

Given that high concentrations of iodate ($IO_3^-$) can be found in wastewater effluents originating from sources such as the food industry and analytical laboratories (Bürgi et al., 2001), the activation of such ions already present in wastewater is an attractive option to diminish the need for additional oxidation agents. Haddad et al. (2019) tested several initial $IO_3^-$ concentrations for the photodegradation of light green SF yellowish (LGSFY) (Haddad et al., 2019). The formation of $IO_2^\bullet$ and $IO^\bullet$ radicals promoted the degradation of the dye, in contrast to UV photolysis alone (Haddad et al., 2019). Given the lack of additional studies, further research with real $IO_3^-$-containing effluents is needed to validate the in situ radical generation.

### 2.4.2 Activation via cavitation

The degradation efficiencies attained through the activation of $IO_4^-$ under cavitation have been observed to not be influenced by the presence of other ions, such as $Ca^{2+}$ and $Cl^-$ (Seid-Mohamadi et al., 2015). However, this method is relatively slower than UV irradiation. For instance, Lee et al. (2016) reported that 120 min were needed to reach 95.7% degradation of perfluorooctanoic acid (PFOA) even at considerable amounts of precursor $IO_4^-$ (e.g., 45 mM) when ultrasound irradiation was used (Lee et al., 2016b). This paper also emphasised the appropriateness of acidic pH to promote $IO_4^-$ activation. They argued that at acidic and basic pH values, $IO_4^-$ and $H_2I_2O_{10}^{4-}$ are the dominant species, respectively. Thus, under acidic conditions, the activation of $IO_4^-$ can result in the formation of $IO_3^\bullet$, which is more active than the I[VI($IO_3^\bullet$)] radical for the decomposition of organic compounds. Therefore, it can

be stated that such an activation method for $IO_4^-$ is appropriate for streams with an acidic nature, such as those from the bleaching stages of pulp and paper mill effluents (Ribeiro et al., 2020). Nonetheless, recent studies have also indicated that the presence of oxygen can inhibit the performance of cavitation activated $IO_4^-$ systems (Hamdaoui and Merouani, 2017).

### 2.4.3 Activation via microwaves

Mohammadi et al. (2016) reported that microwave-assisted activation of $IO_4^-$ to degrade phenol ($C_6H_5OH$) was optimal at alkaline pH, given that phenolic compounds absorb more microwave radiation at an elevated pH (Mohammadi et al., 2016). Nonetheless, further research is needed to elucidate the mechanisms behind microwave activation of $IO_4^-$.

### 2.4.4 Freeze activation

Choi et al. (2018) indicated that the degradation rate of furfuryl alcohol (FFA) was considerably enhanced with increasing $IO_4^-$ concentration, decreasing pH and decreasing temperature below the freezing point (Choi et al., 2018). This method relies on the freeze concentration effect (FCE), where dissolved gases, ions and solutes accumulate and can accelerate specific chemical reactions as ice crystals are formed and separated during the freezing process. The main reactions involved are described in equations (136) - (139) (Grannas et al., 2007; Heger et al., 2005, 2006; Kong et al., 2014; Takenaka and Bandow, 2007).

$$IO_4^- + 2\,H^+ + 2\,e^- \longrightarrow IO_3^- + H_2O \tag{136}$$

$$H_5IO_6 + H^+ + 2\,e^- \longrightarrow IO_3^- + 3\,H_2O \tag{137}$$

$$IO_3^- + 6\,H^+ + 6\,e^- \longrightarrow I^- + 3\,H_2O \tag{138}$$

$$IO_3^- + 6\,H^+ + 5\,e^- \longrightarrow \frac{1}{2}\,I_2 + 3\,H_2O \tag{139}$$

### 2.4.5 Activation via catalysis

Recent studies have focused on improving $TiO_2$-based catalytic treatments with the addition of $IO_4^-$. Gözmen et al. (2009) reached over 65% mineralisation of several dyes after 3 h of illumination, and the enhanced performance was attributed to facile interfacial electron transfer from separated charges in the molecular structure of $TiO_2$ nanoparticles, which promoted the generation of $IO_3^\bullet$ radicals (Gözmen et al., 2009). Manganese-based materials have also been reported as efficient catalysts for the activation of $IO_4^-$. Du et al. (2019) explored the main mechanisms involved in this catalytic activation route (Eqs. 140 - 145) (Du et al., 2019). Lee et al. (2014) doped nZVI with secondary metals such as Cu or Ni for the efficient activation of $IO_4^-$

to degrade selected organic compounds at neutral pH (Lee et al., 2014). They indicated that the bimetallic catalysis of nZVI was effective for the degradation of organic compounds, including benzoic acid ($C_7H_6O_2$), carbamazepine ($C_{15}H_{12}N_2O$), and 2,4,6-trichlorophenol ($C_6H_2Cl_3OH$). Other works have also combined physical methods with a nZVI/$IO_4^-$ system. For instance, Seid-Mohammadi et al. (2019) applied ultrasound coupled with nZVI for the activation of $IO_4^-$ to degrade phenol ($C_6H_5OH$) (Seid-Mohammadi et al., 2019). Reduction of $H^+$ into $H^\bullet$ in the presence of nZVI assisted by ultrasonic waves resulted in the formation of $^\bullet OH$, $IO_3^\bullet$ and $IO_4^\bullet$ radicals. Finally, carbonaceous materials, such as activated carbon and biochar, can also be considered potential catalysts for $IO_4^-$ activation (Ashoori et al., 2019; Mahapatra et al., 2012; Palansooriya et al., 2020; Premarathna et al., 2019; Tadda et al., 2016; Vithanage et al., 2017). Li et al. (2017) reported that the use of granular activated carbon (GAC) contributed to the formation of triiodide ($I_3^-$) and pentaiodide ($I_5^-$), which induced a positive charge on the catalyst surface to promote the interaction with $IO_4^-$ and, as a result, increased the generation of $IO_3^\bullet$ radicals (Li et al., 2017a).

$$Mn^{2+} + 2\,H_2O \longleftrightarrow Mn{-}(OH)_2 + 2\,H^+ \tag{140}$$

$$Mn^{2+} + 2\,IO_4^- + O_2 + 3\,H_2O \longrightarrow Mn{-}O(OH)_2 + 2\,IO_3^- + 4\,H^+ + 2\,O_2^{\bullet-} \tag{141}$$

$$Mn{-}O(OH)_2 \longrightarrow MnO_2 + H_2O \tag{142}$$

$$IO_4^- + 2\,O_2^{\bullet-} + H_2O \longrightarrow IO_3^- + 2\,{}^1O_2 + 2\,OH^- \tag{143}$$

$$2\,O_2^{\bullet-} + 2\,H_2O \longrightarrow {}^1O_2 + H_2O_2 + 2\,OH^- \tag{144}$$

$$Mn{-}O(OH)_2 + IO_4^- \longrightarrow Mn{-}(OH)_2 + IO_3^- + {}^1O_2 \tag{145}$$

### 2.5 Alternative radicals

Information about other oxidative species that have been less frequently investigated, including reactive nitrogen species (RNS), such as $NO^\bullet$ and $NO_2^\bullet$ radicals, as well as carbonate radicals ($CO_3^{\bullet-}$), can be found in Appendix C of the Supplementary Material.

## 3 Environmental and economic review

In addition to its technical feasibility, both the environmental and economic implications of a technology are key intertwined drivers for its further commercialization. Therefore, previously

reported environmental and economic analyses of different AOPs are discussed in this section in terms of the carbon footprint and operational costs per reference unit of treated wastewater, respectively. As it is outside of the scope of this review, for additional information on the technical aspects and industrial implementation of different $^{\bullet}OH$ radical-based AOPs, the reader is referred to previous works with this specific focus (Barrera-Díaz et al., 2014; Boczkaj and Fernandes, 2017; Brillas et al., 2009; Cuerda-Correa et al., 2020; Peleyeju and Arotiba, 2018; Wang and Chen, 2020; Wang and Zhuan, 2020). Similarly, other publications already offer a comparison in terms of the technical performance of $SO_4^{\bullet-}$ radical-based AOPs (Boczkaj and Fernandes, 2017; Devi et al., 2016; Giannakis et al., 2021; Guerra-Rodríguez et al., 2018; Seibert et al., 2020).

## 3.1 Hydroxyl radicals

Given their prevalent interest in the field, $^{\bullet}OH$ radical-based AOPs represent the largest body of research regarding environmental and economic assessments. Specific literature details are shown in Tables 1 and 2, of which the main quantitative results are depicted in Figures 8 and 9. These visualisations are intended to provide an understanding of the variability in results across the literature and not as a direct comparison among treatments, given that they were conducted under a diverse set of experimental conditions (i.e., target pollutant, oxidant/chemical load, reactor volume, operation time, water matrix, etc.).

### 3.1.1 Environmental aspects

Ozonation is typically found as a baseline for environmental comparison, with an environmental impact ranging between 0.2 and 0.3 kg $CO_2$-eq/m$^3$ for several types of wastewater treated (Arzate et al., 2019; Muñoz et al., 2009; Prieto-Rodríguez et al., 2013; Zepon Tarpani and Azapagic, 2018). Similar environmental impacts have been reported for micropollutant degradation via $H_2O_2/O_3$ (i.e., 0.29 kg $CO_2$-eq/m$^3$) (Muñoz et al., 2009). In terms of environmental assessment, catalytic ozonation has not been widely studied. Rough estimates on surface water disinfection purposes have located its impact between 0.11 and 0.13 kg $CO_2$-eq/m$^3$, depending on the use of hollow fibres or catalytic ceramic membranes, respectively (Wang et al., 2019). Regarding photocatalytic ozonation, despite the lack of reported environmental impacts, a lower energy requirement has been observed compared to ozonation and photocatalysis alone (Mecha et al., 2017). Depending on the photocatalyst used, such reduction can be ca. 16-72% and 46-82% lower, respectively (Mecha et al., 2017).

Regarding Fenton processes, both iron and $H_2O_2$ are abundant and safe compounds that do not represent a major hazard to the environment if properly dosed and stored. In addition, the overall operating conditions of the Fenton reaction are relatively simple. Nonetheless, the acidic conditions that need to be attained, followed by subsequent neutralisation and sludge treatment, represent a main drawback for scale-up, both in terms of cost and environmental impact optimisation (Morone et al., 2019; Vasquez-Medrano et al., 2018). Therefore, there are few environmental or cost assessments available regarding solely the Fenton reaction (Pesqueira et al., 2020). As a guideline, it has been reported that to remove 1 g COD per litre of pharmaceutical wastewater in a conventional homogeneous Fenton system, approximately 150 kg $CO_2$-eq/m$^3$ is emitted, of which ca. 80% of the impact is due to sludge and catalyst disposal

(Rodríguez et al., 2016). Under similar conditions, it is estimated that the impact of a heterogeneous Fenton system would be 5 times lower (Rodríguez et al., 2016).

As a key advantage over the classical Fenton reaction, in the photo-Fenton reaction, the iron sludge waste is significantly reduced. The environmental impact of such a setup applied to herbicide-containing wastewater is estimated to be ca. 1.3 kg $CO_2$-eq/$m^3$ to attain over 80% TOC removal, where the major impact contribution belongs to the consumption of $H_2O_2$ and electricity of the UV lamp (Farré et al., 2007). Under similar conditions, the solar photo-Fenton system is estimated to reduce the impact factor down to 1.1 kg $CO_2$-eq/$m^3$ (Farré et al., 2007). Lower impact values in solar photo-Fenton systems applied to other types of wastewater have also been reported in the range of 0.25 to 0.86 kg $CO_2$-eq/$m^3$ (Arzate et al., 2019; Muñoz et al., 2005; Prieto-Rodríguez et al., 2013; Zepon Tarpani and Azapagic, 2018). However, when compared to simpler AOPs such as ozonation, the contribution to climate change of the solar photo-Fenton process as a whole, including the impact derived from its infrastructure, is 2 to 4 times higher. This is related to the fact that solar photo-Fenton operation is limited to daylight hours and, therefore, requires the construction of a storage infrastructure for downtime hours (Arzate et al., 2019). In addition to the energy source used in the photo-Fenton system, attention should be given to the manufacturing process involved. There is a growing interest in the use of magnetic nanoparticles for wastewater treatment, especially due to their easy, fast and cost-effective recovery from the reaction medium, which allows for further reuse (Wang et al., 2016b). Life cycle assessments of different nanoparticle synthesis routes have been reported, including magnetite nanoparticles coated with ZnO or $TiO_2$, which are commonly applied as photocatalysts (Lee et al., 2016a). Their normalised environmental impact is estimated to be up to 7 times greater than that of other standard Fenton catalyst nanoparticles, given that the photocatalyst synthesis process is much more complex and involves a higher consumption of chemicals and energy (Feijoo et al., 2020).

Regarding electro-Fenton, due to its nature, the associated energy consumption is substantial, being the main contributor to the overall carbon footprint. It also needs to be run at low pH values, meaning that chemicals to acidify and neutralise the wastewater before and after electrochemical treatment are still needed (Brillas and Martínez-Huitle, 2015). In relative terms, solar photo-Fenton and solar photoelectro-Fenton are more environmentally friendly than electro-Fenton by approximately one order of magnitude (Pesqueira et al., 2020). Additionally, an environmental assessment of the degradation of $\alpha$-methylphenylglycine has shown a significantly lower environmental impact when applying solar photo-Fenton (i.e., 4 to 6.8 kg $CO_2$-eq/$m^3$) compared to solar photoelectro-Fenton (i.e., 28 to 60 kg $CO_2$-eq/$m^3$) under the same conditions (Serra et al., 2011).

Life cycle assessments of other typologies of UV-based advanced oxidation processes have been reported for the degradation of endocrine disruptors such as 17$\alpha$-ethynylestradiol (EE2) in wastewater. Their estimates of the environmental impact showed that the addition of $H_2O_2$ to UV treatment could reduce the total environmental impact of conventional UV photolysis alone by approximately 88% (Foteinis et al., 2018). Nonetheless, UV/$H_2O_2$ is significantly more energy-intensive than other methods, such as oxidation with $H_2O_2/O_3$. In fact, they are approximately 5 to 20 times more energy-consuming, depending on the process conditions (Katsoyiannis et al., 2011). Treatment with UV/$O_3$ is estimated to be even more energy intensive than UV/$H_2O_2$, ca. 6 times greater. Therefore, the higher the energy requirements are, the higher the potential impact (Pesqueira et al., 2020). When comparing photocatalytic oxidation with simple photolysis, a reduction in environmental factors up to 97% can be achieved (Foteinis

et al., 2018). In absolute terms, it has been estimated that to remove 1 g COD per litre of olive mill wastewater, 5,200 kg $CO_2$-eq/$m^3$ of treated wastewater is released during operation, which is strongly related to the energy consumption of the process and the use of non-environmentally friendly materials such as high-pressure mercury UV lamps (Chatzisymeon et al., 2013). In other studies concerning kraft pulp mill wastewater, it has also been reported that the carbon footprint and energy requirements are ca. 2.4 times greater than those of a conventional photo-Fenton process. Since in both cases the consumption of energy is the main contributor to the environmental indicators, substituting the use of UV lamps with solar energy has been proven to reduce most of the impact categories by a factor of 90-95% (Muñoz et al., 2005). In such scenarios, solar photocatalytic oxidation has a global warming potential approximately 37% lower than that of the solar photo-Fenton process (Muñoz et al., 2005).

Finally, electrochemical oxidation is considered one of the most environmentally friendly $^{\bullet}$OH based AOPs, as they have been reported to have an associated carbon footprint 30 times lower than that of the photocatalytic oxidation of olive mill wastewater via UV/$TiO_2$ under similar conditions (Chatzisymeon et al., 2013).

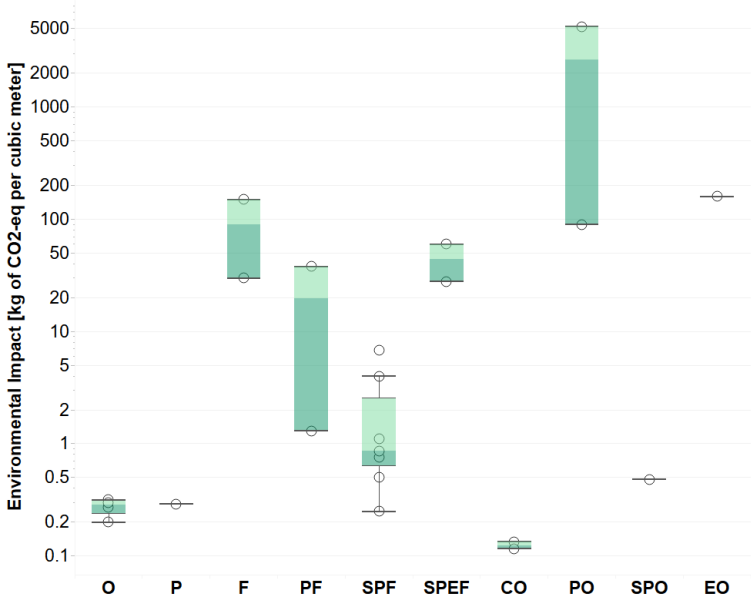


**Figure 8:** Reported environmental impacts in kg $CO_2$-eq per cubic meter of wastewater for different $^{\bullet}$OH radical-based AOPs (*O:* Ozonation, *P:* Peroxone, *F:* Fenton, *PF:* Photo-Fenton, *SPF:* Solar photo-Fenton, *SPEF:* Solar photoelectro-Fenton, *CO:* Catalytic ozonation, *PO:* Photocatalytic oxidation, *SPO:* Solar photocatalytic oxidation, *EO:* Electrochemical oxidation).

**Table 1:** Overview of reported environmental assessments for $^{\bullet}$OH-based AOPs.[1]

| Treatment | Water Matrix | Pollution Load | Efficiency | Time | Calculation Basis | Environmental Impact | Ref. |
|---|---|---|---|---|---|---|---|
| $O_3$ | Effluent from MWTP | 0.04-0.08 mg/L of 66 detected pollutants | 98% | 60 min | 1 $m^3$ of secondary effluent | 0.2-0.3 kg $CO_2$-eq | (Arzate et al., 2019; Prieto-Rodríguez et al., 2013) |
| | Effluent from WWTP | $1.1{\cdot}10^{-6}$-$1.34{\cdot}10^{-2}$ mg/L of 53 detected pollutants | ∼90% | 30 min | 1 $m^3$ of effluent | 0.27 kg $CO_2$-eq | (Muñoz et al., 2009) |
| | | $9{\cdot}10^{-6}$-$1.99{\cdot}10^{-3}$ mg/L of 9 detected PPCPs | 65-99% | - | 1000 $m^3$ of reclaimed water | 316 kg $CO_2$-eq | (Arzate et al., 2019; Zepon Tarpani and Azapagic, 2018) |
| $H_2O_2/O_3$ | Effluent from WWTP | $1.1{\cdot}10^{-6}$-$1.34{\cdot}10^{-2}$ mg/L of 53 detected pollutants | ∼90% | 30 min | 1 $m^3$ of effluent | 0.29 kg $CO_2$-eq | (Muñoz et al., 2009) |
| $UV/H_2O_2$ | Effluent from MWTP | 0.2 mg/L of 17$\alpha$-EE2 | 90% | 10 min | 1 $\mu$g 17$\alpha$-EE2 removal per litre of treated wastewater | 13.8 $\mu$Pt | (Foteinis et al., 2018; Frontistis et al., 2011) |
| Fenton | Pharmaceutical wastewater | 8,000 ± 2,000 mg/L COD | 84-89% | 60 min | 1 g/L COD removal (homogeneous Fenton) | 0.15 kg $CO_2$-eq | (Rodríguez et al., 2016) |
| | | | 84-88% | 60 min | 1 g/L COD removal (heterogeneous Fenton) | 0.03 kg $CO_2$-eq | (Rodríguez et al., 2016) |
| Photo-Fenton | Herbicide synthetic wastewater | 50 ± 2 mg/L TOC | 83% | 510 min | 80% TOC removal in 1.25 L wastewater | $1.62{\cdot}10^{-3}$ kg $CO_2$-eq | (Farré et al., 2007) |
| | Kraft pulp mill wastewater | 441 mg/L DOC | 15% | 75 min | 15% DOC removal in 1 $m^3$ wastewater | 38 kg $CO_2$-eq | (Muñoz et al., 2005) |
| Solar Photo-Fenton | Effluent from MWTP | 0.2 mg/L of 17$\alpha$-EE2 | 90% | 2 min | 1.0 $\mu$g 17$\alpha$-EE2 removal per litre of treated wastewater | 10 $\mu$Pt | (Foteinis et al., 2018; Frontistis et al., 2011) |
| | | 0.04-0.08 mg/L of 66 detected pollutants | 98% | 20 min | 1 $m^3$ of secondary effluent | 0.5-0.86 kg $CO_2$-eq | (Arzate et al., 2019; Prieto-Rodríguez et al., 2013) |

**Table 1:** *Cont.* Overview of reported environmental assessments for $^{\bullet}$OH-based AOPs.[1]

| | | | | | | | |
|---|---|---|---|---|---|---|---|
| | | $9{\cdot}10^{-6}$-$1.99{\cdot}10^{-3}$ mg/L of 9 detected PPCPs | 65-99% | - | 1000 $m^3$ of reclaimed water | 249 kg $CO_2$-eq | (Arzate et al., 2019; Zepon Tarpani and Azapagic, 2018) |
| | Herbicide synthetic wastewater | 50 ± 2 mg/L TOC | 83% | 510 min | 80% TOC removal in 1.25 L wastewater | $1.38{\cdot}10^{-3}$ kg $CO_2$-eq | (Farré et al., 2007) |
| | Kraft pulp mill wastewater | 441 mg/L DOC | 15% | 75 min | 15% DOC removal in 1 $m^3$ wastewater | 0.76 kg $CO_2$-eq | (Muñoz et al., 2005) |
| | Synthetic wastewater | 500 mg/L of $\alpha$-MPG | 100% | 180 min | 90% TOC removal in 250 mL solution | 1.0-$1.7{\cdot}10^{-3}$ kg $CO_2$-eq | (Serra et al., 2011) |
| Solar Photoelectro-Fenton | Synthetic wastewater | 500 mg/L of $\alpha$-MPG | 100% | 130-260 min | 90% TOC removal in 250 mL solution | $7.0{\cdot}10^{-3}$-$1.5{\cdot}10^{-2}$ kg $CO_2$-eq | (Serra et al., 2011) |
| Catalytic Ozonation | Surface water | 2.7-3.7 mg/L COD | >80% | 100 min | 34,100 $m^3$/day of clean water produced | 3,960-4,550 kg $CO_2$-eq | (Schlichter et al., 2004; Wang et al., 2019) |
| Photocatalytic Oxidation | Effluent from MWTP | 0.2 mg/L of 17$\alpha$-EE2 | 90% | 7 min | 1 $\mu$g 17$\alpha$-EE2 removal per litre of treated wastewater | 9.2 $\mu$Pt | (Foteinis et al., 2018; Frontistis et al., 2011) |
| | Kraft pulp mill wastewater | 441 mg/L DOC | 15% | 180 min | 15% DOC removal in 1 $m^3$ wastewater | 90 kg $CO_2$-eq | (Muñoz et al., 2005) |
| | Olive mill wastewater | 5,100 mg/L COD | 18% | 240 min | 1 g COD removal per litre of OMW | 5.2 kg $CO_2$-eq | (Chatzisymeon et al., 2013) |
| Solar Photocatalytic Oxidation | Kraft pulp mill wastewater | 441 mg/L DOC | 15% | 180 min | 15% DOC removal in 1 $m^3$ wastewater | 0.48 kg $CO_2$-eq | (Muñoz et al., 2005) |
| Electrochemical Oxidation | Olive mill wastewater | 10,000 mg/L COD | 28% | 420 min | 1 g COD removal per litre of OMW | 0.16 kg $CO_2$-eq | (Chatzisymeon et al., 2013) |

[1] *17$\alpha$-EE2:* 17$\alpha$-ethynylestradiol, *$\alpha$-MPG:* $\alpha$-methylphenylglycine, *COD:* Chemical oxygen demand, *DOC:* Dissolved organic carbon, *MWTP:* Municipal wastewater treatment plant, *OMW:* Olive mill wastewater, *PPCPs:* Pharmaceuticals and personal care products, *Pt:* Unit for environmental score, *WWTP:* Wastewater treatment plant, *TOC:* Total organic carbon.

### 3.1.2 Economic aspects

From the perspective of future industrial implementation, one of the main strengths of classical $^{\bullet}OH$ radical-based AOPs is that they are estimated to be two orders of magnitude cheaper than other technologies, such as $SO_4^{\bullet-}$ radical-based AOPs, mainly due to the lower cost of the oxidants (Fernandes et al., 2019b).

In terms of cost analysis among chemical-based activation methods, generation via combined $H_2O_2/O_3$ is the most economical and time-efficient solution, with an estimated treatment cost of \$0.01 per litre (i.e., ∼8.3 €/m$^3$) of wastewater treated to attain a degradation efficiency higher than 95% for several VOCs. Under similar conditions, ozonation processes can imply an operational cost of approximately \$0.02-0.06 per litre (i.e., ∼16.6-49.8 €/m$^3$), while $H_2O_2$ stays in a narrower range of \$0.01-0.02 per litre (i.e., ∼8.3-16.6 €/m$^3$). When coupling these chemical precursors with UV irradiation, UV/$H_2O_2$ and UV/$O_3$ have been reported to cost \$0.14 and \$0.21 per litre (i.e., ∼116.2 and 174.3 €/m$^3$) of treated household wastewater for a similar 53% COD reduction, respectively (Chong et al., 2012). Typically, UV/$H_2O_2/O_3$ is estimated to be 2-3 times more expensive because of the use of both types of precursors (Poyatos et al., 2009). On the other hand, reported treatment costs for catalytic ozonation have shown very dispersed results depending on the pollutant to be degraded. For instance, oxalic acid ($(COOH)_2$) has a cost of approximately 3.65 €/m$^3$ of treated wastewater, while dichloroacetic acid ($CHCl_2COOH$) shows an increase up to 10.75 €/m$^3$. Photocatalytic ozonation may lower both prices to 1.51 and 5.16 €/m$^3$, respectively, while significantly increasing removal efficiencies (Mehrjouei et al., 2014).

The costs of independently applying cavitation treatments have been pointed out to be too high compared to other AOPs, given the high energy requirements from the pieces of equipment involved (Fedorov et al., 2022). Enhancing the energy efficiency of the cavitation system is not trivial; moreover, its study at the laboratory scale has several limitations in terms of reproducibility and design towards scale-up implementation (Sirés et al., 2014). For these reasons, it is recommended to primarily consider it as part of a hybrid technology or as a preliminary treatment in a wastewater plant so that it can enhance pollutant degradation while reducing energy consumption and the subsequent environmental and economic impacts (Fedorov et al., 2022; Poyatos et al., 2009).

Regarding the operational costs of Fenton treatments in comparison to ozonation, divergent studies have been reported, as they strongly depend on the type of wastewater investigated. For instance, attaining 70% COD removal in olive mill wastewater has been reported to cost 36 times more in an ozonation plant, whereas the costs to effectively degrade phenols in wastewater via a Fenton system would be ca. 1.4-9.6 times higher than those for ozonation (Cañizares et al., 2009a; Krichevskaya et al., 2011). In a photo-Fenton process under optimal conditions, a total cost of 5.2 €/m$^3$ has been reported for over 90% degradation in pesticide-containing wastewater (Alalm et al., 2015a). When used as tertiary treatment, operational treatment costs can be increased by \$0.2-0.6 per cubic meter (i.e., ∼0.17-0.50 €/m$^3$) of treated wastewater with different micropollutants (Arzate et al., 2019). In a solar photo-Fenton plant, due to the mitigated energy consumption, achieving over 97% degradation of several pharmaceuticals is estimated to yield a total cost of approximately 3.06 €/m$^3$ (Alalm et al., 2015b). Other cost analyses in textile wastewater have shown electro-Fenton oxidation to range between \$1.6 to \$2.0 with the basis of 1 kg COD removal per cubic meter (i.e., ∼1.4-1.7 €/kg COD·m$^3$) of synthetic wastewater containing remazol black B (Suhan et al., 2020). Under the same conditions, the

anodic Fenton treatment reported costs in the range of \$1.4-3.4 (i.e., ~1.2-2.8 €/kg COD·m$^3$) (Suhan et al., 2020). Similarly, an industrial textile wastewater sample was degraded under solar photoelectro-Fenton treatment with operating costs estimated as \$1.56 per cubic meter (i.e., ~1.3 €/m$^3$) for a COD removal efficiency up to 83% (GilPavas et al., 2018).

For other photocatalytic oxidation systems, total estimated costs can be found ranging from ca. 7.8 up to 75.35 €/m$^3$, as there is a strong dependence on the type of pollutant and operating parameters selected, such as the COD removal efficiency and UV/catalyst amount (Alalm et al., 2015a; Mehrjouei et al., 2014). When taking into consideration the maintenance of the UV and catalytic systems as well as the catalyst post-separation treatment, operational costs have been reported to increase by \$15.0 per litre (i.e., ~12,458 €/m$^3$) of household wastewater treated (Chong et al., 2012). In a solar photoelectrocatalytic oxidation setup to degrade several common dyes, operating costs were reported as \$9.4 per cubic meter (i.e., ~7.8 €/m$^3$) of treated wastewater (Pirkarami et al., 2014).

Finally, regarding electrochemical oxidation, operational costs can be up to one order of magnitude lower than those of simple ozonation and slightly cheaper than a Fenton equivalent for several compounds (Cañizares et al., 2009a). For instance, for 85% COD removal in synthetic wastewater containing butyric acid, electrochemical oxidation implied an operational cost of 11 €/m$^3$ of treated wastewater, whereas ozonation and Fenton treatments led to 205 and 35 €/m$^3$, respectively (Cañizares et al., 2009a).

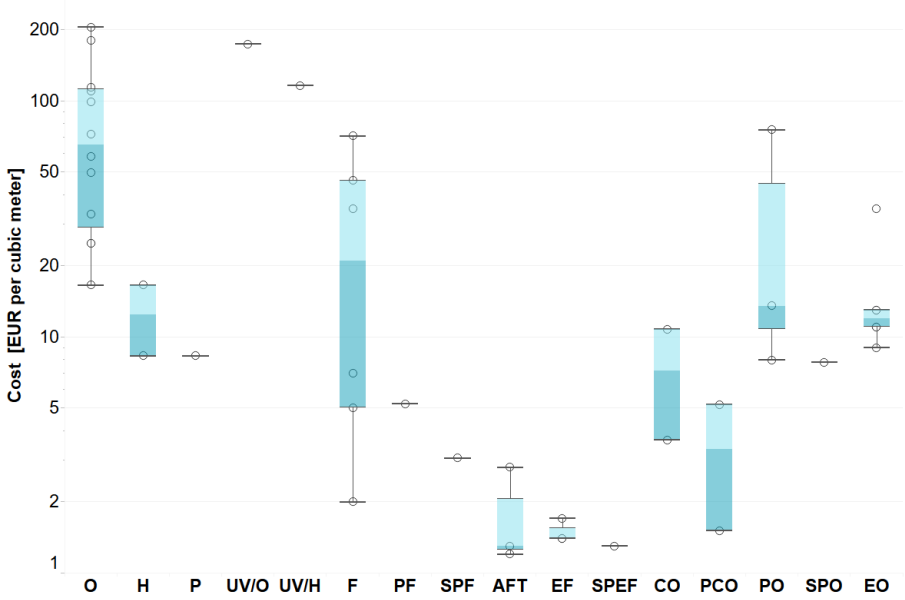


**Figure 9:** Reported costs in €/m$^3$ of wastewater for different $^{\bullet}$OH radical-based AOPs (*O:* Ozonation; *H:* Hydrogen peroxide, *P:* Peroxone, *UV/O:* UV/Ozone, *UV/H:* UV/Hydrogen peroxide, *F:* Fenton, *PF:* Photo-Fenton, *SPF:* Solar photo-Fenton, *AFT:* Anodic Fenton treatment, *EF:* Electro-Fenton, *SPEF:* Solar photoelectro-Fenton, *CO:* Catalytic ozonation, *PCO:* Photocatalytic ozonation, *PO:* Photocatalytic oxidation, *SPO:* Solar photocatalytic oxidation, *EO:* Electrochemical oxidation).

**Table 2:** Overview of reported cost analyses for •OH-based AOPs.[2]

| Treatment | Target Pollutant | Pollution Load | Efficiency | Time | Other | Cost | Ref. |
|---|---|---|---|---|---|---|---|
| $O_3$ | Acid Orange 7 | ~20 mg/L | >90% | 69.1 min | 12.4 mg/L $O_3$ | \$0.04/L (~33.2 €/m$^3$)[3] | (Chong et al., 2012; Tezcanli-Güyer and Ince, 2004) |
| | Butyric acid | ~2,000 mg/L COD | 85% | - | - | 205 €/m$^3$ | (Cañizares et al., 2009a) |
| | 4-Chlorophenol | ~2,000 mg/L COD | 85% | - | - | 114 €/m$^3$ | (Cañizares et al., 2009a) |
| | DEG | 116.6 mg/L | 90% | 90 min | - | 13.0 €/kg pollutant | (Krichevskaya et al., 2011; Turan-Ertas and Gurol, 2002) |
| | | 636 mg/L | 92% | 90 min | - | 2.7 €/kg pollutant | (Krichevskaya et al., 2011) |
| | Effluent from decentralised WWTP with household sludge and chemicals | 21.5 mg/L COD | 53% | 38.4 min | - | \$0.03/L (~24.9 €/m$^3$)[3] | (Chong et al., 2012) |
| | EG | 682 mg/L | 91% | 180 min | - | 5.1 €/kg pollutant | (Krichevskaya et al., 2011) |
| | Eriochrome Black T | ~2,000 mg/L COD | 85% | - | - | 99 €/m$^3$ | (Cañizares et al., 2009a) |
| | 2-Naphthol | ~2,000 mg/L COD | 85% | - | - | 72 €/m$^3$ | (Cañizares et al., 2009a) |
| | Olive mill wastewater | ~2,000 mg/L COD | 70% | - | - | 181 €/m$^3$ | (Cañizares et al., 2009a) |
| | Phenol | 235.3 mg/L | >90% | 27.4 min | 2 mg/L $O_3$ | \$0.03/L (~24.9 €/m$^3$)[3] | (Chong et al., 2012; Kidak and Ince, 2007) |
| | | 22 mg/L | 100% | ~20 min | 56.4 mg/L $O_3$ | 2.1 €/kg pollutant | (Krichevskaya et al., 2011) |
| | | 100 mg/L | 100% | 15 min | - | 4.7 €/kg pollutant | (Canton et al., 2003; Krichevskaya et al., 2011) |
| | | 231 mg/L | 99% | 120 min | - | 0.7 €/kg pollutant | (Krichevskaya et al., 2011) |

**Table 2:** *Cont.* Overview of reported cost analyses for $^{\bullet}$OH-based AOPs.[2]

| | | | | | | | |
|---|---|---|---|---|---|---|---|
| | | 1155 mg/L | 90% | 5.8 min | - | 0.7 €/kg pollutant | (Krichevskaya et al., 2011) |
| | 2-Propanol | ∼2,000 mg/L COD | 85% | - | - | 110 €/m$^3$ | (Cañizares et al., 2009a) |
| | TCE | 2.5 mg/L | >60% | 36.6 min | 6 mg/L $O_3$ | \$0.07/L (∼58.1 €/m$^3$)[3] | (Chong et al., 2012; Nakano et al., 2003) |
| | VOCs | 155.51 mg/L | >95% | 120 min | 18.9 g $O_3$ | \$0.02/L (∼16.6 €/m$^3$)[3] | (Fernandes et al., 2019b) |
| | | | | 357.6 min | 69.38 g $O_3$ | \$0.06/L (∼49.8 €/m$^3$)[3] | (Fernandes et al., 2019b) |
| $H_2O_2$ | VOCs | 155.51 mg/L | >95% | 181.5 min | 31.11 g $H_2O_2$ | \$0.01/L (∼8.3 €/m$^3$)[3] | (Fernandes et al., 2019b) |
| | | | | | 62.23 g $H_2O_2$ | \$0.02/L (∼16.6 €/m$^3$)[3] | (Fernandes et al., 2019b) |
| $H_2O_2/O_3$ | VOCs | 155.51 mg/L | >95% | 30 min | 5.82 g $O_3$, 5.93-12.05 g $H_2O_2$ | \$0.01/L (∼8.3 €/m$^3$)[3] | (Fernandes et al., 2019b) |
| $UV/O_3$ | Effluent from decentralised WWTP with household sludge and chemicals | 21.5 mg/L COD | 53% | 14.2 min | - | \$0.21/L (∼174.3 €/m$^3$)[3] | (Chong et al., 2012) |
| $UV/H_2O_2$ | Effluent from decentralised WWTP with household sludge and chemicals | 21.5 mg/L COD | 53% | 4.5 min | - | \$0.14/L (∼116.2 €/m$^3$)[3] | (Chong et al., 2012) |
| Fenton | Butyric acid | ∼2,000 mg/L COD | 85% | 210 min | - | 35 €/m$^3$ | (Cañizares et al., 2009a) |
| | 4-Chlorophenol | ∼2,000 mg/L COD | 85% | 210 min | - | 2 €/m$^3$ | (Cañizares et al., 2009a) |
| | DEG | 106 mg/L | 40% | 30 min | - | 84 €/kg pollutant | (Krichevskaya et al., 2011; Turan-Ertas and Gurol, 2002) |
| | EG | 1,000 mg/L | 40% | 120 min | - | 4.9 €/kg pollutant | (Krichevskaya et al., 2011) |
| | Eriochrome Black T | ∼2,000 mg/L COD | 85% | 210 min | - | 46 €/m$^3$ | (Cañizares et al., 2009a) |

**Table 2:** *Cont.* Overview of reported cost analyses for $^{\bullet}$OH-based AOPs.[2]

| | | | | | | | |
|---|---|---|---|---|---|---|---|
| | MTBE | 2 mg/L | 99% | 60 min | - | 29 €/kg pollutant | (Krichevskaya et al., 2011) |
| | | 88 mg/L | 98.9% | 120 min | - | 13.8 €/kg pollutant | (Krichevskaya et al., 2011) |
| | 2-Naphthol | ∼2,000 mg/L COD | 85% | 300 min | - | 7 €/m$^3$ | (Cañizares et al., 2009a) |
| | Olive mill wastewater | ∼2,000 mg/L COD | 70% | 300 min | - | 5 €/m$^3$ | (Cañizares et al., 2009a) |
| | Phenol | 0.05 mg/L | 100% | 60 min | - | 6.7 €/kg pollutant | (Krichevskaya et al., 2011) |
| | | 110 mg/L | 90% | 6 min | - | 6.65 €/kg pollutant | (Krichevskaya et al., 2011) |
| | 2-Propanol | ∼2,000 mg/L COD | 85% | 300 min | - | 71 €/m$^3$ | (Cañizares et al., 2009a) |
| Photo-Fenton | Pesticide wastewater (mostly chlorpyrifos, lambda-cyhalothrin and diazinon) | 7,000 ± 450 mg/L COD | 90.7% | 120 min | 1 g/L $H_2O_2$, 4 g/L $FeSO_4{\cdot}7H_2O$ | 5.20 €/m$^3$ | (Alalm et al., 2015a) |
| Solar Photo-Fenton | Amoxicillin, ampicillin, diclofenac and paracetamol | 100 mg/L | >97% | 120 min | 1.5 g/L $H_2O_2$, 0.5 g/L $FeSO_4{\cdot}7H_2O$ | 3.06 €/m$^3$ | (Alalm et al., 2015b) |
| Anodic Fenton Treatment | Remazol Black B | 100 mg/L | 90% | 50 min | 1 mM $Fe^{2+}$ | \$3.360/kg COD·m$^3$ (∼2.8 €/kg COD·m$^3$)[3] | (Suhan et al., 2020) |
| | | | 92.4% | 50 min | 1.5 mM $Fe^{2+}$ | \$1.422/kg COD·m$^3$ (∼1.2 €/kg COD·m$^3$)[3] | (Suhan et al., 2020) |
| | | | 96% | 50 min | 2 mM $Fe^{2+}$ | \$1.570/kg COD·m$^3$ (∼1.3 €/kg COD·m$^3$)[3] | (Suhan et al., 2020) |
| Electro-Fenton | Remazol Black B | 100 mg/L | 88.5% | 50 min | 750 mg/L $H_2O_2$, 1 mM $Fe^{2+}$ | \$1.998/kg COD·m$^3$ (∼1.7 €/kg COD·m$^3$)[3] | (Suhan et al., 2020) |
| | | | 94% | 50 min | 750 mg/L $H_2O_2$, 1.5 mM $Fe^{2+}$ | \$1.689/kg COD·m$^3$ (∼1.4 €/kg COD·m$^3$)[3] | (Suhan et al., 2020) |
| | | | 96% | 50 min | 750 mg/L $H_2O_2$, 2 mM $Fe^{2+}$ | \$1.656/kg COD·m$^3$ (∼1.4 €/kg COD·m$^3$)[3] | (Suhan et al., 2020) |

**Table 2:** *Cont.* Overview of reported cost analyses for $^{\bullet}$OH-based AOPs.[2]

| | | | | | | | |
|---|---|---|---|---|---|---|---|
| Solar Photoelectro-Fenton | COD | 545 mg/L | 83% | 15 min | - | \$1.56/m$^3$ (~1.3 €/m$^3$) | (GilPavas et al., 2018) |
| Catalytic Ozonation | Dichloroacetic acid | 128.9 mg/L | 10% | 60 min | 25 ± 5 mg/L $O_3$ | 10.75 €/m$^3$ | (Mehrjouei et al., 2014) |
| | Oxalic acid | 90 mg/L | 25% | 60 min | 25 ± 5 mg/L $O_3$ | 3.65 €/m$^3$ | (Mehrjouei et al., 2014) |
| Photocatalytic Ozonation | Dichloroacetic acid | 128.9 mg/L | 65% | 20 min | 70 ± 5 mg/L $O_3$, 4 UVA lamps (50% rel. intensity) | 5.16 €/m$^3$ | (Mehrjouei et al., 2014) |
| | Oxalic acid | 90 mg/L | ~100% | 20 min | 70 ± 5 mg/L $O_3$, 4 UVA lamps (75% rel. intensity) | 1.51 €/m$^3$ | (Mehrjouei et al., 2014) |
| Photocatalytic Oxidation | Dichloroacetic acid | 128.9 mg/L | 30% | 60 min | 7 UVA lamps (75% rel. intensity) | 75.35 €/m$^3$ | (Mehrjouei et al., 2014) |
| | Effluent from decentralised WWTP with household sludge and chemicals | 21.5 mg/L COD | 53% | 3.4 min | - | \$15.01/L (~12,458 €/m$^3$)[3] | (Chong et al., 2012) |
| | Oxalic acid | 90 mg/L | >95% | 60 min | 7 UVA lamps (100% rel. intensity) | 13.55 €/m$^3$ | (Mehrjouei et al., 2014) |
| | Pesticides (mostly chlorpyrifos, lambda-cyhalothrin and diazinon) | 7,000 ± 450 mg/L COD | 79.6% | 120 min | 1.5 g/L $TiO_2$ | 7.98 €/m$^3$ | (Alalm et al., 2015a) |
| Solar Photo-electrocatalytic Oxidation | Reactive Red 19, Acid Orange 7, Acid Red 18 | 30 mg/L | ~90% | 30 min | 0.6 mg/L Nano-Ni-$TiO_2$ | \$9.42/m$^3$ (~7.8 €/m$^3$)[3] | (Pirkarami et al., 2014) |
| Electrochemical Oxidation | Butyric acid | ~2,000 mg/L COD | 85% | - | - | 11 €/m$^3$ | (Cañizares et al., 2009a) |
| | 4-Chlorophenol | ~2,000 mg/L COD | 85% | - | - | 13 €/m$^3$ | (Cañizares et al., 2009a) |
| | Eriochrome Black T | ~2,000 mg/L COD | 85% | - | - | 35 €/m$^3$ | (Cañizares et al., 2009a) |

**Table 2:** *Cont.* Overview of reported cost analyses for $^{\bullet}$OH-based AOPs.[2]

| | | | | | | |
|---|---|---|---|---|---|---|
| 2-Naphthol | ∼2,000 mg/L COD | 85% | - | - | 13 €/m$^3$ | (Cañizares et al., 2009a) |
| Olive mill wastewater | ∼2,000 mg/L COD | 70% | - | - | 11 €/m$^3$ | (Cañizares et al., 2009a) |
| 2-Propanol | ∼2,000 mg/L COD | 85% | - | - | 9 €/m$^3$ | (Cañizares et al., 2009a) |

[2] *COD:* Chemical oxygen demand, *DEG:* Diethyleneglycol, *EG:* Ethylene glycol, *WWTP:* Wastewater treatment plant.

[3] Calculated based on the exchange rate 1 USD = 0.8316 EUR provided on the 8th of February 2021 by the European Central Bank (European Central Bank, 2021).

## 3.2 Other radicals

As most studies have primarily focused on $^{\bullet}OH$ radical-based AOPs, the number of available publications regarding other radicals is rather limited, mostly due to their recent incorporation into AOP research trends. There is a knowledge gap regarding the quantification of environmental and economic indicators specifically tailored to other radical-based AOPs, which hinders a comprehensive comparison among these novel technologies.

In the SR-AOP domain, thermal activation of a sulfate precursor is an effective and relatively efficient method for pollutant degradation at the laboratory scale. For large scale wastewater treatment plants, the high energy requirements involved hinder their feasibility, both in terms of operational costs and environmental impact. However, it should be considered that many industries already discharge water effluents at high temperatures, above 30°C (Pulat et al., 2009). Therefore, if such intrinsic energy could be re-used for thermal activation, this technique would become more cost-efficient and environmentally friendly (Ike et al., 2018a). In terms of the activation of precursors via a metal catalyst, as previously discussed, the nature of the metal determines the environmental friendliness of a treatment. For instance, treatments based on cobalt catalysts are considered the least preferred alternatives due to the derived potential health risks (Han et al., 2019; Leyssens et al., 2017). Cavitation activation processes may not be as cost-efficient and sustainable as other methods due to their high energy requirements unless applied in combination with other AOPs (Fedorov et al., 2022; Poyatos et al., 2009; Sirés et al., 2014). Similarly, in UV irradiation, an excessive use of electricity from the grid may result in unfavourable environmental impacts if not powered by renewable energy sources (Chatzisymeon et al., 2013).

Regarding the environmental impact of chlorine-based AOPs, the application of solar-based technologies for the activation of chlorine radicals can considerably aid in reducing the $CO_2$ emissions expected from the application of UV irradiation methods. However, there is a need to define the type and concentration of the residual chemicals and degradation products released into the treated effluents to evaluate their potential toxicity effects. Similarly, the information available on the economic analysis of chlorine-based AOPs is scarce in the literature. In a recent study, Guo et al. (2018) concluded that a UV/chlorine system could considerably contribute to saving electrical energy up to 93.5% compared to a UV/$H_2O_2$ process for PPCP degradation in synthetic effluents (Guo et al., 2018). Previously, it was also shown that the higher efficiency of a UV/chlorine treatment resulted in lower associated costs (25-50%) compared to UV/$H_2O_2$ (Boal et al., 2015). UV/chlorine also demonstrates higher efficiencies than other technologies, such as UV/persulfate oxidation processes, for the degradation of organic matter (Fang et al., 2020). Therefore, it can be argued that they are more economical than conventional radicals given the higher process efficiencies reported. However, detailed economic assessments in scaled-up installations are required to evaluate their feasibility for real applications (Cho et al., 2014).

Although there has been significant progress in the field of iodine radicals for the treatment of polluted wastewater, there is still room for environmental and economic studies to allow for a deeper understanding of their viability for industrial applications. Regarding their environmental implications, the generation of toxic nitro-products is a major concern that needs to be investigated further for this type of AOP (Rayaroth et al., 2022). For economic considerations, it is advantageous that the precursors required to provide iodine radicals such as sodium iodate ($NaIO_3$) and sodium periodate ($NaIO_4$) are low-cost chemicals (Rezaeivalla, 2006). Moreover, according to the recent literature, these AOP systems can also operate with low precursor

concentrations (Belghit et al., 2020).

# 4 Future outlook in a sustainable economy

Current wastewater treatment plants are typically highly energy-consuming. Recently, Zawartka et al. (2020) reported an extensive life cycle assessment of a system for wastewater collection, transport and treatment. In particular, they indicated that under regular operation, a conventional wastewater treatment facility is estimated to consume 631.24 kWh of electricity from the grid per year and per 1 PE (person-equivalent), with a corresponding carbon footprint of 1.16240 kg $CO_2$-eq/PE (Zawartka et al., 2020). When expressed under the functional unit of one cubic meter of treated wastewater, reported carbon footprint values may range from 0.1 to 2.4 kg $CO_2$-eq (Li et al., 2017b; Maktabifard et al., 2020; Wang et al., 2016a). Similarly, a recent study by Maktabifard et al. (2020) investigated the carbon footprint of six full-scale wastewater treatment plants, and for those plants fully dependent on the power grid, indirect emissions due to energy consumption accounted for approximately 69–72% of the entire carbon footprint (Maktabifard et al., 2020).

Regarding the energy consumption of AOPs, Chatzisymeon et al. (2013) performed a comparative life cycle assessment on the environmental footprint of three methods, i.e., UV heterogeneous photocatalysis (UV/$TiO_2$), wet air oxidation (WAO) and electrochemical oxidation with boron-doped diamond electrodes (eAOPs), all of which are based on $^{\bullet}$OH generation. The electrochemical treatment displayed the lowest impact values and therefore was designated as the most environmentally friendly alternative. In fact, for the removal of 1 g of COD, 0.16 kg $CO_2$-eq/L treated olive mill wastewater was estimated. This value is minor compared to 0.88 kg $CO_2$-eq/L for WAO and 5.2 kg $CO_2$-eq/L for UV/$TiO_2$ (Table 1). From their results, it can be affirmed that not only is the carbon footprint of an electrochemical treatment significantly lower than that of conventional wastewater treatment but also that the environmental impact associated with AOP operation is strongly dependent on energy requirements for all process conditions under study (Chatzisymeon et al., 2013). Muñoz et al. (2005) also performed a comparative environmental assessment on another set of $^{\bullet}$OH radical-based AOPs, including heterogeneous photocatalysis and photo-Fenton, and under two scenarios corresponding to whether electricity was supplied from a solar energy source or from the general grid. The outcomes of their analysis demonstrated that the solar energy scenario could reduce the environmental impact by over 90% in all impact categories for most AOPs under study (Table 1) (Muñoz et al., 2005).

Typically, the co-generation of industrial chemical waste, both in terms of quantity and concentration, is another key parameter when evaluating the sustainability of wastewater treatment plants (Foley et al., 2010). For instance, Arzate et al. (2019) reported that in a solar photo-Fenton process, a large amount of acid is needed in relation to the concentration of total inorganic carbon so that the effect of this scavenger can be mitigated and the Fenton reaction can be carried out at the desired pH. Afterwards, the effluent is also neutralised with the addition of proportional quantities of a strong base. As a result, the chemicals used to acidify and neutralise the wastewater stream eventually showed a higher impact than the use of $H_2O_2$ and iron themselves, representing approximately 40-45% of the overall carbon footprint under different reactor configurations (Table 1) (Arzate et al., 2019).

Considering the abovementioned energy and chemical issues, renewable energy-driven elec-

trochemical AOPs dedicated to the generation of oxidative radicals without added precursors, that is, systems that can promote the generation of radicals from species already present in the influent wastewater, showcase a competitive advantage over other technologies from an economic and environmental perspective. Saving energy and chemicals, and hence avoiding their corresponding environmental impacts and secondary waste streams, is possible through eAOPs while attaining high degradation efficiencies. In addition, eAOPs are robust and safe in performance and usually do not require excessive amounts of auxiliary chemicals to alter the pH of the wastewater (Radjenovic and Sedlak, 2015). Regarding their potential toxicological effects, eAOPs are more effective in minimising the risk of nitro-product formation than other AOPs (Rayaroth et al., 2022). However, there is still a reason why eAOPs have not been extensively rolled out industrially. This commercial limitation is due to the associated risk of the formation of halogenated degradation products, such as chlorine- and bromine-containing compounds (Divyapriya and Nidheesh, 2021). In addition, the high costs of the electrode materials and the negative effects that scavengers may entail add up to the burdens for their industrial scale-up.

Consequently, there is no perfect solution when selecting the most sustainable wastewater treatment technology. On the one hand, it is necessary to conduct an economic evaluation to guarantee that a treatment is not only efficient in removing pollutants but also industrially feasible. Table 3 summarises the key findings on the economic considerations of various AOPs together with their possibilities for improvement. On the other hand, not all economically viable projects are justified for execution if that comes at the expense of the environment. Thus, it is necessary to quantify their potential environmental and toxicological impacts together with the measures to minimise them. Table 4 includes the results of the environmental assessments of various AOPs with further recommendations.

**Table 3:** Summary of economic considerations of various AOPs.

| AOPs | Economic Remarks | Improvement Possibilities |
|---|---|---|
| Chlorine-based processes | Chlorine-based methods have shown a lower energy demand due to their fast reaction kinetics (Boal et al., 2015; Guo et al., 2018), but they rely on complex chemical precursors (Chuang et al., 2017; Zhang et al., 2020a). | Using chlorine-rich effluents as the source of chlorine radicals as well as visible light activation routes. |
| Electrochemical processes | eAOPs allow for operation at room temperature and atmospheric pressure, with limited or no need for precursor chemicals (Radjenovic and Sedlak, 2015). However, the costs derived from the power supply and the production and maintenance of the electrodes are currently the main economic obstacles (Sirés and Brillas, 2012). | Generating oxidative radicals from species already present in wastewater, relying on renewable energy sources and developing non-active electrodes from low-cost materials. |
| Fenton and Fenton-related processes | Fenton processes rely on a relatively low-cost catalyst (i.e., iron), but when it comes to photo-Fenton or electro-Fenton treatments, energy consumption plays a key role in the economy of the process (Alalm et al., 2015b). | For the photo-Fenton process, implementing solar-based technologies as energy sources may reduce operational energy costs. The electro-Fenton process can also satisfy economic considerations by the continuous (re)generation of the reactants. |
| Iodine-based processes | Precursors such as sodium iodate and sodium periodate need to be added to the wastewater matrix, although they are considered low-cost chemicals (Rezaeivalla, 2006). | Applying this technique to wastewater matrices naturally rich in iodine. |
| PDS-based processes | PDS is a relatively expensive oxidation agent (Clara et al., 2021). | Promoting the in situ generation of PDS and $SO_4^{\bullet -}$ radicals from $SO_4^{2-}$ ions. |
| Photo(catalytic) processes | UV-based treatments are highly energy-consuming (Chatzisymeon et al., 2013). When combined with nanocatalysis, the synthesis and regeneration of nanomaterials are the main challenges for their wider application (Feijoo et al., 2020). | Implementing solar-based technologies as well as nanocatalysts that have a longer lifetime and are produced through low-cost methods. Developing novel photocatalysts that combine pollutant degradation with energy or $H_2$ production. |

**Table 4:** Summary of environmental considerations of various AOPs.

| AOPs | Environmental Remarks | Improvement Possibilities |
|---|---|---|
| Electrochemical processes | In the presence of halogens, eAOPs may form toxic halogenated byproducts, such as chlorate, perchlorate and bromate (Bergmann and Rollin, 2007; Jung et al., 2010). | Specific pre-treatment unit operations can be added to separate halogens. |
| Fenton and Fenton-related processes | The need for acidification, neutralisation and sludge post-treatment steps are the main environmental drawbacks for Fenton and Fenton-related processes (Morone et al., 2019; Vasquez-Medrano et al., 2018). In addition, Fenton-like processes rely on metals of increased toxicity potential (e.g., cobalt, copper) (Han et al., 2019). | Natural-based materials such as ashes can be applied for the neutralisation and transformation of the sludge into valuable materials such as biochar.<br>Strict quality controls should be implemented to detect metal leaching when iron cannot be used as a catalyst.<br>Opting for solar photo-Fenton systems to reduce sludge formation and electricity consumption as well as electro-Fenton for chemical regeneration. |
| PDS-based processes | Increased PDS and $SO_4{}^{2-}$ concentrations, either from using excessive amounts of reactants or after their recombination during the treatment, may not be allowed for discharge into the environment (Honarmandrad et al., 2023; Priyadarshini et al., 2022).<br>Regarding activation routes, the thermal activation of PDS is highly energy-consuming, and catalytic activation with metals such as cobalt entails negative ecological and health risks (Han et al., 2019; Ike et al., 2018a). | Generating radicals without added precursors and avoiding the use of hazardous catalysts. |
| Photo(catalytic) processes | UV-based processes are highly energy-consuming (Chatzisymeon et al., 2013), and when combined with nanocatalysis, the accidental release of nanocatalysts into the environment is of toxicological concern (Jiang et al., 2014). | Relying on renewable energy sources, safe nanomaterials and stricter quality control mechanisms for the treated effluents. |

# 5 Conclusions

Due to the growing challenges that water pollution causes in the social, environmental and economic spheres, it is imperative to improve current wastewater treatments to ensure safe water reuse. To this end, conventional technologies need to be enhanced to achieve higher cleaning standards. Several methods have been developed to address polluted wastewater, among which AOPs have been shown to effectively degrade recalcitrant and non-biodegradable compounds. Nonetheless, taking the leap from laboratory studies to full-scale exploitation faces several limitations, not only from a technological point of view but also because there is still a need to reduce associated treatment costs and make these systems more environmentally friendly. In this regard, key aspects are as follows:

- In environmental terms, it is particularly important that AOPs minimise the consumption of chemicals and energy, promote synergistic effects and prevent the formation of toxic byproducts, such as halogenated and nitro-compounds, while achieving maximum degradation efficiencies.
- The generation of radicals without the addition of chemical precursors poses a competitive advantage to push AOPs for further commercialization, both from environmental and economic points of view.
- Relying on renewable sources as well as coupling pollutant degradation with energy and/or $H_2$ production would not only entail significant environmental and economic improvements but would also make AOPs less vulnerable in the current crisis of the energy market.
- Renewable energy-driven electrochemical AOPs are a promising technique to generate oxidative radicals from other species already present in influent wastewater. However, other issues, such as scavenging effects, the formation of toxic halogenated degradation products and the elevated costs of the electrodes, need to be further optimised.
- The robustness of each radical type and activation method should be further tested for recalcitrant compounds with different chemical structures, real wastewater matrices of diverse origins and variable operating conditions (e.g., energy, oxidant and/or catalyst consumption) before assessing their overall suitability for wastewater treatment.
- Most studies have focused on investigating specific radicals separately, typically $^{\bullet}OH$ or $SO_4^{\bullet-}$, but comparative assessments in terms of degradation efficiency, underlying mechanisms, technical feasibility, operational costs and environmental impacts across different radical types and generation methods are needed to elucidate the most suitable treatment for a given application.

# Acknowledgements

The research leading to these results received funding from the European Union's EU Framework Programme for Research and Innovation Horizon 2020 under Grant Agreement No 861369 (MSCA-ETN InnovEOX) and from the KU Leuven Industrial Research Council under grant numbers C24E/19/040 (SO4ELECTRIC) and C3/20/094 (Sani-TRouBLe).

# Competing interests

The authors declare no competing interests.

# References


Alalm, M. G., Tawfik, A., and Ookawara, S. (2015a). Comparison of solar $TiO_2$ photocatalysis and solar photo-Fenton for treatment of pesticides industry wastewater: Operational conditions, kinetics and costs. *J. Water Process Eng.*, 8:55–63.

Alalm, M. G., Tawfik, A., and Ookawara, S. (2015b). Degradation of four pharmaceuticals by solar photo-Fenton process: Kinetics and costs estimation. *J. Environ. Chem. Eng.*, 3(1):46–51.

Alaton, I. A., Balcioglu, I. A., and Bahnemann, D. W. (2002). Advanced oxidation of a reactive dyebath effluent: Comparison of $O_3$, $H_2O_2$/UV-C and $TiO_2$/UV-A processes. *Water Res.*, 36(5):1143–1154.

Alkhuraiji, T. S., Boukari, S. O., and Alfadhl, F. S. (2017). Gamma irradiation-induced complete degradation and mineralization of phenol in aqueous solution: Effects of reagent. *J. Hazard. Mater.*, 328:29–36.

Amadelli, R., De Battisti, A., Girenko, D., Kovalyov, S., and Velichenko, A. (2000). Electrochemical oxidation of trans-3,4-dihydroxycinnamic acid at $PbO_2$ electrodes: Direct electrolysis and ozone mediated reactions compared. *Electrochim. Acta*, 46(2):341–347.

Ameta, R., K. Chohadia, A., Jain, A., and Punjabi, P. B. (2018). Chapter 3 - Fenton and Photo-Fenton processes. In Ameta, S. C. and Ameta, R., editors, *Advanced Oxidation Processes for Waste Water Treatment*, pages 49–87. Academic Press.

Amor, C., Marchão, L., Lucas, M. S., and Peres, J. A. (2019). Application of Advanced Oxidation Processes for the treatment of recalcitrant agro-industrial wastewater: A review. *Water*, 11(2).

Anglada, A., Urtiaga, A., and Ortiz, I. (2009). Contributions of electrochemical oxidation to waste-water treatment: Fundamentals and review of applications. *Emerg. Technol.*, 84(12):1747–1755.

Anipsitakis, G. P. and Dionysiou, D. D. (2003). Degradation of organic contaminants in water with sulfate radicals generated by the conjunction of peroxymonosulfate with cobalt. *Environ. Sci. Technol.*, 37(20):4790–4797.

Anipsitakis, G. P. and Dionysiou, D. D. (2004a). Radical generation by the interaction of transition metals with common oxidants. *Environ. Sci. Technol.*, 38(13):3705–3712.

Anipsitakis, G. P. and Dionysiou, D. D. (2004b). Transition metal/UV-based advanced oxidation technologies for water decontamination. *Appl. Catal. B-Environ.*, 54(3):155–163.

Antonin, V. S., Santos, M. C., Garcia-Segura, S., and Brillas, E. (2015). Electrochemical incineration of the antibiotic ciprofloxacin in sulfate medium and synthetic urine matrix. *Water Res.*, 83:31–41.

Ao, X. and Liu, W. (2017). Degradation of sulfamethoxazole by medium pressure UV and oxidants: Peroxymonosulfate, persulfate, and hydrogen peroxide. *Chem. Eng. J.*, 313:629–637.

Arellano, M., Pazos, M., and Ángeles Sanromán, M. (2019). Sulfate radicals-based technology as a promising strategy for wastewater. *Water*, 11.

Arevalo, E. and Calmano, W. (2007). Studies on electrochemical treatment of wastewater contaminated with organotin compounds. *J. Hazard. Mater.*, 146(3):540–545.

Arzate, S., Pfister, S., Oberschelp, C., and Sánchez-Pérez, J. (2019). Environmental impacts of an Advanced Oxidation Process as tertiary treatment in a wastewater treatment plant. *Sci. Total Environ.*, 694:133572.

Ashoori, N., Teixido, M., Spahr, S., LeFevre, G. H., Sedlak, D. L., and Luthy, R. G. (2019). Evaluation of pilot-scale biochar-amended woodchip bioreactors to remove nitrate, metals, and trace organic contaminants from urban stormwater runoff. *Water Res.*, 1(154):1–11.

Babuponnusami, A. and Muthukumar, K. (2014). A review on Fenton and improvements to the Fenton process for wastewater treatment. *J. Environ. Chem. Eng.*, 2(1):557–572.

Balkema, A. J., Preisig, H. A., Otterpohl, R., and Lambert, F. J. (2002). Indicators for the sustainability assessment of wastewater treatment systems. *Urban Water J.*, 4(2):153–161.

Barrera-Díaz, C., Cañizares, P., Fernández, F. J., Natividad, R., and Rodrigo, M. A. (2014). Electrochemical Advanced Oxidation Processes: An overview of the current applications to actual industrial effluents. *J. Mex. Chem. Soc.*, 58:256–275.

Belghit, A., Merouani, S., Hamdaoui, O., Alghyamah, A., and Bouhelassa, M. (2020). Influence of processing conditions on the synergism between UV irradiation and chlorine toward the degradation of refractory organic pollutants in UV/chlorine advanced oxidation system. *Sci. Total Environ.*, 736:139623.

Bendjama, H., Merouani, S., Hamdaoui, O., and Bouhelassa, M. (2018). Efficient degradation method of emerging organic pollutants in marine environment using UV/periodate process: Case of chlorazol black. *Mar. Pollut. Bull.*, 126:557–564.

Bergmann, M. H. and Rollin, J. (2007). Product and by-product formation in laboratory studies on disinfection electrolysis of water using boron-doped diamond anodes. *Catal. Today*, 124(3):198–203.

Boal, A. K., Rhodes, C., and Garcia, S. (2015). Pump-and-treat groundwater remediationusing Chlorine/Ultraviolet Advanced Oxidation Processes. *Ground Water Monit. R.*, 35(2):93–100.

Boczkaj, G. and Fernandes, A. (2017). Wastewater treatment by means of advanced oxidation processes at basic pH conditions: A review. *Chem. Eng. J.*, 320:608–633.

Bokare, A. D. and Choi, W. (2014). Review of iron-free Fenton-like systems for activating $H_2O_2$ in Advanced Oxidation Processes. *J. Hazard. Mater.*, 275:121–135.

Bokare, A. D. and Choi, W. (2015). Singlet-oxygen generation in alkaline periodate solution. *Environ. Sci. Technol.*, 49(24):14392–14400.

Boretti, A. and Rosa, L. (2019). Reassessing the projections of the World Water Development Report. *npj Clean Water*, 2.

Bürgi, H., Schaffner, T. H., and Seiler, J. P. (2001). The toxicology of iodate: A review of the literature. *Thyroid*, 11(5):449–456.

Brienza, M. and Katsoyiannis, I. A. (2017). Sulfate radical technologies as tertiary treatment for the removal of emerging contaminants from wastewater. *Sustainability*, 9(9).

Brillas, E. and Martínez-Huitle, C. A. (2015). Decontamination of wastewaters containing synthetic organic dyes by electrochemical methods. An updated review. *Appl. Catal. B-Environ.*, 166-167:603–643.

Brillas, E., Sirés, I., and Oturan, M. A. (2009). Electro-Fenton process and related electrochemical technologies based on Fenton's reaction chemistry. *Chem. Rev.*, 109(12):6570–6631.

Bu, L., Zhou, S., Shi, Z., Deng, L., and Gao, N. (2017). Removal of 2-MIB and geosmin by electrogenerated persulfate: Performance, mechanism and pathways. *Chemosphere*, 168:1309–1316.

Cai, J., Zhou, M., Pan, Y., Du, X., and Lu, X. (2019). Extremely efficient electrochemical degradation of organic pollutants with co-generation of hydroxyl and sulfate radicals on Blue-$TiO_2$ nanotubes anode. *Appl. Catal. B-Environ.*, 257:117902.

Cai, W.-W., Peng, T., Yang, B., Xu, C., Liu, Y.-S., Zhao, J.-L., Gu, F.-L., and Ying, G.-G. (2020). Kinetics and mechanism of reactive radical mediated fluconazole degradation by the UV/chlorine process: Experimental and theoretical studies. *Chem. Eng. J.*, 402:126224.

Cañizares, P., Paz, R., Sáez, C., and Rodrigo, M. A. (2009a). Costs of the electrochemical oxidation of wastewaters: A comparison with ozonation and Fenton oxidation processes. *J. Environ. Manage.*, 90(1):410–420.

Cañizares, P., Sáez, C., Sánchez-Carretero, A., and Rodrigo, M. A. (2009b). Synthesis of novel oxidants by electrochemical technology. *J. Appl. Electrochem.*, 39(2143):2143–2149.

Cako, E., Gunasekaran, K. D., Cheshmeh Soltani, R. D., and Boczkaj, G. (2020). Ultrafast degradation of brilliant cresyl blue under hydrodynamic cavitation based advanced oxidation processes (AOPs). *Water Resour. Ind.*, 24:100134.

Can, W., Yao-Kun, H., Qing, Z., and Min, J. (2014). Treatment of secondary effluent using a three-dimensional electrode system: COD removal, biotoxicity assessment, and disinfection effects. *Chem. Eng. J.*, 243:1–6.

Canton, C., Esplugas, S., and Casado, J. (2003). Mineralization of phenol in aqueous solution by ozonation using iron or copper salts and light. *Appl. Catal. B-Environ.*, 43(2):139–149.

Carter, K. E. and Farrell, J. (2008). Oxidative destruction of perfluorooctane sulfonate using boron-doped diamond film electrodes. *Environ. Sci. Technol.*, 42(16):6111–6115.

Chakma, S., Praneeth, S., and Moholkar, V. S. (2017). Mechanistic investigations in sono-hybrid (ultrasound/$Fe^{2+}$/UVC) techniques of persulfate activation for degradation of azorubine. *Ultrason. Sonochem.*, 38:652–663.

Chatzisymeon, E., Foteinis, S., Mantzavinos, D., and Tsoutsos, T. (2013). Life Cycle Assessment of Advanced Oxidation Processes for olive mill wastewater treatment. *J. Clean. Prod.*, 54:229–234.

ChemSpider (2021). Ozonide. `http://www.chemspider.com/Chemical-Structure.10140300.html`.

Chen, L., Lei, C., Li, Z., Yang, B., Zhang, X., and Lei, L. (2018a). Electrochemical activation of sulfate by BDD anode in basic medium for efficient removal of organic pollutants. *Chemosphere*, 210:516–523.

Chen, X., Oh, W.-D., and Lim, T.-T. (2018b). Graphene- and CNTs-based carbocatalysts in persulfates activation: Material design and catalytic mechanisms. *Chem. Eng. J.*, 354:941–976.

Chen, Y., Xie, P., Wang, Z., Shang, R., and Wang, S. (2017). UV/persulfate preoxidation to improve coagulation efficiency of *Microcystis aeruginosa*. *J. Hazard. Mater.*, 322:508–515.

Cheng, Z., Ling, L., Wu, Z., Fang, J., Westerhoff, P., and Shang, C. (2020). Novel visible light-driven photocatalytic chlorine activation process for carbamazepine degradation in drinking water. *Environ. Sci. Technol.*, 54(18):11584–11593.

Chiang, Y.-P., Liang, Y.-Y., Chang, C.-N., and Chao, A. C. (2006). Differentiating ozone direct and indirect reactions on decomposition of humic substances. *Chemosphere*, 65(11):2395–2400.

Cho, K., Qu, Y., Kwon, D., Zhang, H., Cid, C. A., Aryanfar, A., and Hoffmann, M. R. (2014). Effects of anodic potential and chloride ion on overall reactivity in electrochemical reactors designed for solar-powered wastewater treatment. *Environ. Sci. Technol.*, 48(4):2377–2384.

Choi, Y., Yoon, H.-I., Lee, C., Vetráková, L., Heger, D., Kim, K., and Kim, J. (2018). Activation of periodate by freezing for the degradation of aqueous organic pollutants. *Environ. Sci. Technol.*, 52(9):5378–5385.

Chong, M. N., Sharma, A. K., Burn, S., and Saint, C. P. (2012). Feasibility study on the application of advanced oxidation technologies for decentralised wastewater treatment. *J. Clean. Prod.*, 35:230–238.

Chuang, Y.-H., Chen, S., Chinn, C. J., and Mitch, W. A. (2017). Comparing the UV/Monochloramine and UV/Free Chlorine Advanced Oxidation Processes (AOPs) to the UV/Hydrogen Peroxide AOP under scenarios relevant to potable reuse. *Environ. Sci. Technol.*, 51(23):13859–13868.

Clara, V. S. M., Costa, E. P., Souza, F. A., Machado, E. C., de Araujo, J. C., and Amorim, C. C. (2021). Persulfate mediated solar photo-Fenton aiming at wastewater treatment plant effluent improvement at neutral pH: emerging contaminant removal, disinfection, and elimination of antibiotic-resistant bacteria. *Environ. Sci. Pollut. Res.*, 28(14):17355–17368.

Comninellis, C. and Chen, G. (2010). *Electrochemistry for the Environment*. Springer, New York, 1st edition.

Considine, D. M. and Considine, G. D., editors (2007). *Ozone Generation*. Springer US, USA, 8th edition.

Crini, G. and Lichtfouse, E. (2019). Advantages and disadvantages of techniques used for wastewater treatment. *Environ. Chem. Lett.*, 17:145–155.

Cuerda-Correa, E. M., Alexandre-Franco, M. F., and Fernández-González, C. (2020). Advanced Oxidation Processes for the removal of antibiotics from water. An overview. *Water*, 12(1).

Deng, Y. and Zhao, R. (2015). Advanced Oxidation Processes (AOPs) in wastewater treatment. *Water Pollut.*, 1:167–176.

Destaillats, H., Colussi, A. J., Joseph, J. M., and Hoffmann, M. R. (2000). Synergistic effects of sonolysis combined with ozonolysis for the oxidation of azobenzene and methyl orange. *J. Phys. Chem. A*, 104(39):8930–8935.

Devi, P., Das, U., and Dalai, A. K. (2016). In-situ chemical oxidation: Principle and applications of peroxide and persulfate treatments in wastewater systems. *Sci. Total Environ.*, 571:643–657.

Dewil, R., Mantzavinos, D., Poulios, I., and Rodrigo, M. A. (2017). New perspectives for Advanced Oxidation Processes. *J. Environ. Manage.*, 195:93–99.

Dhaka, S., Kumar, R., Khan, M. A., Paeng, K.-J., Kurade, M. B., Kim, S.-J., and Jeon, B.-H. (2017). Aqueous phase degradation of methyl paraben using UV-activated persulfate method. *Chem. Eng. J.*, 321:11–19.

Divyapriya, G. and Nidheesh, P. (2021). Electrochemically generated sulfate radicals by boron doped diamond and its environmental applications. *Curr. Opin. Solid State Mater Sci.*, 25(3):100921.

Du, J., Tang, S., Faheem, Ling, H., Zheng, H., Xiao, G., Luo, L., and Bao, J. (2019). Insights into periodate oxidation of bisphenol A mediated by manganese. *Chem. Eng. J.*, 369:1034–1039.

Du, Y., Wang, W.-L., Zhang, D.-Y., Zhou, T.-H., Lee, M.-Y., Wu, Q.-Y., Hu, H.-Y., He, Z.-M., and Huang, T.-Y. (2020). Degradation of non-oxidizing biocide benzalkonium chloride and bulk dissolved organic matter in reverse osmosis concentrate by UV/chlorine oxidation. *J. Hazard. Mater.*, 396:122669.

Duan, X., He, X., Wang, D., Mezyk, S. P., Otto, S. C., Marfil-Vega, R., Mills, M. A., and Dionysiou, D. D. (2017). Decomposition of iodinated pharmaceuticals by UV-254 nm-assisted Advanced Oxidation Processes. *J. Hazard. Mater.*, 323:489–499.

Duan, X., Sun, H., and Wang, S. (2018). Metal-free carbocatalysis in Advanced Oxidation Reactions. *Acc. Chem. Res.*, 51(3):678–687.

Duan, X., Yang, S., Wacławek, S., Fang, G., Xiao, R., and Dionysiou, D. D. (2020). Limitations and prospects of Sulfate Radical-Based Advanced Oxidation Processes. *J. Environ. Chem. Eng.*, 8(4):103849.

European Central Bank (2021). Euro foreign exchnage reference rates. `https://www.ecb.europa.eu/stats/policy_and_exchange_rates/euro_reference_exchange_rates/html/eurofxref-graph-usd.en.html`.

Fang, Z., Huang, R., How, Z. T., Jiang, B., Chelme-Ayala, P., Shi, Q., Xu, C., and Gamal El-Din, M. (2020). Molecular transformation of dissolved organic matter in process water from oil and gas operation during UV/$H_2O_2$, UV/chlorine, and UV/persulfate processes. *Sci. Total Environ.*, 730:139072.

Farhat, A., Keller, J., Tait, S., and Radjenovic, J. (2015). Removal of persistent organic contaminants by electrochemically activated sulfate. *Environ. Sci. Technol.*, 49:14326–14333.

Farhat, A., Keller, J., Tait, S., and Radjenovic, J. (2017). Assessment of the impact of chloride on the formation of chlorinated by-products in the presence and absence of electrochemically activated sulfate. *Chem. Eng. J.*, 330:1265–1271.

Farré, M. J., García-Montaño, J., Ruiz, N., Muñoz, I., Domènech, X., and Peral, J. (2007). Life Cycle Assessment of the removal of diuron and linuron herbicides from water using three environmentally friendly technologies. *Environ. Technol.*, 28(7):819–830.

Fedorov, K., Dinesh, K., Sun, X., Darvishi Cheshmeh Soltani, R., Wang, Z., Sonawane, S., and Boczkaj, G. (2022). Synergistic effects of hybrid advanced oxidation processes (AOPs) based on hydrodynamic cavitation phenomenon - A review. *Chem. Eng. J.*, 432:134191.

Fedorov, K., Plata-Gryl, M., Khan, J. A., and Boczkaj, G. (2020). Ultrasound-assisted heterogeneous activation of persulfate and peroxymonosulfate by asphaltenes for the degradation of BTEX in water. *J. Hazard. Mater.*, 397:122804.

Fedorov, K., Sun, X., and Boczkaj, G. (2021). Combination of hydrodynamic cavitation and SR-AOPs for simultaneous degradation of BTEX in water. *Chem. Eng. J.*, 417:128081.

Feijoo, S., González-Rodríguez, J., Fernández, L., Vázquez-Vázquez, C., Feijoo, G., and Moreira, M. T. (2020). Fenton and photo-Fenton nanocatalysts revisited from the perspective of Life Cycle Assessment. *Catalysts*, 10(1).

Fernandes, A., Gagol, M., Makoś, P., Khan, J. A., and Boczkaj, G. (2019a). Integrated photocatalytic advanced oxidation system ($TiO_2$/UV/$O_3$/$H_2O_2$) for degradation of volatile organic compounds. *Sep. Purif. Technol.*, 224:1–14.

Fernandes, A., Makoś, P., Khan, J. A., and Boczkaj, G. (2019b). Pilot scale degradation study of 16 selected volatile organic compounds by Hydroxyl and Sulfate Radical based Advanced Oxidation Processes. *J. Clean. Prod.*, 208:54–64.

Fernandes, A., Makoś, P., Wang, Z., and Boczkaj, G. (2020). Synergistic effect of $TiO_2$ photocatalytic advanced oxidation processes in the treatment of refinery effluents. *Chem. Eng. J.*, 391:123488.

Fischbacher, A., Löppenberg, K., von Sonntag, C., and Schmidt, T. C. (2015). A new reaction pathway for bromite to bromate in the ozonation of bromide. *Environ. Sci. Technol.*, 49(19):11714–11720.

Foley, J., de Haas, D., Hartley, K., and Lant, P. (2010). Comprehensive life cycle inventories of alternative wastewater treatment systems. *Water Res.*, 44(5):1654–1666.

Foteinis, S., Borthwick, A. G., Frontistis, Z., Mantzavinos, D., and Chatzisymeon, E. (2018). Environmental sustainability of light-driven processes for wastewater treatment applications. *J. Clean. Prod.*, 182:8–15.

Frontistis, Z., Xekoukoulotakis, N. P., Hapeshi, E., Venieri, D., Fatta-Kassinos, D., and Mantzavinos, D. (2011). Fast degradation of estrogen hormones in environmental matrices by photo-Fenton oxidation under simulated solar radiation. *Chem. Eng. J.*, 178:175–182.

Gagol, M., Cako, E., Fedorov, K., Soltani, R. D. C., Przyjazny, A., and Boczkaj, G. (2020). Hydrodynamic cavitation based advanced oxidation processes: Studies on specific effects of inorganic acids on the degradation effectiveness of organic pollutants. *J. Mol. Liq.*, 307:113002.

Gagol, M., Przyjazny, A., and Boczkaj, G. (2018). Wastewater treatment by means of advanced oxidation processes based on cavitation - A review. *Chem. Eng. J.*, 338:599–627.

Gansäuer, A. and Bluhm, H. (2000). Reagent-controlled transition-metal-catalyzed radical reactions. *Chem. Rev.*, 100(8):2771–2788.

Gao, Y.-Q., Gao, N.-Y., Deng, Y., Yang, Y.-Q., and Ma, Y. (2012). Ultraviolet (UV) light-activated persulfate oxidation of sulfamethazine in water. *Chem. Eng. J.*, 195-196:248–253.

Garcia-Segura, S., Keller, J., Brillas, E., and Radjenovic, J. (2015). Removal of organic contaminants from secondary effluent by anodic oxidation with a boron-doped diamond anode as tertiary treatment. *J. Hazard. Mater.*, 283:551–557.

Garcia-Segura, S., Ocon, J. D., and Chong, M. N. (2018). Electrochemical oxidation remediation of real wastewater effluents - A review. *Process Saf. Environ. Prot.*, 113:48–67.

Garrido-Cardenas, J., Esteban-García, B., Agüera, A., Sánchez-Pérez, J., and Manzano-Agugliaro, F. (2020). Wastewater treatment by Advanced Oxidation Process and their worldwide research trends. *Int. J. Environ. Res. Public Health*, 17.

Ghanbari, F. and Moradi, M. (2017). Application of peroxymonosulfate and its activation methods for degradation of environmental organic pollutants: Review. *Chem. Eng. J.*, 310:41–62.

Ghanbari, F., Moradi, M., and Gohari, F. (2016). Degradation of 2,4,6-trichlorophenol in aqueous solutions using peroxymonosulfate/activated carbon/UV process via sulfate and hydroxyl radicals. *J. Water Process Eng.*, 9:22–28.

Giannakis, S., Lin, K. Y. A., and Ghanbari, F. (2021). A review of the recent advances on the treatment of industrial wastewaters by Sulfate Radical-based Advanced Oxidation Processes (SR-AOPs). *Chem. Eng. J.*, 406:127083.

GilPavas, E., Dobrosz-Gómez, I., and Ángel Gómez-García, M. (2018). Optimization of solar-driven photo-electro-Fenton process for the treatment of textile industrial wastewater. *J. Water Process Eng.*, 24:49–55.

Grannas, A. M., Bausch, A. R., and Mahanna, K. M. (2007). Enhanced aqueous photochemical reaction rates after freezing. *J. Phys. Chem. A*, 111(43):11043–11049.

Guan, Y.-H., Ma, J., Li, X.-C., Fang, J.-Y., and Chen, L.-W. (2011). Influence of pH on the formation of sulfate and hydroxyl radicals in the UV/Peroxymonosulfate system. *Environ. Sci. Technol.*, 45(21):9308–9314.

Guerra-Rodríguez, S., Rodríguez, E., Singh, D. N., and Rodríguez-Chueca, J. (2018). Assessment of Sulfate Radical-Based Advanced Oxidation Processes for water and wastewater treatment: A review. *Water*, 10(12).

Guo, K., Wu, Z., Yan, S., Yao, B., Song, W., Hua, Z., Zhang, X., Kong, X., Li, X., and Fang, J. (2018). Comparison of the UV/chlorine and UV/$H_2O_2$ processes in the degradation of PPCPs in simulated drinking water and wastewater: Kinetics, radical mechanism and energy requirements. *Water Res.*, 147:184–194.

Guo, Y., Zhou, J., Lou, X., Liu, R., Xiao, D., Fang, C., Wang, Z., and Liu, J. (2014). Enhanced degradation of tetrabromobisphenol A in water by a UV/base/persulfate system: Kinetics and intermediates. *Chem. Eng. J.*, 254:538–544.

Gözmen, B., Turabik, M., and Hesenov, A. (2009). Photocatalytic degradation of Basic Red 46 and Basic Yellow 28 in single and binary mixture by UV/$TiO_2$/periodate system. *J. Hazard. Mater.*, 164(2):1487–1495.

Haddad, A., Merouani, S., Hannachi, C., Hamdaoui, O., and Hamrouni, B. (2019). Intensification of light green SF yellowish (LGSFY) photodegradation in water by iodate ions: Iodine radicals implication in the degradation process and impacts of water matrix components. *Sci. Total Environ.*, 652:1219–1227.

Hamdaoui, O. and Merouani, S. (2017). Improvement of sonochemical degradation of Brilliant blue R in water using periodate ions: Implication of iodine radicals in the oxidation process. *Ultrason. Sonochem.*, 37:344–350.

Han, Z., Li, J., Han, X., Ji, X., and Zhao, X. (2019). A comparative study of iron-based PAN fibrous catalysts for peroxymonosulfate activation in decomposing organic contaminants. *Chem. Eng. J.*, 358:176–187.

He, S., Chen, Y., Li, X., Zeng, L., and Zhu, M. (2022). Heterogeneous photocatalytic activation of persulfate for the removal of organic contaminants in water: A critical review. *ACS ES&T Eng.*, 2(4):527–546.

He, X., de la Cruz, A. A., and Dionysiou, D. D. (2013). Destruction of cyanobacterial toxin cylindrospermopsin by hydroxyl radicals and sulfate radicals using UV-254 nm activation of hydrogen peroxide, persulfate and peroxymonosulfate. *J. Photochem. Photobiol. A*, 251:160–166.

He, Z., Song, S., Ying, H., Xu, L., and Chen, J. (2007). p-Aminophenol degradation by ozonation combined with sonolysis: Operating conditions influence and mechanism. *Ultrason. Sonochem.*, 14(5):568–574.

Heger, D., Jirkovský, J., and Klán, P. (2005). Aggregation of methylene blue in frozen aqueous solutions studied by absorption spectroscopy. *J. Phys. Chem. A*, 109(30):6702–6709.

Heger, D., Klánová, J., and Klán, P. (2006). Enhanced protonation of cresol red in acidic aqueous solutions caused by freezing. *J. Phys. Chem. B*, 110(3):1277–1287.

Herrero, O., Pérez Martín, J., Fernández Freire, P., Carvajal López, L., Peropadre, A., and Hazen, M. (2012). Toxicological evaluation of three contaminants of emerging concern by use of the *Allium cepa* test. *Mutat. Res. Genet. Toxicol. Environ. Mutagen.*, 743(1):20–24.

Herrmann, H. (2007). On the photolysis of simple anions and neutral molecules as sources of $O^-$/OH, $SOx^-$ and Cl in aqueous solution. *Phys. Chem. Chem. Phys.*, 9:3935–3964.

Hoigné, J. (1988). *The Chemistry of Ozone in Water*, pages 121–141. Springer US, Boston.

Hoigné, J. (1998). *Chemistry of Aqueous Ozone and Transformation of Pollutants by Ozonation and Advanced Oxidation Processes*, pages 83–141. Springer Berlin Heidelberg, Berlin, Heidelberg.

Honarmandrad, Z., Sun, X., Wang, Z., Naushad, M., and Boczkaj, G. (2023). Activated persulfate and peroxymonosulfate based advanced oxidation processes (AOPs) for antibiotics degradation - A review. *Water Resour. Ind.*, 29:100194.

House, D. A. (1962). Kinetics and mechanism of oxidations by peroxydisulfate. *Chem. Rev.*, 62(3):185–203.

Hsueh, C., Huang, Y., Wang, C., and Chen, C. (2005). Degradation of azo dyes using low iron concentration of Fenton and Fenton-like system. *Chemosphere*, 58(10):1409–1414.

Hu, P. and Long, M. (2016). Cobalt-catalyzed sulfate radical-based advanced oxidation: A review on heterogeneous catalysts and applications. *Appl. Catal. B-Environ.*, 181:103–117.

Huang, B., Wu, Z., Zhou, H., Li, J., Zhou, C., Xiong, Z., Pan, Z., Yao, G., and Lai, B. (2021). Recent advances in single-atom catalysts for advanced oxidation processes in water purification. *J. Hazard. Mater.*, 412:125253.

Huang, N., Wang, T., Wang, W.-L., Wu, Q.-Y., Li, A., and Hu, H.-Y. (2017). UV/chlorine as an advanced oxidation process for the degradation of benzalkonium chloride: Synergistic effect, transformation products and toxicity evaluation. *Water Res.*, 114:246–253.

Ike, I. A., Linden, K. G., Orbell, J. D., and Duke, M. (2018a). Critical review of the science and sustainability of persulphate Advanced Oxidation Processes. *Chem. Eng. J.*, 338:651–669.

Ike, I. A., Orbell, J. D., and Duke, M. (2018b). Activation of persulfate at waste heat temperatures for humic acid degradation. *ACS Sustain. Chem. Eng.*, 6(3):4345–4353.

Ismail, L., Ferronato, C., Fine, L., Jaber, F., and Chovelon, J.-M. (2017). Elimination of sulfaclozine from water with $SO_4^{\bullet -}$ radicals: Evaluation of different persulfate activation methods. *Appl. Catal. B-Environ.*, 201:573–581.

Jawad, A., Li, Y., Lu, X., Chen, Z., Liu, W., and Yin, G. (2015). Controlled leaching with prolonged activity for Co–LDH supported catalyst during treatment of organic dyes using bicarbonate activation of hydrogen peroxide. *J. Hazard. Mater.*, 289:165–173.

Ji, Y., Bai, J., Li, J., Luo, T., Qiao, L., Zeng, Q., and Zhou, B. (2017). Highly selective transformation of ammonia nitrogen to $N_2$ based on a novel solar-driven photoelectrocatalytic-chlorine radical reactions system. *Water Res.*, 125:512–519.

Jiang, C., Jia, J., and Zhai, S. (2014). Mechanistic understanding of toxicity from nanocatalysts. *Int. J. Mol. Sci.*, 15(8):13967–13992.

Jiménez, S., Andreozzi, M., Micó, M. M., Álvarez, M. G., and Contreras, S. (2019). Produced water treatment by advanced oxidation processes. *Sci. Total Environ.*, 666:12–21.

Joshi, A., Locke, B., Arce, P., and Finney, W. (1995). Formation of hydroxyl radicals, hydrogen peroxide and aqueous electrons by pulsed streamer corona discharge in aqueous solution. *J. Hazard. Mater.*, 41(1):3–30.

Jung, Y. J., Baek, K. W., Oh, B. S., and Kang, J.-W. (2010). An investigation of the formation of chlorate and perchlorate during electrolysis using Pt/Ti electrodes: The effects of pH and reactive oxygen species and the results of kinetic studies. *Water Res.*, 44(18):5345–5355.

Kang, J.-W. and Hoffmann, M. R. (1998). Kinetics and mechanism of the sonolytic destruction of methyl tert-butyl ether by ultrasonic irradiation in the presence of ozone. *Environ. Sci. Technol.*, 32(20):3194–3199.

Kang, Y.-G., Yoon, H., Lee, W., ju Kim, E., and Chang, Y.-S. (2018). Comparative study of peroxide oxidants activated by nZVI: Removal of 1,4-Dioxane and Arsenic(III) in contaminated waters. *Chem. Eng. J.*, 334:2511–2519.

Katsoyiannis, I. A., Canonica, S., and von Gunten, U. (2011). Efficiency and energy requirements for the transformation of organic micropollutants by ozone, $O_3/H_2O_2$ and $UV/H_2O_2$. *Water Res.*, 45(13):3811–3822.

Khan, A. U. and Kasha, M. (1994). Singlet molecular oxygen evolution upon simple acidification of aqueous hypochlorite: Application to studies on the deleterious health effects of chlorinated drinking water. *Proc. Natl. Acad. Sci. U.S.A.*, 91(26):12362–12364.

Khan, J. A., Sayed, M., Shah, N. S., Khan, S., Zhang, Y., Boczkaj, G., Khan, H. M., and Dionysiou, D. D. (2020). Synthesis of eosin modified $TiO_2$ film with co-exposed 001 and 101 facets for photocatalytic degradation of para-aminobenzoic acid and solar $H_2$ production. *Appl. Catal. B-Environ.*, 265:118557.

Kidak, R. and Ince, N. (2007). Catalysis of advanced oxidation reactions by ultrasound: A case study with phenol. *J. Hazard. Mater.*, 146(3):630–635.

Kim, C., Ahn, J.-Y., Kim, T. Y., Shin, W. S., and Hwang, I. (2018a). Activation of persulfate by nanosized zero-valent iron (NZVI): Mechanisms and transformation products of NZVI. *Environ. Sci. Technol.*, 52(6):3625–3633.

Kim, I., Yamashita, N., and Tanaka, H. (2009). Performance of UV and $UV/H_2O_2$ processes for the removal of pharmaceuticals detected in secondary effluent of a sewage treatment plant in Japan. *J. Hazard. Mater.*, 166(2):1134–1140.

Kim, J., Lee, C., and Yoon, J. (2018b). Electrochemical peroxodisulfate (PDS) generation on a self-doped $TiO_2$ Nanotube Array Electrode. *Ind. Eng. Chem. Res.*, 57(33):11465–11471.

Kim, J.-G., Yousef, A. E., and Dave, S. (1999). Application of ozone for enhancing the microbiological safety and quality of foods: A review. *J. Food Prot.*, 62(9):1071–1087.

Kläning, U. K. and Sehested, K. (1978). Photolysis of periodate and periodic acid in aqueous solution. *J. Chem. Soc. Faraday Trans.*, 74:2818–2838.

Kläning, U. K., Sehested, K., and Wolff, T. (1981). Laser flash photolysis and pulse radiolysis of iodate and periodate in aqueous solution. Properties of iodine(VI). *J. Chem. Soc. Faraday Trans.*, 77:1707–1718.

Kong, X., Thomson, E. S., Papagiannakopoulos, P., Johansson, S. M., and Pettersson, J. B. C. (2014). Water accommodation on ice and organic surfaces: Insights from environmental molecular beam experiments. *J. Phys. Chem. B*, 118(47):13378–13386.

Krichevskaya, M., Klauson, D., Portjanskaja, E., and Preis, S. (2011). The cost evaluation of Advanced Oxidation Processes in laboratory and pilot-scale experiments. *Ozone Sci. Eng.*, 33(3):211–223.

Kurokawa, Y., Maekawa, A., Takahashi, M., and Hayashi, Y. (1990). Toxicity and carcinogenicity of potassium bromate - A new renal carcinogen. *Environ. Health Persp.*, 87:309–335.

Lado Ribeiro, A. R., Moreira, N. F. F., Li Puma, G., and Silva, A. M. T. (2019). Impact of water matrix on the removal of micropollutants by advanced oxidation technologies. *Chem. Eng. J.*, 363:155–173.

Lee, H., Yoo, H.-Y., Choi, J., Nam, I.-H., Lee, S., Lee, S., Kim, J.-H., Lee, C., and Lee, J. (2014). Oxidizing capacity of periodate activated with iron-based bimetallic nanoparticles. *Environ. Sci. Technol.*, 48(14):8086–8093.

Lee, J., von Gunten, U., and Kim, J.-H. (2020). Persulfate-based Advanced Oxidation: Critical assessment of opportunities and roadblocks. *Environ. Sci. Technol.*, 54(6):3064–3081.

Lee, K. M., Lai, C. W., Ngai, K. S., and Juan, J. C. (2016a). Recent developments of zinc oxide based photocatalyst in water treatment technology: A review. *Water Res.*, 88:428–448.

Lee, Y.-C., Chen, M.-J., Huang, C.-P., Kuo, J., and Lo, S.-L. (2016b). Efficient sonochemical degradation of perfluorooctanoic acid using periodate. *Ultrason. Sonochem.*, 31:499–505.

Leyssens, L., Vinck, B., Van Der Straeten, C., Wuyts, F., and Maes, L. (2017). Cobalt toxicity in humans - A review of the potential sources and systemic health effects. *Toxicology*, 387:43–56.

Li, B., Wang, Y.-F., Zhang, L., and Xu, H.-Y. (2022). Enhancement strategies for efficient activation of persulfate by heterogeneous cobalt-containing catalysts: A review. *Chemosphere*, 291:132954.

Li, G., He, J., Wang, D., Meng, P., and Zeng, M. (2015). Optimization and interpretation of $O_3$ and $O_3/H_2O_2$ oxidation processes to pretreat hydrocortisone pharmaceutical wastewater. *Environ. Technol.*, 36(8):1026–1034.

Li, X., Liu, X., Lin, C., Qi, C., Zhang, H., and Ma, J. (2017a). Enhanced activation of periodate by iodine-doped granular activated carbon for organic contaminant degradation. *Chemosphere*, 181:609–618.

Li, Y., Wang, X., Butler, D., Liu, J., and Qu, J. (2017b). Energy use and carbon footprints differ dramatically for diverse wastewater-derived carbonaceous substrates: An integrated exploration of biokinetics and life-cycle assessment. *Sci. Rep.*, 7:243.

Liang, C. and Bruell, C. J. (2008). Thermally activated persulfate oxidation of trichloroethylene: Experimental investigation of reaction orders. *Ind. Eng. Chem. Res.*, 47(9):2912–2918.

Liang, C., Bruell, C. J., Marley, M. C., and Sperry, K. L. (2004a). Persulfate oxidation for in situ remediation of TCE I. Activated by ferrous ion with and without a persulfate-thiosulfate redox couple. *Chemosphere*, 55(9):1213–1223.

Liang, C., Bruell, C. J., Marley, M. C., and Sperry, K. L. (2004b). Persulfate oxidation for in-situ remediation of TCE II. Activated by chelated ferrous ion. *Chemosphere*, 55(9):1235–1233.

Liang, T., Magers, D. B., Raston, P. L., Allen, W. D., and Douberly, G. E. (2013). Dipole moment of the HOOO radical: Resolution of a structural enigma. *J. Phys. Chem. Lett.*, 4(21):3584–3589.

Liao, C.-H. and Gurol, M. D. (1995). Chemical oxidation by photolytic decomposition of hydrogen peroxide. *Environ. Sci. Technol.*, 29(12):3007–3014.

Lin, D., Fu, Y., Li, X., Wang, L., Hou, M., Hu, D., Li, Q., Zhang, Z., Xu, C., Qiu, S., Wang, Z., and Boczkaj, G. (2022). Application of persulfate-based oxidation processes to address diverse sustainability challenges: A critical review. *J. Hazard. Mater.*, 440:129722.

Lin, H., Wu, J., and Zhang, H. (2013). Degradation of bisphenol A in aqueous solution by a novel electro/$Fe^{3+}$/peroxydisulfate process. *Sep. Purif. Technol.*, 117:18–23.

Lin, Y.-T., Liang, C., and Chen, J.-H. (2011). Feasibility study of ultraviolet activated persulfate oxidation of phenol. *Chemosphere*, 82(8):1168–1172.

Loos, G., Scheers, T., Van Eyck, K., Van Schepdael, A., Adams, E., Van der Bruggen, B., Cabooter, D., and Dewil, R. (2018). Electrochemical oxidation of key pharmaceuticals using a boron doped diamond electrode. *Sep. Purif. Technol.*, 195:184–191.

Luo, C., Jiang, J., Ma, J., Pang, S., Liu, Y., Song, Y., Guan, C., Li, J., Jin, Y., and Wu, D. (2016). Oxidation of the odorous compound 2,4,6-trichloroanisole by UV activated persulfate: Kinetics, products, and pathways. *Water Res.*, 96:12–21.

Lutze, H. V., Bakkour, R., Kerlin, N., von Sonntag, C., and Schmidt, T. C. (2014). Formation of bromate in sulfate radical based oxidation: Mechanistic aspects and suppression by dissolved organic matter. *Water Res.*, 53:370–377.

Lutze, H. V., Kerlin, N., and Schmidt, T. C. (2015). Sulfate radical-based water treatment in presence of chloride: Formation of chlorate, inter-conversion of sulfate radicals into hydroxyl radicals and influence of bicarbonate. *Water Res.*, 72:349–360.

Macías-Quiroga, I. F., Henao-Aguirre, P. A., Marín-Flórez, A., Arredondo-López, S. M., and Sanabria-González, N. R. (2020). Bibliometric analysis of advanced oxidation processes (AOPs) in wastewater treatment: Global and Ibero-American research trends. *Environ. Sci. Pollut. Res.*

Mahapatra, K., Ramteke, D., and Paliwal, L. (2012). Production of activated carbon from sludge of food processing industry under controlled pyrolysis and its application for methylene blue removal. *J. Anal. Appl. Pyrolysis*, 95:79–86.

Mailloux, R. (2015). Teaching the fundamentals of electron transfer reactions in mitochondria and the production and detection of reactive oxygen species. *Redox Biol.*, 141:381–398.

Maktabifard, M., Zaborowska, E., and Makinia, J. (2020). Energy neutrality versus carbon footprint minimization in municipal wastewater treatment plants. *Bioresour. Technol.*, 300:122647.

Malato-Rodríguez, S. (2004). Solar detoxification and disinfection. In Cleveland, C. J., editor, *Encyclopedia of Energy*, pages 587–596. Elsevier, New York.

Martí, E., Riera, J. L., and Sabater, F. (2010). *Effects of Wastewater Treatment Plants on Stream Nutrient Dynamics Under Water Scarcity Conditions*, pages 173–195. Springer Berlin Heidelberg, Berlin, Heidelberg.

Martínez-Huitle, C. A. and Ferro, S. (2006). Electrochemical oxidation of organic pollutants for the wastewater treatment: Direct and indirect processes. *Chem. Soc. Rev.*, 35(12):1324–1340.

Masschelein, W. J. (1998). Ozone Generation: Use of air, oxygen or air simpsonized with oxygen. *Ozone Sci. Eng.*, 20(3):191–203.

Matzek, L. W. and Carter, K. E. (2016). Activated persulfate for organic chemical degradation: A review. *Chemosphere*, 151:178–188.

Mecha, A. C. and Chollom, M. N. (2020). Photocatalytic ozonation of wastewater: A review. *Environ. Chem. Lett.*, 18:1491–1507.

Mecha, A. C., Onyango, M. S., Ochieng, A., and Momba, M. N. (2017). Ultraviolet and solar photocatalytic ozonation of municipal wastewater: Catalyst reuse, energy requirements and toxicity assessment. *Chemosphere*, 186:669–676.

Mehrjouei, M., Müller, S., and Möller, D. (2014). Energy consumption of three different advanced oxidation methods for water treatment: A cost-effectiveness study. *J. Clean. Prod.*, 65:178–183.

Milh, H., Schoenaers, B., Stesmans, A., Cabooter, D., and Dewil, R. (2020). Degradation of sulfamethoxazole by heat-activated persulfate oxidation: Elucidation of the degradation mechanism and influence of process parameters. *Chem. Eng. J.*, 379:122234.

Minakata, D., Kamath, D., and Maetzold, S. (2017). Mechanistic insight into the reactivity of Chlorine-Derived Radicals in the aqueous-phase UV-Chlorine Advanced Oxidation Process: Quantum Mechanical Calculations. *Environ. Sci. Technol.*, 51(12):6918–6926.

Moad, G. and Solomon, D. H. (1989). 8 - Azo and Peroxy Initiators. In Allen, G. and Bevington, J. C., editors, *Comprehensive Polymer Science and Supplements*, pages 97–121. Pergamon, Amsterdam.

Mohammadi, A. S., Asgari, G., Poormohammadi, A., and Ahmadian, M. (2016). Oxidation of phenol from synthetic wastewater by a novel Advanced Oxidation Process: Microwave-assisted periodate. *J. Sci. Ind. Res. (India)*, 75(4):267–272.

Morone, A., Mulay, P., and Kamble, S. P. (2019). 8-Removal of pharmaceutical and personal care products from wastewater using advanced materials. In Prasad, M. N. V., Vithanage, M., and Kapley, A., editors, *Pharmaceuticals and Personal Care Products: Waste Management and Treatment Technology*, pages 173–212. Butterworth-Heinemann.

Muga, H. E. and Mihelcic, J. R. (2008). Sustainability of wastewater treatment technologies. *J. Environ. Manage.*, 88(3):437–447.

Muñoz, I., Rieradevall, J., Torrades, F., Peral, J., and Domènech, X. (2005). Environmental assessment of different solar driven Advanced Oxidation Processes. *Sol. Energy*, 79(4):369–375.

Muñoz, I., Rodríguez, A., Rosal, R., and Fernández-Alba, A. R. (2009). Life Cycle Assessment of urban wastewater reuse with ozonation as tertiary treatment: A focus on toxicity-related impacts. *Sci. Total Environ.*, 407(4):1245–1256.

Nakano, Y., Okawa, K., Nishijima, W., and Okada, M. (2003). Ozone decomposition of hazardous chemical substance in organic solvents. *Water Res.*, 37(11):2595–2598.

Neta, P., Huie, R. E., and Ross, A. B. (1988). Rate constants for reactions of inorganic radicals in aqueous solution. *J. Phys. Chem. Ref. Data*, 17(3):1027–1284.

Neyens, E. and Baeyens, J. (2003). A review of classic Fenton's peroxidation as an advanced oxidation technique. *J. Hazard. Mater.*, 98(1):33–50.

Nidheesh, P. V. (2015). Heterogeneous Fenton catalysts for the abatement of organic pollutants from aqueous solution: A review. *RSC Adv.*, 5(51):40552–40577.

Nikravesh, B., Shomalnasab, A., Nayyer, A., Aghababaei, N., Zarebi, R., and Ghanbari, F. (2020). UV/Chlorine process for dye degradation in aqueous solution: Mechanism, affecting factors and toxicity evaluation for textile wastewater. *J. Environ. Chem. Eng.*, 8(5):104244.

O'Dowd, K. and Pillai, S. C. (2020). Photo-Fenton disinfection at near neutral pH: Process, parameter optimization and recent advances. *J. Environ. Chem. Eng.*, 8(5):104063.

Oh, S.-Y., Kim, H.-W., Park, J.-M., Park, H.-S., and Yoon, C. (2009). Oxidation of polyvinyl alcohol by persulfate activated with heat, $Fe^{2+}$, and zero-valent iron. *J. Hazard. Mater.*, 168(1):346–351.

Oh, W.-D., Dong, Z., and Lim, T. (2016). Generation of sulfate radical through heterogeneous catalysis for organic contaminants removal: Current development, challenges and prospects. *Appl. Catal. B-Environ.*, 194:169–201.

Oh, W.-D. and Lim, T.-T. (2019). Design and application of heterogeneous catalysts as peroxydisulfate activator for organics removal: An overview. *Chem. Eng. J.*, 358:110–133.

Olvera-Vargas, H., Oturan, N., Oturan, M. A., and Brillas, E. (2015). Electro-Fenton and solar photoelectro-Fenton treatments of the pharmaceutical ranitidine in pre-pilot flow plant scale. *Sep. Purif. Technol.*, 146:127–135.

Oturan, N. and Oturan, M. A. (2018). Chapter 8 - Electro-Fenton Process: Background, New Developments and Applications. In Martínez-Huitle, C. A., Rodrigo, M. A., and Scialdone, O., editors, *Electrochemical Water and Wastewater Treatment*, pages 193–221. Butterworth-Heinemann.

Palansooriya, K. N., Yang, Y., Tsang, Y. F., Sarkar, B., Hou, D., Cao, X., Meers, E., Rinklebe, J., Kim, K.-H., and Ok, Y. S. (2020). Occurrence of contaminants in drinking water sources and the potential of biochar for water quality improvement: A review. *Crit. Rev. Env. Sci. Tec.*, 50(6):549–611.

Pan, Y., Cheng, S., Yang, X., Ren, J., Fang, J., Shang, C., Song, W., Lian, L., and Zhang, X. (2017). UV/chlorine treatment of carbamazepine: Transformation products and their formation kinetics. *Water Res.*, 116:254–265.

Pardieck, D. L., Bouwer, E. J., and Stone, A. T. (1992). Hydrogen peroxide use to increase oxidant capacity for in situ bioremediation of contaminated soils and aquifers: A review. *J. Contam. Hydrol.*, 9(3):221–242.

Paul (Guin), J., Naik, D., Bhardwaj, Y., and Varshney, L. (2014). Studies on oxidative radiolysis of ibuprofen in presence of potassium persulfate. *Radiat. Phys. Chem.*, 100:38–44.

Peleyeju, M. G. and Arotiba, O. A. (2018). Recent trend in visible-light photoelectrocatalytic systems for degradation of organic contaminants in water/wastewater. *Environ. Sci. Water Res. Technol.*, 4:1389–1411.

Pesqueira, J. F., Pereira, M. F. R., and Silva, A. M. (2020). Environmental impact assessment of advanced urban wastewater treatment technologies for the removal of priority substances and contaminants of emerging concern: A review. *J. Clean. Prod.*, 261:121078.

Pignatello, J. J., Oliveros, E., and MacKay, A. (2006). Advanced Oxidation Processes for organic contaminant destruction based on the Fenton reaction and related chemistry. *Crit. Rev. Env. Sci. Tec.*, 36(1):1–84.

Pinedo Escobar, J. A., Moctezuma, E., and Serrano Rosales, B. (2020). Heterojunctions for photocatalytic wastewater treatment: Positive holes, hydroxyl radicals and activation mechanism under UV and visible light. *Int. J. Chem. React. Eng.*, 18(7):20190159.

Pirkarami, A., Olya, M. E., and Raeis Farshid, S. (2014). UV/Ni-$TiO_2$ nanocatalyst for electrochemical removal of dyes considering operating costs. *Water Resour. Ind.*, 5:9–20.

Popiel, S., Nalepa, T., Dzierżak, D., Stankiewicz, R., and Witkiewicz, Z. (2009). Rate of dibutylsulfide decomposition by ozonation and the $O_3/H_2O_2$ Advanced Oxidation Process. *J. Hazard. Mater.*, 164(2):1364–1371.

Poyatos, J. M., Muñio, M. M., Almecija, M. C., Torres, J. C., Hontoria, E., and Osorio, F. (2009). Advanced Oxidation Processes for wastewater treatment: State of the art. *Water Air Soil Pollut.*, 205(187).

Premarathna, K., Rajapaksha, A. U., Sarkar, B., Kwon, E. E., Bhatnagar, A., Ok, Y. S., and Vithanage, M. (2019). Biochar-based engineered composites for sorptive decontamination of water: A review. *Chem. Eng. J.*, 372:536–550.

Prieto-Rodríguez, L., Oller, I., Klamerth, N., Agüera, A., Rodríguez, E., and Malato, S. (2013). Application of solar AOPs and ozonation for elimination of micropollutants in municipal wastewater treatment plant effluents. *Water Res.*, 47(4):1521–1528.

Priyadarshini, M., Das, I., Ghangrekar, M. M., and Blaney, L. (2022). Advanced oxidation processes: Performance, advantages, and scale-up of emerging technologies. *J. Environ. Manage.*, 316:115295.

PubChem (2021). Hydroperoxyl radical. `https://pubchem.ncbi.nlm.nih.gov/compound/Hydroperoxy-radical`.

Pulat, E., Etemoglu, A., and Can, M. (2009). Waste-heat recovery potential in Turkish textile industry: Case study for city of Bursa. *Renew. Sustain. Energy Rev.*, 13(3):663–672.

Radjenovic, J. and Petrovic, M. (2016). Sulfate-mediated electrooxidation of X-ray contrast media on boron-doped diamond anode. *Water Res.*, 94:128–135.

Radjenovic, J. and Petrovic, M. (2017). Removal of sulfamethoxazole by electrochemically activated sulfate: Implications of chloride addition. *J. Hazard. Mater.*, 333:242–249.

Radjenovic, J. and Sedlak, D. L. (2015). Challenges and opportunities for electrochemical processes as next-generation technologies for the treatment of contaminated water. *Environ. Sci. Technol.*, 49(19):11292–11302.

Rastogi, A., Al-Abed, S. R., and Dionysiou, D. D. (2009). Sulfate radical-based ferrous-peroxymonosulfate oxidative system for PCBs degradation in aqueous and sediment systems. *Appl. Catal. B-Environ.*, 85(3):171–179.

Raviv, M. and Antignus, Y. (2004). UV radiation effects on pathogens and insect pests of greenhouse-grown crops. *Photochem. Photobiol.*, 79(3):219–226.

Rayaroth, M. P., Aravindakumar, C. T., Shah, N. S., and Boczkaj, G. (2022). Advanced oxidation processes (AOPs) based wastewater treatment - unexpected nitration side reactions - a serious environmental issue: A review. *Chem. Eng. J.*, 430:133002.

Rezaeivalla, M. (2006). Sodium periodate ($NaIO_4$) - A versatile reagent in organic synthesis. *Synlett*, (20):3550–3551.

Ribeiro, J. P., Marques, C. C., Portugal, I., and Nunes, M. I. (2020). AOX removal from pulp and paper wastewater by Fenton and photo-Fenton processes: A real case-study. *Energy Rep.*, 6:770–775.

Robl, S., Wörner, M., Maier, D., and Braun, A. M. (2012). Formation of hydrogen peroxide by VUV-photolysis of water and aqueous solutions with methanol. *Photochem. Photobiol. Sci.*, 11:1041–1050.

Rodríguez, R., Espada, J., Pariente, M., Melero, J., Martínez, F., and Molina, R. (2016). Comparative Life Cycle Assessment (LCA) study of heterogeneous and homogenous Fenton processes for the treatment of pharmaceutical wastewater. *J. Clean. Prod.*, 124:21–29.

Rodriguez, S., Vasquez, L., Costa, D., Romero, A., and Santos, A. (2014). Oxidation of Orange G by persulfate activated by Fe(II), Fe(III) and zero valent iron (ZVI). *Chemosphere*, 101:86–92.

Saeli, M., Tobaldi, D. M., Seabra, M. P., and Labrincha, J. A. (2019). Mix design and mechanical performance of geopolymeric binders and mortars using biomass fly ash and alkaline effluent from paper-pulp industry. *J. Clean. Prod.*, 208:1188–1197.

Salmerón, I., Oller, I., and Malato, S. (2020). Electro-oxidation process assisted by solar energy for the treatment of wastewater with high salinity. *Sci. Total Environ.*, 705:135831.

Scaria, J. and Nidheesh, P. V. (2022). Comparison of hydroxyl-radical-based advanced oxidation processes with sulfate radical-based advanced oxidation processes. *Curr. Opin. Chem. Eng.*, 36:100830.

Schlichter, B., Mavrov, V., and Chmiel, H. (2004). Study of a hybrid process combining ozonation and microfiltration/ultrafiltration for drinking water production from surface water. *Desalination*, 168:307–317.

Schmitz, K. S. (2017). Chapter 15 - Reaction Rates and Mechanisms. In Schmitz, K. S., editor, *Physical Chemistry*, pages 695–760. Elsevier, Boston.

Scialdone, O., Guarisco, C., and Galia, A. (2011). Oxidation of organics in water in microfluidic electrochemical reactors: Theoretical model and experiments. *Electrochim. Acta*, 58:463–473.

Seibert, D., Zorzo, C. F., Borba, F. H., de Souza, R. M., Quesada, H. B., Bergamasco, R., Baptista, A. T., and Inticher, J. J. (2020). Occurrence, statutory guideline values and removal of contaminants of emerging concern by Electrochemical Advanced Oxidation Processes: A review. *Sci. Total Environ.*, 748:141527.

Seid-Mohamadi, A., Asgari, G., Shokoohi, R., and Adabi, S. (2015). Phenol disgrace via periodate in integrating by using supersonic radiation. *J. Med. Life*, 8(3):233–237.

Seid-Mohammadi, A., Asgari, G., Shokoohi, R., Baziar, M., Mirzaei, N., Adabi, S., and Partoei, K. (2019). Degradation of phenol using US/Periodate/nZVI system from aqueous solutions. *Glob. Nest J.*, 21(3):360–357.

Serra, A., Domènech, X., Brillas, E., and Peral, J. (2011). Life Cycle Assessment of solar photo-Fenton and solar photoelectro-Fenton processes used for the degradation of aqueous alpha-methylphenylglycine. *J. Environ. Monit.*, 13:167–174.

Serrano, K., Michaud, P., Comninellis, C., and Savall, A. (2002). Electrochemical preparation of peroxodisulfuric acid using boron doped diamond thin film electrodes. *Electrochim. Acta*, 48(4):431–436.

Shah, N. S., Rizwan, A. D., Khan, J. A., Sayed, M., Khan, Z. U. H., Murtaza, B., Iqbal, J., Din, S. U., Imran, M., Nadeem, M., Al-Muhtaseb, A. H., Muhammad, N., Khan, H. M., Ghauri, M., and Zaman, G. (2018). Toxicities, kinetics and degradation pathways investigation of ciprofloxacin degradation using iron-mediated $H_2O_2$ based Advanced Oxidation Processes. *Process Saf. Environ.*, 117:473–482.

Sharma, K., Dutta, V., Sharma, S., Raizada, P., Hosseini-Bandegharaei, A., Thakur, P., and Singh, P. (2019). Recent advances in enhanced photocatalytic activity of bismuth oxyhalides for efficient photocatalysis of organic pollutants in water: A review. *J. Ind. Eng. Chem.*, 78:1–20.

Sharpe, A. G. (1992). *Inorganic Chemistry.* Longman Scientific and Technical, UK, 3rd edition.

Shemer, H. and Narkis, N. (2005). Trihalomethanes aqueous solutions sono-oxidation. *Water Res.*, 39(12):2704–2710.

Sigma Aldrich (2020). OXONE®, monopersulfate compound. `https://www.sigmaaldrich.com/catalog/product/sial/228036?lang=en&region=BE`.

Sirés, I. and Brillas, E. (2012). Remediation of water pollution caused by pharmaceutical residues based on electrochemical separation and degradation technologies: A review. *Environ. Int.*, 40:212–229.

Sirés, I., Brillas, E., Oturan, M. A., Rodrigo, M. A., and Panizza, M. (2014). Electrochemical Advanced Oxidation Processes: Today and tomorrow. A review. *Environ. Sci. Pollut. Res.*, 21:8336–8367.

Soltani, R. D. C., Mashayekhi, M., Naderi, M., Boczkaj, G., Jorfi, S., and Safari, M. (2019a). Sonocatalytic degradation of tetracycline antibiotic using zinc oxide nanostructures loaded on nano-cellulose from waste straw as nanosonocatalyst. *Ultrason. Sonochem.*, 55:117–124.

Soltani, R. D. C., Miraftabi, Z., Mahmoudi, M., Jorfi, S., Boczkaj, G., and Khataee, A. (2019b). Stone cutting industry waste-supported zinc oxide nanostructures for ultrasonic assisted decomposition of an anti-inflammatory non-steroidal pharmaceutical compound. *Ultrason. Sonochem.*, 58:104669.

Song, H., Yan, L., Jiang, J., Ma, J., Zhang, Z., Zhang, J., Liu, P., and Yang, T. (2018). Electrochemical activation of persulfates at BDD anode: Radical or nonradical oxidation? *Water Res.*, 128:393–401.

Soumia, F. and Petrier, C. (2016). Effect of potassium monopersulfate (oxone) and operating parameters on sonochemical degradation of cationic dye in an aqueous solution. *Ultrason. Sonochem.*, 32:343–347.

Srinivasan, A. and Thiruvenkatachari, V. (2009). Perchlorate: Health effects and technologies for its removal from water resources. *Int. J. Environ. Res. Public Health*, 6(4):1418–1442.

Särkkä, H., Bhatnagar, A., and Sillanpää, M. (2015). Recent developments of electro-oxidation in water treatment - A review. *J. Electroanal. Chem.*, 754:46–56.

Steffen, C. and Wetzel, E. (1993). Chlorate poisoning: Mechanism of toxicity. *Toxicology*, 84(1):217–231.

Steter, J. R., Brillas, E., and Sirés, I. (2018). Solar photoelectro-Fenton treatment of a mixture of parabens spiked into secondary treated wastewater effluent at low input current. *Appl. Catal. B-Environ.*, 224:410–418.

Suhan, M. B. K., Shuchi, S. B., Anis, A., Haque, Z., and Islam, M. S. (2020). Comparative degradation study of remazol black B dye using electro-coagulation and electro-Fenton process: Kinetics and cost analysis. *Environ. Nanotechnol. Monit. Manag.*, 14:100335.

Summerfelt, S. T. (2003). Ozonation and UV irradiation - An introduction and examples of current applications. *Aquac. Eng.*, 28(1):21–36.

Tadda, M., Ahsan, A., Shitu, A., ElSergany, M., Arunkumar, T., Jose, B., Razzaque, M. A., and Daud, N. N. (2016). A review on activated carbon: Process, application and prospects. *JACEPR*, 2(1):7–13.

Takenaka, N. and Bandow, H. (2007). Chemical kinetics of reactions in the unfrozen solution of ice. *J. Phys. Chem. A*, 111(36):8780–8786.

Tan, C., Dong, Y., Fu, D., Gao, N., Ma, J., and Liu, X. (2018). Chloramphenicol removal by zero valent iron activated peroxymonosulfate system: Kinetics and mechanism of radical generation. *Chem. Eng. J.*, 334:1006–1015.

Tan, C., Gao, N., Zhou, S., Xiao, Y., and Zhuang, Z. (2014). Kinetic study of acetaminophen degradation by UV-based Advanced Oxidation Processes. *Chem. Eng. J.*, 253:229–236.

Tang, T., Lu, G., Wang, R., Qiu, Z., Huang, K., Lian, W., Tao, X., Dang, Z., and Yin, H. (2019). Rate constants for the reaction of hydroxyl and sulfate radicals with organophosphorus esters (OPEs) determined by competition method. *Ecotox. Environ. Safe.*, 170:300–305.

Tezcanli-Güyer, G. and Ince, N. (2004). Individual and combined effects of ultrasound, ozone and UV irradiation: A case study with textile dyes. *Ultrasonics*, 42(1):603–609.

Thomas, N., Dionysiou, D. D., and Pillai, S. C. (2021). Heterogeneous Fenton catalysts: A review of recent advances. *J. Hazard. Mater.*, 404:124082.

Tran, N. H., Reinhard, M., and Gin, K. Y.-H. (2018). Occurrence and fate of emerging contaminants in municipal wastewater treatment plants from different geographical regions - A review. *Water Res.*, 133:182–207.

Tröster, I., Fryda, M., Herrmann, D., Schäfer, L., Hänni, W., Perret, A., Blaschke, M., Kraft, A., and Stadelmann, M. (2002). Electrochemical advanced oxidation process for water treatment using DiaChem® electrodes. *Diam. Relat. Mater.*, 11(3):640–645.

Turan-Ertas, T. and Gurol, M. D. (2002). Oxidation of diethylene glycol with ozone and modified Fenton processes. *Chemosphere*, 47(3):293–301.

Urtiaga, A., Gómez, P., Arruti, A., and Ortiz, I. (2014). Electrochemical removal of tetrahydrofuran from industrial wastewaters: Anode selection and process scale-up. *J. Chem. Technol. Biotechnol.*, 89:1243–1250.

Ushani, U., Lu, X., Wang, J., Zhang, Z., Dai, J., Tan, Y., Wang, S., Li, W., Niu, C., Cai, T., Wang, N., and Zhen, G. (2020). Sulfate radicals-based advanced oxidation technology in various environmental remediation: A state-of-the-art review. *Chem. Eng. J.*, 402:126232.

Vasquez-Medrano, R., Prato-Garcia, D., and Vedrenne, M. (2018). Chapter 4 - Ferrioxalate-mediated processes. In Ameta, S. C. and Ameta, R., editors, *Advanced Oxidation Processes for Waste Water Treatment*, pages 89–113. Academic Press.

Vidal-Dorsch, D. E., Bay, S. M., Maruya, K., Snyder, S. A., Trenholm, R. A., and Vanderford, B. J. (2012). Contaminants of emerging concern in municipal wastewater effluents and marine receiving water. *Environ. Toxicol. Chem.*, 31(12):2674–2682.

Vithanage, M., Herath, I., Joseph, S., Bundschuh, J., Bolan, N., Ok, Y. S., Kirkham, M., and Rinklebe, J. (2017). Interaction of arsenic with biochar in soil and water: A critical review. *Carbon*, 113:219–230.

Waldemer, R. H., Tratnyek, P. G., Johnson, R. L., and Nurmi, J. T. (2007). Oxidation of chlorinated ethenes by heat-activated persulfate: Kinetics and products. *Environ. Sci. Technol.*, 41:1010–1015.

Wang, H., Yang, Y., Keller, A. A., Li, X., Feng, S., Dong, Y.-N., and Li, F. (2016a). Comparative analysis of energy intensity and carbon emissions in wastewater treatment in USA, Germany, China and South Africa. *Appl. Energ.*, 184:873–881.

Wang, J. and Chen, H. (2020). Catalytic ozonation for water and wastewater treatment: Recent advances and perspectives. *Sci. Total Environ.*, 704:135249.

Wang, J. and Wang, S. (2018a). Activation of persulfate (PS) and peroxymonosulfate (PMS) and application for the degradation of emerging contaminants. *Chem. Eng. J.*, 334:1502–1517.

Wang, J. and Zhuan, R. (2020). Degradation of antibiotics by advanced oxidation processes: An overview. *Sci. Total Environ.*, 701:135023.

Wang, L. K., Hung, Y.-T., and Shammas, N. K. (2005). *Physicochemical Treatment Processes*, volume 3. Springer.

Wang, N., Zheng, T., Zhang, G., and Wang, P. (2016b). A review on Fenton-like processes for organic wastewater treatment. *J. Environ. Chem. Eng.*, 4(1):762–787.

Wang, S. (2008). A comparative study of Fenton and Fenton-like reaction kinetics in decolourisation of wastewater. *Dyes Pigm.*, 76(3):714–720.

Wang, S. and Wang, J. (2018b). Degradation of carbamazepine by radiation-induced activation of peroxymonosulfate. *Chem. Eng. J.*, 336:595–601.

Wang, S. and Wang, J. (2020). Treatment of membrane filtration concentrate of coking wastewater using PMS/chloridion oxidation process. *Chem. Eng. J.*, 379:122361.

Wang, X., Anctil, A., and Masten, S. J. (2019). Energy consumption and environmental impact analysis of ozonation catalytic membrane filtration system for water treatment. *Environ. Eng. Sci.*, 36(2):149–157.

Wang, X., Sun, M., Zhao, Y., Wang, C., Ma, W., Wong, M. S., and Elimelech, M. (2020). In situ electrochemical generation of Reactive Chlorine Species for efficient ultrafiltration membrane self-cleaning. *Environ. Sci. Technol.*

Wang, Y., Lin, X., Shao, Z., Shan, D., Li, G., and Irini, A. (2017). Comparison of Fenton, UV-Fenton and nano-$Fe_3O_4$ catalyzed UV-Fenton in degradation of phloroglucinol under neutral and alkaline conditions: Role of complexation of $Fe^{3+}$ with hydroxyl group in phloroglucinol. *Chem. Eng. J.*, 313:938–945.

Wardman, P. (1989). Reduction potentials of one-electron couples involving free radicals in aqueous solution. *J. Phys. Chem. Ref. Data*, 18:1637–1755.

Weber, W. J., Hopkins, C. B., and Bloom, R. (1970). Physicochemical treatment of wastewater. *J. Water Pollut. Control Fed.*, 42(1):83–99.

Wei, Z., Villamena, F. A., and Weavers, L. K. (2017). Kinetics and mechanism of ultrasonic activation of persulfate: An in situ EPR spin trapping study. *Environ. Sci. Technol.*, 51(6):3410–3417.

Wordofa, D. N., Walker, S. L., and Liu, H. (2017). Sulfate radical-induced disinfection of pathogenic *Escherichia coli O157:H7* via iron-activated persulfate. *Environ. Sci. Technol.*, 4:154–160.

Wu, W., Huang, Z.-H., and Lim, T.-T. (2014). Recent development of mixed metal oxide anodes for electrochemical oxidation of organic pollutants in water. *Appl. Catal. A-Gen.*, 480:58–78.

Xiao, R., Luo, Z., Wei, Z., Luo, S., Spinney, R., Yang, W., and Dionysiou, D. D. (2018). Activation of peroxymonosulfate/persulfate by nanomaterials for sulfate radical-based advanced oxidation technologies. *Curr. Opin. Chem. Eng.*, 19:51–58.

Xiao, S., Qu, J., Zhao, X., Liu, H., and Wan, D. (2009). Electrochemical process combined with UV light irradiation for synergistic degradation of ammonia in chloride-containing solutions. *Water Res.*, 43(5):1432–1440.

Xu, X., Ye, Q., Tang, T., and Wang, D. (2008). HgO oxidative absorption by $K_2S_2O_8$ solution catalyzed by $Ag^+$ and $Cu^{2+}$. *J. Hazard. Mater.*, 158(2):410–416.

Xu, X.-R. and Li, X.-Z. (2010). Degradation of azo dye Orange G in aqueous solutions by persulfate with ferrous ion. *Sep. Purif. Technol.*, 72(1):105–111.

Yan, D. Y. S. and Lo, I. M. C. (2013). Removal effectiveness and mechanisms of naphthalene and heavy metals from artificially contaminated soil by iron chelate-activated persulfate. *Environ. Pollut.*, 178:15–22.

Yin, S., Han, J., Zhou, T., and Xu, R. (2015). Recent progress in g-$C_3N_4$ based low cost photocatalytic system: Activity enhancement and emerging applications. *Catal. Sci. Technol.*, 5:5048–5061.

Yogranjan, Bal, L. M., Satpute, G., and Srivastava, A. (2017). Chapter 19 - Plant stress signaling through corresponding nanobiotechnology. In Oprea, A. E. and Grumezescu, A. M., editors, *Nanotechnology Applications in Food*, pages 381–391. Academic Press.

Yuan, R., Ramjaun, S. N., Wang, Z., and Liu, J. (2011). Effects of chloride ion on degradation of Acid Orange 7 by sulfate radical-based Advanced Oxidation Process: Implications for formation of chlorinated aromatic compounds. *J. Hazard. Mater.*, 196:173–179.

Yun, E.-T., Yoo, H.-Y., Kim, W., Kim, H.-E., Kang, G., Lee, H., Lee, S., Park, T., Lee, C., Kim, J.-H., and Lee, J. (2017). Visible-light-induced activation of periodate that mimics dye-sensitization of $TiO_2$: Simultaneous decolorization of dyes and production of oxidizing radicals. *Appl. Catal. B-Environ.*, 203:475–484.

Zaharia, C., Suteu, D., Muresan, A., Muresan, R., and Popescu, A. (2009). Textile wastewater treatment by homogeneous oxidation with hydrogen peroxide. *Environ. Eng. Manag. J.*, 8(6):1359–1369.

Zawartka, P., Burchart-Korol, D., and Blaut, A. (2020). Model of carbon footprint assessment for the life cycle of the system of wastewater collection, transport and treatment. *Sci. Rep.*, 10:5799.

Zepon Tarpani, R. R. and Azapagic, A. (2018). Life cycle environmental impacts of advanced wastewater treatment techniques for removal of pharmaceuticals and personal care products (PPCPs). *J. Environ. Manage.*, 215:258–272.

Zhang, B.-T., Zhang, Y., Teng, Y., and Fan, M. (2015). Sulfate radical and its application in decontamination technologies. *Crit. Rev. Env. Sci. Tec.*, 45(16):1756–1800.

Zhang, T., Chen, Y., Wang, Y., Roux, J. L., Yang, Y., and Croué, J.-P. (2014). Efficient peroxydisulfate activation process not relying on sulfate radical generation for water pollutant degradation. *Environ. Sci. Technol.*, 48:5868–5875.

Zhang, X., Guo, K., Wang, Y., Qin, Q., Yuan, Z., He, J., Chen, C., Wu, Z., and Fang, J. (2020a). Roles of bromine radicals, HOBr and $Br_2$ in the transformation of flumequine by the UV/chlorine process in the presence of bromide. *Chem. Eng. J.*, 400:125222.

Zhang, Y., Li, J., Bai, J., Li, X., Shen, Z., Xia, L., Chen, S., Xu, Q., and Zhou, B. (2018). Total organic carbon and total nitrogen removal and simultaneous electricity generation for nitrogen-containing wastewater based on the catalytic reactions of hydroxyl and chlorine radicals. *Appl. Catal. B-Environ.*, 238:168–176.

Zhang, Y., Wang, H., Li, Y., Wang, B., Huang, J., Deng, S., Yu, G., and Wang, Y. (2020b). Removal of micropollutants by an electrochemically driven UV/chlorine process for decentralized water treatment. *Water Res.*, 183:116115.

Zhao, D., Liao, X., Yan, X., Huling, S. G., Chai, T., and Tao, H. (2013). Effect and mechanism of persulfate activated by different methods for PAHs removal in soil. *J. Hazard. Mater.*, 254-255:228–235.

Zhao, L., Chen, Y., Liu, Y., Luo, C., and Wu, D. (2017). Enhanced degradation of chloramphenicol at alkaline conditions by S(-II) assisted heterogeneous Fenton-like reactions using pyrite. *Chemosphere*, 188:557–566.

Zhou, M., Oturan, M. A., and Sirés, I. (2018). *Electro-Fenton Process.* Springer Singapore.

Zhou, Y., Jiang, J., Gao, Y., Ma, J., Pang, S.-Y., Li, J., Lu, X.-T., and Yuan, L.-P. (2015). Activation of peroxymonosulfate by benzoquinone: A novel nonradical oxidation process. *Environ. Sci. Technol.*, 49:12941–12950.

Zhu, Y., Zhu, R., Xi, Y., Zhu, J., Zhu, G., and He, H. (2019). Strategies for enhancing the heterogeneous Fenton catalytic reactivity: A review. *Appl. Catal. B-Environ.*, 255:117739.

Zárate-Guzmán, A. I., González-Gutiérrez, L. V., Godínez, L. A., Medel-Reyes, A., Carrasco-Marín, F., and Romero-Cano, L. A. (2019). Towards understanding of heterogeneous Fenton reaction using carbon-Fe catalysts coupled to in-situ $H_2O_2$ electro-generation as clean technology for wastewater treatment. *Chemosphere*, 224:698–706.